UNIVERSITY OF HULL

SCHOOL OF ENVIRONMENTAL SCIENCES

Seasonal Growth Dynamics and Blue Carbon Storage

of the Intertidal Seagrass *Zostera noltei*

By

Aidan Jackson

BSc Marine Biology

August 2023

A thesis submitted in fulfilment of the requirements for the degree MSc (by Research)

Biological Science

Supervisor: Professor Rodney Forster

Contents

List of figures

List of tables

Abstract

The primary objective of this study was to assess the carbon assimilation potential of a bed of the intertidal seagrass, *Zostera noltei,* at Spurn Point on the East Yorkshire coastline at the mouth of the Humber Estuary. This population of seagrass, prior to this report, had not been subject to scientific investigation since 1936. Environmental factors that influenced the bed during the study period were thoroughly considered. Two field-based techniques were used to estimate the annual carbon assimilation. Short-term (< 1 h) gas-exchange enclosure experiments were conducted at sites with varying percentages of *Zostera noltei* cover. The findings yielded a peak photosynthetic carbon assimilation value of 58.8 mg C m^{-2} h^{-1}. By combining the photosynthetic rate measurements with logger data recording incident irradiance measurements for the seagrass bed throughout the study period, hourly values were extrapolated to monthly and growing season estimates and converted to carbon drawdown. Additional MINI-PAM photosynthesis-irradiance analysis gave estimates of the irradiances at which half the photosynthetic capacity was achieved. Dark respiration rates measured in the field were low and variable. For modelling net primary production, a respiratory loss of 10% of the maximum photosynthetic rate was set. An estimate was made of 57.5 gC m^{-2} over this period. The area of the *Zostera noltei* bed as of 2022, was estimated at 10,467.4 m^2. Therefore, the bed size multiplied by our productivity factor per square meter estimated an overall productivity during the growth season for the bed to be 602 kg carbon fixed.

Keywords

Introduction

Background

Seagrasses are flowering plants that have vascular systems and are commonly found in marine and estuarine environments. The global scientific community recognises 65 different species of seagrasses, each with its own unique evolutionary history (Gruber et al., 2022). For example, estuarine seagrasses have evolved from terrestrial ancestors, which has resulted in certain physiological adaptations regarding water retention and additionally nutrient extraction from the water column (Gruber et al., 2022). To adjust to their environment, estuarine seagrasses have also reduced their structural tissue to increase their buoyancy enhancing their ability to photosynthesise when submerged. When it comes to reproduction, estuarine seagrasses can reproduce sexually or asexually. In sexual reproduction, their pollen is typically released into the water column and is carried by currents to fertilise other plants (Barañano et al., 2022).

There are four species of seagrass that can be found in the UK and British Isles, consisting of two species of eelgrass: *Zostera marina*, which is the larger of the two, and *Zostera noltei* which is also named dwarf eelgrass. The two species were relatively widespread in the UK but now have a restricted distribution. The *Zostera marina* populations tend to be found in the shallow sublittoral or lower shore, whereas *Zostera noltei* occurs more commonly at the higher intertidal elevations. The third and fourth species which belong to a different phylogenetic group (widgeon weeds) are rarer in the UK, only inhabiting very northern areas of England and also Scotland, they are named, *Ruppia maritima* and *Ruppia cirrhosa* (Lefebvre et al., 2009; Tyler-Walters & d'Avack, 2015). Whilst both *Ruppia* species are considered to be stable by the IUCN Red List, the *Zostera* species are considered as declining. The IUCN listing considers their global status and not only that of the UK (IUCN Red List, 2022). All species of seagrass in the UK are covered under the UK Biodiversity Action Plan (1994) and are deemed to be nationally scarce (Foden & Brazier, 2007). One study estimated the historic losses of seagrass in the UK at around 44% since 1936 with 39% being lost since the year 1939, it also suggested that the total losses over history may even be as high as 92% (Green et al., 2021). Due to such losses, conservation efforts to protect and recover beds from further decline are commonly found nationwide (Airoldi & Beck, 2007).

Seagrass beds are considered to be highly productive (Makri et al., 2023). However, they are not solely important for their productivity, they also act as an essential component of the ecosystem in regard to providing habitat to juvenile fish such as cod, crabs, and shrimp (Polte et al., 2005) along with provision of a food source to various nematodes, copepods and also grazing wild fowl such as

brent geese (Lebreton et al., 2012) The ability of the seagrass bed to provide shelter and food to other trophic layers is an important enhancement effect that seagrass beds have on biodiversity (McHenry et al., 2021). Seagrass beds also act as a buffer against wave action on the shore. For example, the presence of a seagrass community such as *Zostera noltei* at the study site of this project (Spurn Point) increases the resistance of the sediment surface to erosion, and can trap sediment (and carbon-rich particles), which assists in mitigating currents (Houseago et al., 2022) or wave energy that may otherwise cause erosion to the coastline (Christianen et al., 2013; Annuar & Anas, 2021). The populations of seagrass can also play a key role in providing cultural value to an area (Scott et al., 2018), through tourism and recreational opportunities (Oracion et al., 2005), perhaps not to the extent of other more high-profile marine protected sights, but rather a more local attraction to an interested demographic.

Figure 1. A Yorkshire Wildlife Trust signage board, located on the peninsula at Spurn, giving information on the population of seagrass present.

This coupled with the influx of grazing birds that the seagrass bed attracts, which also entices ornithologists (Istomina et al., 2016). Seagrass populations add a sense of cultural identity to the area. The *Zostera noltei* population at Spurn Point described in this thesis forms part of the wildlife features at this frequently visited site.

The benefits that seagrass beds can bring are wide, they are also capable of acting as an acidification buffer by regulating the chemical composition of the water in which they are found (Cyronak et al., 2018). Through their photosynthetic activity and uptake of CO_2, there will be a local-scale reversal of the main cause of ocean acidification which is the dissolving of CO_2 into bodies of water, which in turn due to the formation of carbonic acid, lowers the pH of such a body, (Hendriks et al., 2014). In addition, oxygen is produced as a biproduct of photosynthesis and this may counteract any localised oxygen depletion.

Climate Change Impact

Unfortunately, despite the benefits that they bring, seagrass beds have seen a decline globally (Sudo et al., 2021). With the obvious and concerning trend of climate change currently, conditions for seagrasses are only set to deteriorate (Tang & Hadibarata, 2022). Firstly, the most obvious impact to seagrasses globally is the increase in air and water temperatures that are occurring. The gradual increase in average temperatures globally may not have an initial impact, however the occurrence of extreme heat events can cause mortality in seagrass (Bulthuis, 1987), with extreme events deemed 'marine heatwaves' exceeding the temperature tolerances of seagrass such as *Zostera noltei* and *Zostera marina*. Under heat replication experiments between 28°C and 32°C photoinhibition was witnessed alongside an increase in respiration, displaying the negative impact of such temperatures on *Z. marina* (Deguette et al., 2021). The die-off caused by these events alongside the reduced flowering and reproductive ability seen in *Z.noltei* and *Z. marina* after such events (Deguette et al., 2022), may cause a shift in the spatial distribution of certain seagrasses (Short & Neckles, 1999). Alongside the increased marine heatwave events, increased extreme storm events are also apparent (Kowalski et al., 2023). Storm surges have occurred at Spurn Point and caused a breach of the spit, where the North Sea has washed over the neck of the peninsula and exposed the sheltered seagrass bed to currents and wave activity that it otherwise would not experience. If the conditions become severe enough, the blades are susceptible to break off and the root/rhizome matrix may become disturbed. A reduction in blade biomass is a loss in photosynthetic material which in turn will hinder the productivity of the bed as a whole (La Nafie et al., 2012). The effect of ocean acidification on the growth of *Z. noltei* has been seen in the literature to cause a significant reduction in the photosynthetic pigments present within the plant blades (Repolho et al., 2017). Another negative impact as a result of ocean acidification was found during an investigation into the leaf lipid structure of *Z. noltei,* where it was found the fatty acids underwent a remodelling event, typical of a plant that is under new environmental stress (Duarte et al., 2022). The remodelling occurs as a reaction to thermal and low pH stress in order to balance excessive membrane fluidity and stabilise

the chloroplastidial monogalactosyldiacylglycerol and digalactosyldiacylglycerol lipids, membrane fluidity and the aforementioned lipids are essential in photosynthetic activity therefore a remodelling event is an indicator of climate change related stress (Franzitta et al., 2021).

Blue Carbon

Blue carbon is the term used to describe the natural carbon sinks in the marine environment, predominantly mangroves, seagrass beds and salt marshes. It refers to the capacity of the aforementioned ecosystems to fix and bury carbon from the atmosphere. It is estimated that these ecosystems are able to sequester 25% of the human-produced carbon dioxide and as a result prove to be an invaluable resource in battling the current climate crisis (Baez, 2023). The importance of seagrass beds in regard to blue carbon is a highly discussed topic in the scientific literature. They are described as significant carbon sinks, that need maintaining and protecting on a global scale in order to combat climate change (McHenry et al., 2023). Much of the literature attempts to quantify the carbon sinks and portrays highly productive ecosystems that have the potential to sequester carbon at a rate 'much greater than terrestrial forests' (McLeod et al., 2011) or even that seagrass are capable of burying carbon 35 times faster than a rainforest (Macreadie et al., 2014). A recent study on eelgrass (*Zostera marina*) in the Clayoquot Sound region of British Colombia, Canada studied 7 beds in total and found their carbon stocks predominantly within the range from 21.1 ± 1.4 gC m^{-2} to 28.9 ± 1.6 gC m^{-2}. Carbon assimilation was analysed to produce an annual accumulation range of 0.5 to 47 gC m^{-2} y^{-1}. This shows quite a wide range of carbon accumulation between populations, emphasising the importance of understanding the productivity of individual beds to support the importance of such a population (Prior, 2023) and the necessity of any conservation/restoration projects that may be considered. For example, a bed may be highly productive but due to external pressures such as disease (Burdick et al., 1993), pollution (Marino et al., 2021) or trampling (Tyler-Walters, 2008) may have experienced a loss in coverage, hence emphasising the need for restoration projects that attempt to re-establish the potential productivity of any given seagrass bed.

In the study by Gouldsmith & Cooper (2022), a global comparison of organic carbon storage in sediments of seagrass beds was done. The range of organic carbon was between 218 and 38,000 g OC m^{-2}. Values were collected from two other studies that presented blue carbon stock data from 13 different countries including, Bulgaria, Canada, Denmark, Finland, France, Japan, Korea, Mexico, Norway, Portugal, Sweden, the United Kingdom and the USA. The comparison in the study also includes seagrass beds found in Australia, Northern Europe, Denmark, England and the Pacific and suggests a mean value for the entirety of global seagrass stocks at 13,970 g OC m^{-2}.

Zostera noltei at Spurn

The current extent of the *Zostera noltei* bed at Spurn Point is relatively small (10,467.4 m^2) with a predicted short growth season (assumed at the onset of this study to be around 6 months), with blade density increasing through Spring and into Summer and then subsequently being lost through Autumn and Winter (Philippart, 1995). It is important to understand whether *Zostera noltei* has such capabilities for carbon assimilation as others are described to in the literature, as this will provide insight into the significance of their role in assisting to battle climate change. The seagrass can store carbon through growth of the plant material, with photosynthetic activity fixing carbon from the atmosphere and providing the energy needed for the plant to grow (Brun et al., 2003). It is essential to understand that not all carbon assimilated by photosynthesis is sequestered. In order for the carbon sequestered by the seagrass to be stored it must remain part of the plant or be buried into the sediment. The carbon may remain as part of the plant as buried blade and root material. An important additional factor in carbon storage is the settlement of carbon-rich particles (silts and muds) from the estuarine water, into the seagrass bed root/rhizome matrix (Couto et al., 2013).

This study focuses on the remaining population of *Zostera noltei* located at Spurn Point on the Yorkshire coastline, for which the regional extent has had an estimated decline of over 90%. Seagrass beds in Spurn Point were originally mapped in Philip (1936) and showed an extent of roughly 330 hectares. That estimation is considered rough as the original image was hand-sketched and analysed in GIS. In 2022, the maximum extent of surveying *Z. noltei* was 1.05 hectares, which displays the dramatic nature of the decline (Figure 2).

Extent of seagrass from previous surveys

The area of Spurn Point and in particularly, the seagrass present at the site have not previously been the study of scientific publications, and therefore the history of the seagrass coverage in the region has a large gap. Initially the seagrass was mapped in 1936 by Graham Philip, but due to the lack of technology available at the time, it was impossible to give a true and precise representation of the coverage of the seagrass. He did however publish a detailed sketch of the site and coverage. From this it is evident, when compared to the outline of seagrass extent made by surveys in 2022, that a dramatic loss of seagrass has occurred within this albeit, extended period of time.

Figure 2. The historic coverage of Zostera noltei and Zostera marina (Philips, 1936) compared to the current coverage as of 2022 generated in GIS.

The current *Zostera noltei* coverage is represented as the red band in Figure 2, it is overlapped by the pink band that represents the historic *Z. noltei* population which was situated relatively high on the shore. The lower shore pink band in the above figure described by Philips (1936) resembles present-day descriptions of the larger seagrass species, *Zostera marina*. This species is no longer present at Spurn Point but is recorded in the North Sea elsewhere.

Currently the Yorkshire Wildlife Trust manage the site at Spurn and have in recent years begun a rewilding project to re-establish the population across a wider area. It is essential to understand the health and productivity of the current population at Spurn, to build a picture of the ecosystem and to also understand the "Blue Carbon" a re-established bed may be capable of capturing. The

importance of maintaining such populations is paramount, as the loss of such an ecosystem could result in a decline in atmospheric carbon fixed by the plants. More atmospheric carbon leads to faster rates of climate change and in turn more loss (Mazarrasa et al., 2021), a vicious cycle noted by conservation efforts.

Aims of the Project

This project is aimed at trying to quantify the Blue Carbon assimilation performed over the course of the annual growth season, by a population of *Zostera noltei* at Spurn Point. The study attempts to understand the productivity whilst accounting for as many variables as possible. Often when quantifying productivity in marine vegetation, assumptions are made to present final values (Duarte de Paula Costa et al., 2023). Rather than using previously designed assumptions, we aimed to record environmental conditions at the seagrass bed such as light intensity and temperature. Light levels vary considerably dependant on other environmental factors such as:

- weather, where cloud cover may change during the day and greatly alter the incident light intensity,
- time of year, where light intensity varies with solar elevation e.g., depending on the Earth's position in regard to the sun,
- tide times, where during particular tide times the seagrass bed may become immersed during the bright conditions of midday, thus limiting the light that reaches the plant, and exposed during nighttime where light availability is limited.

It was important to record the incident light intensity experienced by the seagrass bed in order to construct calculations and assumptions of the photosynthetic capacity of *Zostera noltei* at varying light intensities. For example, particularly high incident light intensities would be assumed to record more productive instances of photosynthesis than lower light intensities and this must be reflected in the calculation of productivity over the study period. Light intensity is also important to monitor at low levels, as at a certain light intensity respiration will become more dominant than photosynthesis, therefore as a biproduct carbon dioxide will be released into the atmosphere (Alcoverro, Manzanera and Romero, 2001). As a direct result of photosynthesis carbon is fixed into carbohydrates, the carbohydrates may be stored within the root system or as part of the aboveground blade material as new growth or used in respiration. If the blade is not lost between growth seasons through shoot shedding or as a result of grazing or if respiration does not outweigh photosynthesis, then this carbon is stored (Ghosh et al., 2015).

We were also able to record a time series of temperature values at a high temporal resolution to understand the exposure to low and high temperatures encountered as the seagrass became emersed or immersed. This allowed us to make valid assumptions and calculations again on the photosynthetic capacity of the seagrass whilst experiencing different temperatures, over the study period. By taking into account all these variables we believe that our methodology provides a true insight into the productivity of *Zostera noltei* at Spurn Point and provides a methodology that can be used at other intertidal sites.

The hypotheses of this study are as follows:

- The population of *Zostera noltei* at Spurn Point are expected to have environmental pressures that effect the health of the population, due to the limited distribution for example light intensity and exposure to light. The high elevation of the distribution of *Zostera noltei* would suggest that the population is high light and temperature adapted, as a result of extensive periods spent emersed in summer

- The total carbon assimilation of the *Zostera noltei* at Spurn Point should be comparable to other seagrasses in similar studies, where environmental variability is accounted for, with a particular focus on light intensity

- The water quality of the Humber Estuary may prove to be insufficient to sustain expansion of the current population of *Zostera noltei* and that previous nutrient levels may have caused a reduction in distribution at Spurn.

- A consistent measure of percentage cover throughout the growth season should display an increase in biomass from winter into summer as temperatures begin to rise and light conditions become more intense, it will reach its peak percentage cover here. Then a subsequent decline will occur as temperatures fall and light intensity drops when summer becomes winter

- The carbon and nitrogen balance of the above and belowground material will reflect the rapid growth of *Zostera noltei* as it enters its growth period and then the loss of biomass at the end of the growth season. The sediment characteristics will vary slightly across the bed

Materials and Methods

Site description

Spurn Point is a dynamic coastal spit system found on the East Yorkshire Coast (53°34'40"N; 0°6'58"E). Its geomorphological structure displays three main areas (Bateman et al., 2020):

- The dunes, which are found predominantly through the centremost region of the peninsula and the area where the peninsula meets the mainland. The distribution of the dunes has been reduced due to development on Spurn.
- The sandy/gravel-based shoreline, which is situated on the outermost region of the peninsula and is exposed to periods of high wave action from the North Sea. The high wave action has led to the neck of the peninsula becoming severely eroded and as a result of storm action it has been breached on a number of occasions.
- The innermost region of the peninsula is comprised of saltmarsh (*Spartina sp.*) and mudflats. Due to the positioning on the peninsula and the reduced wave action as a result of facing the Humber, these two diverse and complex ecosystems are able to survive.

The *Zostera noltei* population, which is the focus of this project, can be found in patches along the high tide line of the mudflats that are situated on the innermost section of the peninsula, as shown in the figure below.
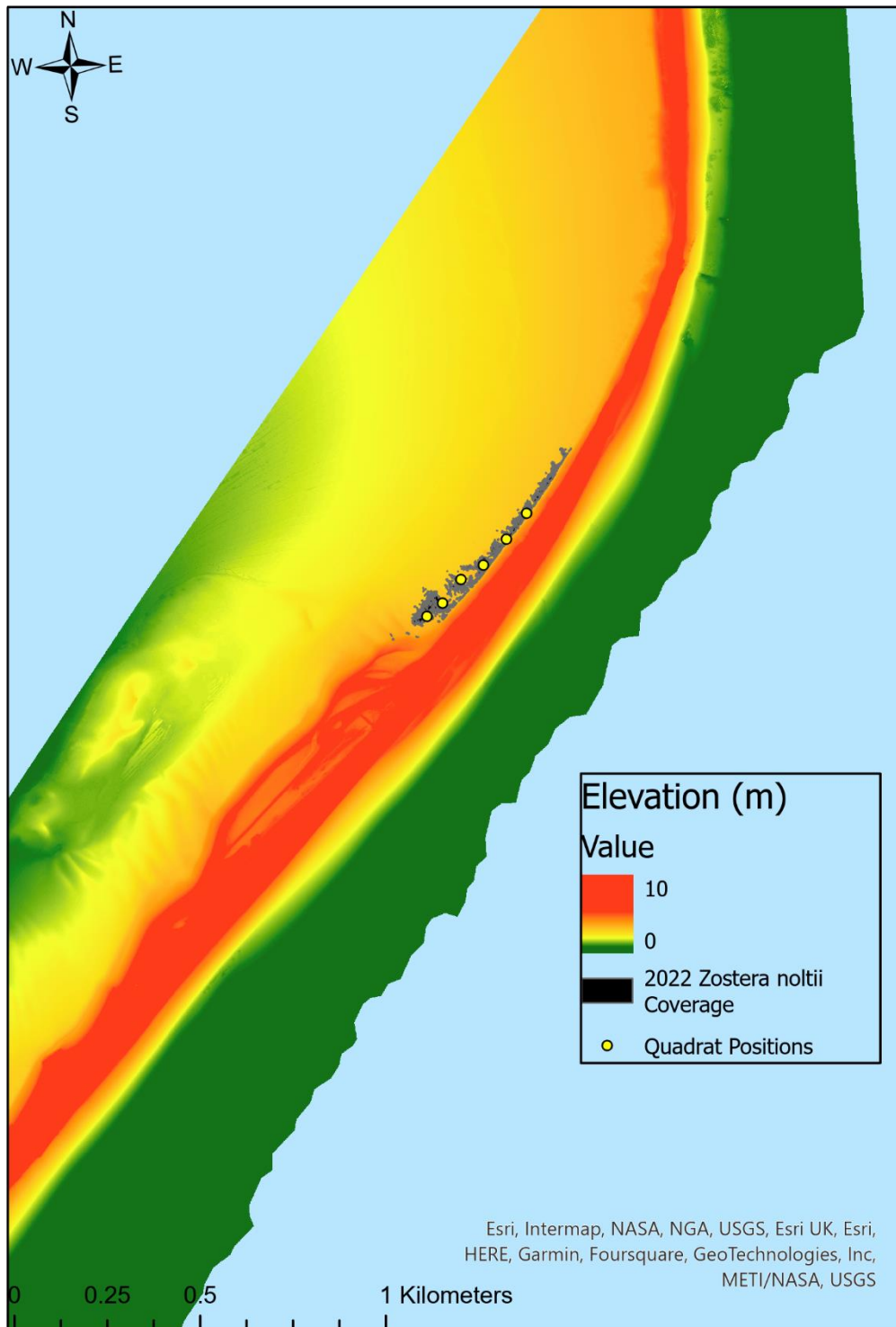
Figure 3. Spurn Point elevation (mCD) map, showing the 2022 Zostera noltei coverage and experimental quadrat positions.

Due to the rare and vulnerable geomorphological features that the Humber Estuary and Spurn Point exhibit, exhibit, intertidal mud and sandflats, subtidal sandbanks and dunes and their importance as biotopes (Wu and Parsons, 2019). The estuary was it was deemed of sufficient interest from a conservational view to be protected within the Natura 2000 Framework. This covers Spurn Head

under several different areas of legislation, including the following – Special Area of Conservation (SAC), Special Protection Areas (SPA), Sites of Special Scientific Interest (SSSI) and a Heritage Coast site (Lonsdale et al., 2022). It is also a designated Area of Outstanding National Beauty and a National Nature Reserve, it is further protected under the Ramsar Convention for Wetlands in the Humber (Bateman et al., 2020).

Photosynthetically Active Radiation and Temperature Analysis

One of a pair of identical waterproof light and temperature loggers (HOBO Pendant MX 2202, Onset Corp. USA) was attached onto a brick using cable ties. Initially, the brick was sat on top of the intertidal sediment surface, however, it was noted that the brick may retain heat differently to that of the surrounding mud and so on 15/07/2022 it was buried beneath the surface with just the logger showing above. The logger was situated next to a patch of *Spartina* which was centrally located in the main *Zostera noltei* patch at Spurn Point, the seagrass was predominantly found on the mudflats surrounding the *Spartina* patches. However, some seagrass was found growing amongst the patches.

Figure 4. An image of the temperature and light data logger, secured to a buried brick by cable ties.

A bamboo stick was driven into the ground next to the brick amongst the *Spartina* so that it could be easily found upon revisiting the site. The logger was set to record data every minute and was left in place at the Spurn seagrass bed for the following seven months. The other logger that made up the pair was placed further along the peninsula, whilst remaining intertidal it was situated on a gravel outcrop named 'The Den', this location was situated at 3.7 m elevation which was slightly lower on the shore than its twin on the seagrass which was at 4.96 m elevation and allowed us to determine

the impact of a known difference in elevation on the temperatures and time spent in illuminated conditions. Between the two loggers we have established a temperature and light timeline that stretches from the 1st of July 2022 until the 5th of January 2023. This allows for an analysis of the time the seagrass spent exposed to photosynthetically active radiation over approximately 7 months with both Summer and Winter seasons recorded, alongside the air and water temperatures experienced by the meadow. The elevation data is retrieved from the Environment Agency Lidar chart datum and was cross referenced with Immingham tidal gauge to ensure accuracy. See Figure 5 for an example of a dome experiment being carried out from a neighbouring *Spartina* patch. It should be noted that the sea level never reaches '0 m', this is because the source of the tidal data presents '0' as 'Admiralty zero' which is essentially the lowest tide in recorded history (Saiful et al., 2012). The tidal maximum on very high spring tides at Spurn Point may rise to above 7 m. Tidal gauge data from Immingham showed neap high tide height to be 4.9-5 m. Hence, the bed of *Z. noltii*, situated at a sea level of 4.5 to 5.0 m, would have a tidal submersion depth of between 0.1 m and 2.0 m for neap and spring high tides respectively. The tidal immersion/emersion cycle can be visualised from the light data as due to the characteristic turbidity of the water of the Humber Estuary, when the logger was submerged the light intensity decreased rapidly, tidal data was cross-referenced to validate the timings of apparent immersion and emersion. The data would be expected to show a sudden drop in irradiance when becoming submerged due to the turbidity of the Humber Estuary, and the temperature may also drop during the middle of a summer's day upon immersion. However, during the evening as air temperatures drop immersion should stabilise the ambient temperature, or even show an increase if the incoming tide is warmer than the cooling air. Calculation of the incident irradiance on an hourly basis during the emersed period was key to the calculations of photosynthetic carbon fixation to be described. Two extreme events of unusually hot weather ('marine heatwaves') were recorded during the measurement period.

Short-term gas exchange measurements

The uptake of carbon dioxide during short periods of seagrass photosynthesis in the light, and release by community respiration in the dark were measured using a variation of the 'bell jar' method, in which a transparent acrylic dome was used to isolate an area and an infrared CO_2 monitor was used to measure the fluxes in CO_2 (ppm) over a set period of time. The set up in this experiment was a simplified version in comparison to others in the literature, primarily as it was a completely closed system with no built-in method of circulation (Plus et al., 2001). However, the system was still capable of capturing fluxes in CO_2 as a result of any photosynthetic or respiratory activity (Silva, 2004). See 'Bell Jar Method' for a description of the equipment and how it was used.

Choice of sites

Three sample areas of different *Zostera noltei* densities were selected for estimation of carbon dioxide exchange. Seagrass coverage of the areas was judged by eye with the aim of being as close as possible to the values of 0%, 50% and 100% coverage. After each experiment was completed, a digital photograph was taken of the area covered and later analysed through an image analysis software (ImageJ). The process was the same as for the quadrat analysis described later (see 'Seasonal Growth Quadrat Analysis'). The image was cropped to a square over the area covered by the transparent acrylic dome to give a more accurate representation of the percentage cover of *Zostera* within the isolated dome.

Bell Jar Method

This study uses a variation of a bell jar technique (Plus et al., 2001) and the equipment used is as follows;

- A 50 cm diameter hemispherical acrylic dome (Talbot Designs),
- A carbon dioxide monitor (A37 CO_2 Meter; Uni-T Ltd, China) attached to the inside of the dome using Velcro,
- A waterproof light and temperature logger (HOBO Pendant MX 2202, Onset Corp. USA).
- A section of blackout cloth to reduce incident irradiance to zero.

Figure 5. An example of the set-ups in use at Spurn to measure changes in CO_2. On the left is the covered experiment with zero irradiance and on the right is the ambient solar light period. The irradiance/temperature logger is underneath the dome in the photos and the CO_2 monitor can be seen attached by Velcro on the inside of the dome in the picture showing the illuminated period.

A data logger within the dome measured and stored ambient temperature and visible light which enabled CO_2 uptake by the seagrass to be studied in relation to photosynthetically active radiation

(PAR), which is the section of the light spectrum that plants use to create sugars and sustain life (Gitelson et al., 2021).

Upon beginning the experiment within a selected area, another data logger of the same make and model as previously described was strategically placed close to the seagrass area and set to measure temperature and light every 2 seconds. The carbon dioxide meter was given time to equilibrate with the atmospheric CO_2 concentrations and then was attached to the inside of the dome.

Photosynthesis in ambient light – The dome was then placed over the selected area and pushed slightly down into the mudflat surrounding the salt marsh, in order to create an air-tight seal and therefore an isolated environment within. The volume of air trapped within the dome was 0.0327 m^3 and the area of sediment surface covered was 0.1963 m^2. The time when the dome was sealed into the mud was recorded as well as the initial reading of CO_2 that the monitor gave. The monitor was then checked every five minutes from there onwards for a total of fifteen minutes, recording the value displayed and the time (noting the time of day during the steps of the experiment was useful for later retrieving data from the logger). Varying temperatures and light intensities were observed throughout the day due to natural changes in solar elevation and cloud cover. A time period of 15 minutes was deemed most appropriate in order to avoid large deviations in temperature and humidity within the enclosed space. Typically, the CO_2 concentration decreased by over 100 ppm during this time.

Respiration – The dome was then covered by the blackout cloth immediately after the illuminated period, in order to replicate conditions with no light and analyse respiration rates for a further period of 15 minutes. After the time had expired the cloth was removed and the CO_2 reading alongside the time was recorded.

The data logger recorded light intensity in units of lux therefore a conversion was needed in order to display PAR in units of μmol photon m^{-2} s^{-1}. The reading given in lux was averaged over the period of time of the experiment, it was then divided by a coefficient of 54 (determined by comparison with a calibrated PAR sensor) to provide the PAR value (Canadell et al., 2021). Readings of lux were also reported at 5 minute intervals and again divided by the value of 54 to ensure homogenous results. Thus, the relationship between photosynthetic rate and PAR could be constructed from a series of enclosure experiments made under different solar conditions.

In order to present the data in a format that could give a true reflection of the carbon uptake or release by the seagrass within the domes and the bed in its entirety, various calculations and

conversions were needed to standardise the units. The total assimilation/release values of CO_2 in ppm from the individual 15 minute experiments were used and converted into mg C m^{-3}.

$$0.0409 \times Concentration\ (ppm) \times 44.01$$

The volume of the dome was then calculated and multiplied with the drawdown of CO_2 from a particular experiment, this gave the gas exchange rate relative to the size of the dome. Multiplication then allowed for calculation of hourly drawdown, and standardisation to area gave the hourly drawdown or release of carbon per m^2. This is the most common form of units found across other similar studies (Ouisse et al., 2010) and so allowed for comparisons to be made.

For extrapolation over longer periods of time the carbon drawdown data from the dome enclosure experiments was used alongside the light data retrieved from the fixed position HOBO loggers, to produce a value for the carbon drawdown potential over the study period. Firstly, a value for the maximum photosynthetic rate (P_{max}) was required. This was determined from the CO_2 uptake versus irradiance curves, and MINI-PAM (Walz GmbH, Germany) data (Figure 10 and Figure 22). A mean was taken of the photosynthetic rates (mg C m^{-2} h^{-1}) of the experiments with at least 30% coverage, giving a value of 58.8 mg C m^{-2} h^{-1}. This value was then halved to give 'half P_{max}' and then finally 10% of the P_{max} shown as a negative was used to represent the assumed respiration rate of *Zostera* (Marsh et al., 1986; Philippart, 1995).

The logger data was then downloaded and collated into an Excel spreadsheet, where data was present from the month of July 2022 through until November 2022. This was seen as an appropriate time range to display as it shows light data two months either side of when the CO_2 dome sampling was done, and is the period of peak *Z noltei* biomass for temperate sites (Wyer et al., 1977). The data required from the loggers was an hourly average of light from the months mentioned. The light data was converted to µmol m^{-2} s^{-1}m using the same method as earlier. The average light of each individual hour was categorised into the three different groups (P_{max}, half P_{max} and respiration), and within the respective groups a value for the amount of carbon fixed or released was applied. This was determined by assuming that P_{max} occurs at light intensity values over 300 µmol m^{-2} s^{-1} (Silva et al., 2005). Anything lower than this but above 20 µmol m^{-2} s^{-1} was considered to be at half P_{max}, and anything below 20 µmol m^{-2} s^{-1} was considered to be respiration. As well as literature evidence, the use of these values were later supported by the short-term light curve measurements using variable fluorescence, which saw maximum electron transport rates (ETRs) occur for most temperatures at 300 µmol m^{-2} s^{-1}. Between 20 and 300 µmol m^{-2} s^{-1} ETRs were seen to reach half of their capacity and any lower than this ETRs were effectively 0 (Figure 22). Through the use of pivot tables to condense the large amounts of data and 'IF' functions in Microsoft Excel the average light intensity of any

given hour within the time frame was assigned an 'hourly rate' value. The sum of the hourly rate values within a day gave an approximation for the aggregated photosynthetic/respiration rate of that respective day, noting that only days with at least 24 hours of valid data were used. No correction to photosynthetic rates was made for variability in temperature. The daily integral derived by this calculation is net primary productivity (NPP; mg C m^{-2} d^{-1}), which can be a positive or a negative value depending on the balance of time in the light and in the dark.

It is possible from this analysis to derive a value for the monthly and total carbon that can be fixed or released by a 1 m^{-2} patch of ≥30% coverage of *Zostera noltei* at Spurn Head over a 5-month study period, July- November 2022. The monthly calculation of productivity also allowed the data to be viewed in regard to the distribution of NPP throughout a month. It is expected to show a clear decline, with an increase in the variability of data as weather conditions become more unpredictable at the end of Summer and into Autumn and Winter. A Turkey (HSD) statistical analysis test was conducted on the monthly NPP data to determine whether a difference was present between the NPP of the months when compared to each other.

Estuarine Water Analysis

Investigation into the water nutrient content was necessary in order to gain a full understanding of the conditions and environment that the *Zostera noltei* population at Spurn Point was exposed to. The data was retrieved from an Environment Agency monitoring station that is situated relatively close to the peninsula at Spurn Point, therefore giving a strong indicator of the water quality that submerges the seagrass on a high tide. The key nutrients that are of interest are ammonium and nitrate, as both may become deleterious to seagrass growth at high concentrations (Van Katwijk et al., 1997).

Seasonal Growth Analysis

In order to gain an understanding of the population of *Zostera noltei* inhabiting the intertidal zone at Spurn and their seasonal growth progression, a non-destructive experiment was designed to produce a time series throughout the course of the study period. The experiment consisted of 6 stations with a singular fixed location 1 m^2 quadrat, the station location was selected using an example of stratified sampling (Miller & Ambrose, 2000). Beginning by visually noting the extent of the patch of seagrass at Spurn (prior knowledge of the extent of the patch was already present), and starting at the furthermost edge of the established patch, a quadrat was placed roughly every 100 metres walking back towards the mainland, attempting to remain at a similar elevation. When a quadrat location was determined a 1 x 1 m quadrat was placed onto the mud, two 'soft to wet ground tent pegs' were then driven into the bottom left and right-hand corners of the quadrat. The

tent pegs remained where they were stationed from when they were first placed in early April 2022 until the final field work in late September 2022 allowing 9 replicates to be taken in the study period. This allowed the same exact location to be used in subsequent months and therefore replicates were directly comparable. As the height of the peg tops relative to the sediment surface did not change, this also gave an indication of relatively stable sediment conditions at the site e.g. very limited erosion or deposition in this time period.

The quadrats were placed systematically and a photo was taken from above attempting to be as central as possible, sometimes the use of a wooden platform was needed to mitigate trampling damage to the surrounding seagrass. The photos were then collated into folders on a personal laptop and analysed at a later date (See Appendix). The analysis method included the use of the software ImageJ (based on protocols in the Water Framework Directive monitoring of France and the UK (Foden, 2007; Auby et al., 2014)), where the software opened the image of a quadrat, the image was then cropped to include a square within the quadrat, the number of pixels in the cropped image was then noted. To further analyse the now cropped image of the quadrat it was adjusted via the colour threshold tool within ImageJ, here the brightness threshold was adjusted to best display the area that was covered by *Zostera*. The ROI Manager (Region of Interest) tool in ImageJ then calculated the pixels selected by thresholding (*Zostera* coverage), and from here the percentage cover is calculated.

$$x = \frac{z}{t} 100$$

Where 'x' is the percentage cover, 'z' is the amount of *Zostera* pixels and 't' is the total pixels in the crop. This technique was used over the course of 9 visits to Spurn spanning a 6 month period.

Core Composition Analysis

Due to environmental protection laws over the *Zostera noltei* population at Spurn, the Natural England dispensation for the site allowed only limited numbers of cores that could be taken for analysis with as little damage to the bed and substrate as possible. A total of 18 mini-cores were taken on the 13th September 2022, using 50 ml cut-off test tubes with a 25 mm diameter to a standard depth of around 60 mm (giving a sediment volume of approximately 29.45cm^3). There was some variation in depth due to the inability for the cores to hold onto all the material when removed. The cores were taken at the end of the sampling regime, at each of the quadrat stations. A core was taken from the centre of three of the individual squares within the quadrat, working from the top right-hand corner and moving diagonally downwards. The cores were then bagged and

labelled individually, noting the quadrat and the square that they originated from. Core bags were then stored in the fridge overnight and worked up within a 48-hour period.

When working up, the core bags were gently mixed to homogenise the sediment. 36 oven-suitable crucibles were weighed and recorded. A small subsample of around 1g of sediment was added from each of the cores and weighed again using the same 4 decimal place fine balance that was used to weigh the empty crucibles. This was then recorded with the core number and area that it came from. The remaining material from the bag was then sieved using a 1 mm mesh sieve and any plant/rhizome material was removed, cleaned, measured against a ruler and then weighed in crucibles, again noting the number of the crucible in relation to where the sample had originated from. This gave the wet weight of the material.

The crucibles of sediment and plant material were then put in an oven for 48 hours at 60 °C (Ouisse et al., 2012). After drying, material was allowed to cool in a desiccator so that temperature and any uptake of atmospheric moisture did not impact the final weight. Samples were weighed once more to give a dry weight which was recorded (Machás et al., 2006). This allowed for the dry bulk density of the sediment to be analysed (dry mass of core sample/total core volume), for which the results should follow predictable patterns determined by the grain size of the substrate, where sandy substrates are heavier with a higher dry bulk density than muddy substrates (Flemming & Delafontaine, 2000).

The next step was to analyse the amount of carbon, nitrogen and hydrogen in the plant material. To do this the plant matter was separated into blade material and rhizome material. Approximately 50 mg of each type of matter was weighed and placed into tin foil cups which were then twisted so the material sat in the base of the structure. These were labelled according to the quadrat that they were taken from and analysed using a Leco CHN analyser, where the sample is heated to extreme temperatures under a stream of oxygen (850-1050°C), the released gas was monitored to give a precise reading of the three aforementioned elements and provided a percentage composition of the elements from each given sample.

The results were presented in a table with the percentages of each element found in the samples and also the amount in g kg^{-1}. It was decided that the best way to display the results from this experiment would be to plot the above ground material against the below ground to compare the quantities of the given elements between the material. To do this a mean was taken of the percentages of elements found in both groups, the results would be displayed in a bar chart and the confidence interval to 95% calculated, this would allow a significant difference, if present, to be seen between the elemental composition of the above and below ground matter. One-way ANOVA was

used to confirm if a statistical difference in elemental composition was present between above and below ground material, the null hypotheses was that there would be no significant difference between the elemental composition of the above and below ground material.

The mini-corer used in this analysis, sampled a sediment surface area of 4.909 cm^2. The data given by the cores was originally presented as the wet weight of the plant material found within three cores at the 6 different quadrat locations. The drying process, which was the same as for the sediment samples, gave the weight of the dry blade and rhizome/root matter individually alongside the ratio of blade: rhizome/root per core. The C, H, N analysis showed the carbon content of the plant material which was then used to produce a mean of the total carbon present in the plant material found within each individual core. Within a square meter it is possible to fit 2037 of the mini core samples used. Therefore, 2037 was the multiplier to calculate the value for total seagrass carbon m^{-2}. The ratio of blade to root/rhizome mass was applied to the total plant material carbon from here, to calculate the quantity of carbon in the blades of each core. A mean was taken from the three cores and their respective quadrats. Correlation between percentage cover of seagrass and leaf carbon content was determined using a Spearman's rank test.

Purpose Built Aquarium and Photosynthetic Yield Analysis

In order to later analyse seagrass samples taken from Spurn to determine their health, via pulse amplitude modulation fluorometry, a holding aquarium was built. This enabled the seagrass to be kept alive away from the field in a laboratory and therefore tested under stable and planned conditions.

The tank used was rectangular and made out of Perspex held together by a mix of screws and waterproof adhesive. A hole was drilled into the base of the tank and a connector was attached to the hole to ensure smooth flow. Four equal panels of Perspex were glued together, forming a hollow square column. Attached to the floor of the tank with the hole central in the column, this acted as a drain and kept the water level constant when full, also preventing spillages. A hole with another connector was made in the lower corner of a side panel to make the inflow valve. Attached to the connector was a malleable plastic pipe, this fed under the tank station and into a separate 60 l insulated tank where the other end of the pipe was attached to a salt water suitable 'Aquarium pump'. Placed centrally above the tank were two LED Mitras Lightbar's made by GHL.

In order to replicate tidal/daily light exposure patterns a GHL Profilux 4 aquarium computer was used. A GHL Powerbar was used in tandem with the computer so both the lightbars and the pump could be controlled simultaneously. The computer was setup to replicate North Sea tidal cycles by switching on and off the pump at specific times, it was also designed to simulate the summer season

in regard to light conditions that would be displayed in GMT. The tank was setup in a 'cold room' within the university laboratory, this allowed the temperature to be set and maintained externally.
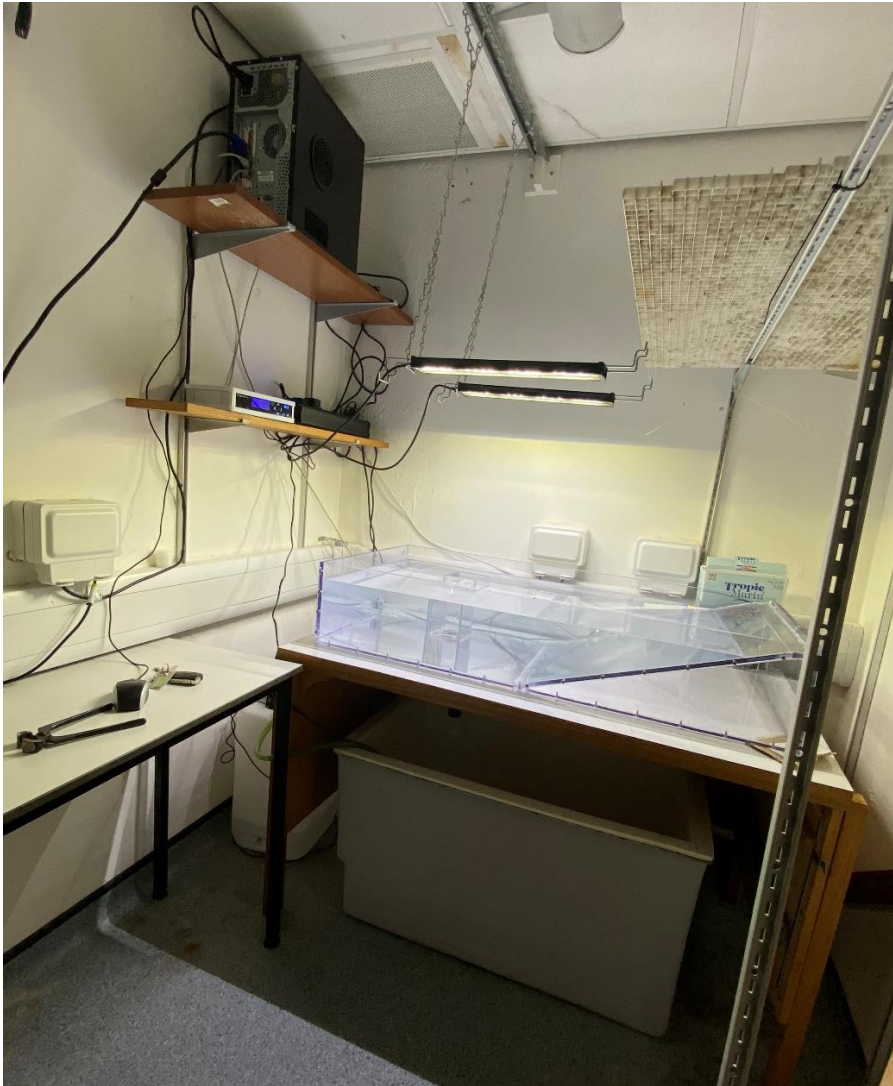
Figure 6. Laboratory cold room/saltwater tank set up.

Cores were taken *in situ* (39.27 cm^3) and the seagrass was separated from the sediment collected and measured. Small plastic stands were filled with sediment and the seagrass was replanted. The stands were heavy enough to stay stable upon filling and draining of the tank and were situated centrally in the tank to remain under direct light from above. The water used in the tank was collected from various areas of the coastal North Sea during the Spring as part of another project at the university. The water was unfiltered so contained similar, or lower, nutrients to that at Spurn. The salinity was regulated to account for changes due to evaporation. Using a conductivity, temperature and depth instrument (CTD) to measure, distilled water was added until the salinity was adjusted to around 20 ppt, which is the average for the Humber estuary (Marshall & Elliott, 1998).

A portable MINI-PAM fluorometer (Walz GmbH, Germany) was used in order to analyse the photosynthetic yield of the seagrass under the following temperatures: 13, 14, 16, 17, 18 and 20°C. The cold room was set to the desired temperature and then monitored from outside using the temperature gauge. The MINI-PAM (Walz GmbH, Germany) was set up against a square piece of blackout cloth in order to negate any background noise from the otherwise white surface of the table. The plants in the experiment were left in the tank partially submerged by the saline water between experiments, they were removed when the temperature had equilibrated, usually around 20 minutes, and then arranged flat on the black cloth with as little overlap as possible between blades. The 'Fibreoptics Holder for Surfaces 2060-A' was used in the experiment in order to log temperature with the fibreoptic cable inserted into a 45° holder, that maintained a close and consistent distance of the PAM measuring beam from the seagrass throughout the experiment. The MINI-PAM (Walz GmbH, Germany) was connected to a laptop using the Wincontrol software (Walz GmbH, Germany), so rapid light curves (RLCs) could be made after a 10 minute period of dark adaptation for each plant. This process was repeated for each temperature stage.

Rapid light curves were established using the seagrass after the room had equilibrated to the desired temperature. The MINI-PAM (Walz GmbH, Germany) produces an RLC by monitoring the fluorescent response of the seagrass material in this study to 12 different actinic light irradiance steps (0-1517 μmol m^{-2} s^{-1}). The steps are separated by a saturating light pulse, from which the PAM software recorded all relevant fluorescence parameters and produce an estimate of the electron transport rate of photosystem II (ETR) (White & Critchley, 1999). ETR was then plotted as a function of the PAR irradiance (μmol m^{-2} s^{-1}) given at each light step. The resulting RLC should show any acclimation to light conditions that the seagrass may possess. It is expected that the curve should show an initial linear rise as the steps increase in irradiance, after which ETR would then reach a maximum rate where photosystem II was light-saturated. There may even be a decline at the very highest light steps, due to the seagrass not being adapted to and therefore being unable to photosynthesise is such strong light (Ralph & Gademann, 2005).

Results

Photosynthetically Active Radiation and Temperature Analysis

An example of the high-resolution recordings obtained by the data logger situated within the seagrass is shown for a full day during the peak of a marine heatwave in July 2022, noting that the day is 6th July where the brick that the logger was attached had not yet been buried below the sediment surface, this particular day was also not a heatwave on land. The time scale was used to

show irradiance and the tide cycle against time and then temperature and tide cycle against time. This would display the impact on both irradiance and temperature that changing tides have on the logger and therefore the seagrass bed. The data (Figure 7**Error! Reference source not found.**a and 7b) give an insight into the time that the seagrass spends either photosynthesising or respiring and allow precise calculation of the duration that the community is exposed to different levels of PAR, and darkness.

An example of high-frequency irradiance and temperature logging in the seagrass bed is shown for 6th July 2022. This day was one of several events during the summer of 2022 in which high air temperatures were recorded over eastern England, giving marine heatwave conditions (Figure 7a and 7b). The data shows three periods of immersion during high tide and two periods of low tide emersion throughout the selected day (low tide at 04:00 and 16:45). Irradiance began to increase at 04:48 as the sun rose over the horizon, and the seagrass bed was exposed to air during low tide. The data presented in Figure 7a shows irradiance increased until a value of 650 µmol m^{-2} s^{-1} at 09:00 at which point a steep decrease to zero irradiance indicated that the incoming tide had submerged the logger. Irradiance remained at zero throughout the first high tide immersion period of the day, then increased sharply at 13:00 as the water column depth became shallow enough for light to reach the sensor. During the subsequent afternoon emersion period, solar irradiance was within the range 500 to 1500 µmol m^{-2} s^{-1}, reflecting alternating periods of clear sky and cloud cover, and reached as high as 2122 µmol m^{-2} s^{-1} at 16:17. PAR values then decreased in the late afternoon and early evening as solar elevation decreased. Fully dark conditions were recorded from 21:00 onwards as the next incoming tide submerged the sensor. Sharp changes in irradiance on the incoming or outgoing tide show the exact point at which the logger (and hence the seagrass bed) is emersed or immersed to be at 4.5 to 5.0 m above chart datum. From Figure 3 using only GIS and an existing digital elevation model from 2021, it was calculated that the seagrass bed is located at an elevation of between 4.8 to 5.0 m above chart datum.
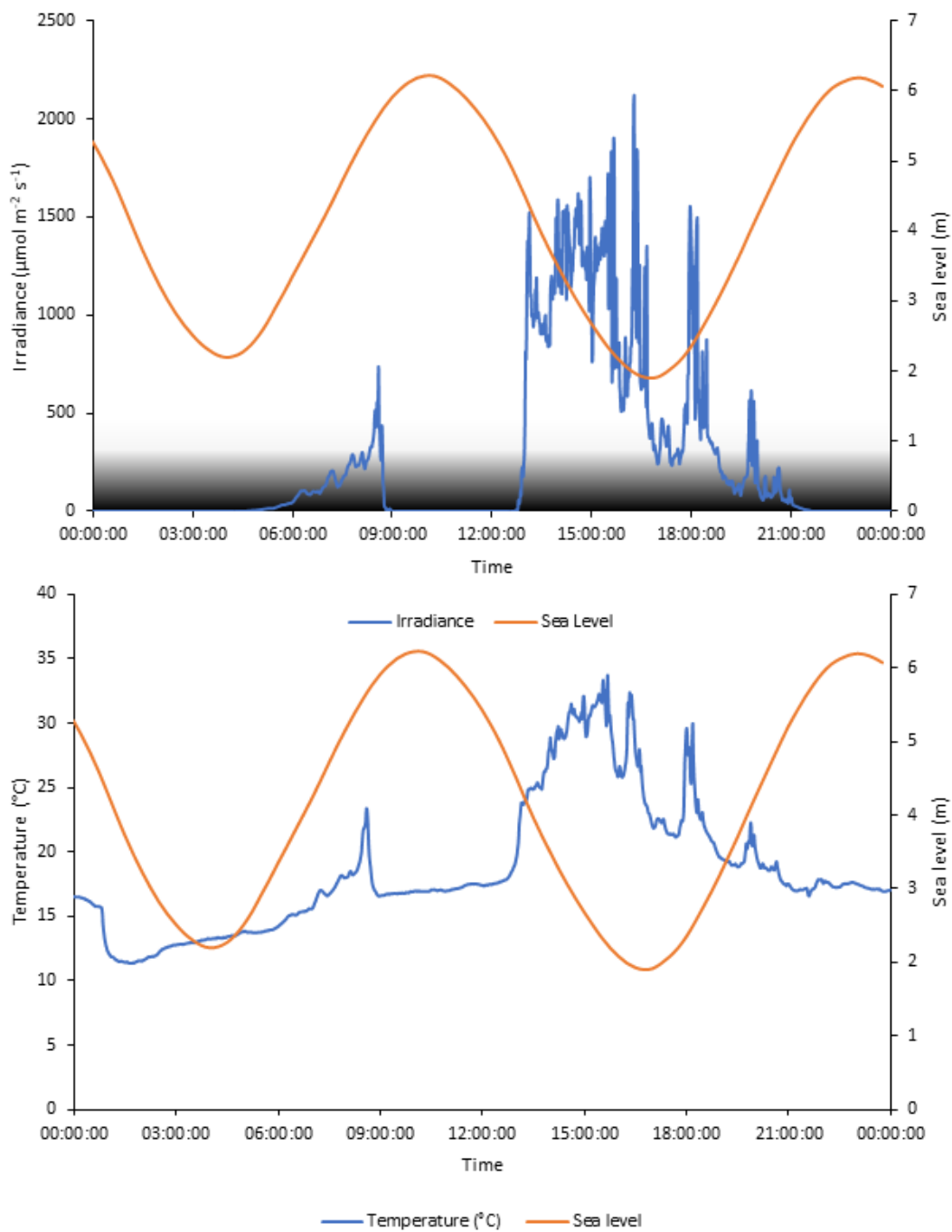
Figure 7a and 7b. An example of high frequency recording of irradiance (7a) and temperature (7b) on the 6th July 2022, in comparison to tidal height data from Immingham. The shading in the graphic reflects the light intensity relative to primary production/respiration, where the darkest shading represents the value of <20 µmol m⁻² s⁻¹ (respiration) and the lighter shading represents ≤300 µmol m⁻² s⁻¹ (half P_{max}).

The tidal maximum recorded by the HOBO loggers was 6.2m. The data in figure 7b showed a temperature decreased sharply as the tide reached a height of 5.5 m on the incoming tide in daylight

e.g. from 23.6 °C at 08:36 to 16.6 °C at 09:00, indicating a transition from warmer air temperatures to cooler estuarine water. An increase in temperature at 12:45 from 17.9 °C to 24.5 °C indicated that the site was again exposed to air. Temperatures increased throughout the afternoon low tide emersion period to a maximum of 33.7 °C at 15:40. Alternating direct sun and cloud conditions increased and decreased the temperature. The incoming evening tide caused a slight reduction in temperature at 20:45. During darkness, a different pattern was observed. A drop in temperature at around 01:00 could be the result of the estuary water being warmer than the early morning air. The tidal cycle, in combination with the high-shore location of the seagrass at Spurn, thus directly controlled both the temperature and the irradiance that the seagrass was exposed to during a 24-hour period in summer. The temperature range measured over the study period reached a maximum on 8th July 2022 at 10:51 am, where the HOBO logger situated amongst the seagrass recorded a temperature of 40.4 °C, and a minimum on 17th September 2022 at 06:21 am where the logger recorded a temperature of 6.22 °C.

A further example of high frequency irradiance and temperature logging in the seagrass bed is shown for the 1st of November 2022. This day gives insight into the shift in temperature and irradiance shown in a winter month (Figure 8a and 8b). As in Figure 8a and 8b, the data shows three periods of immersion at high tide and two periods of emersion during low tide (low tide at 04:45 and 15:00). Due to the change in the time of year the sun did not rise during the first period of emersion and so irradiance remained 0. Irradiance continued at 0 throughout the second period of high tide shown. The second low tide period brought about two irradiance peaks, these were shown as the water on top of the seagrass bed became shallow enough for the irradiance to penetrate through the turbid Humber water e.g. at 14:22 the irradiance was 14.36 μmol m^{-2} s^{-1}. Then again when complete emersion occurred and the bed was exposed to a cloudy mid-afternoon winter day, showing a range of 19-31.51 μmol m^{-2} s^{-1}. The seagrass bed logger only recorded a total of 11 minutes where irradiance was >20 μmol m^{-2} s^{-1}, therefore according to our calculated assumptions on photosynthetic rate (see later section), only 11 minutes were spent photosynthesising at a rate of half P$_{max}$. Irradiance then began to decline as the solar elevation decreased in the late afternoon, reflecting the earlier setting time of the winter sun, until it reached 0 at 16:50.
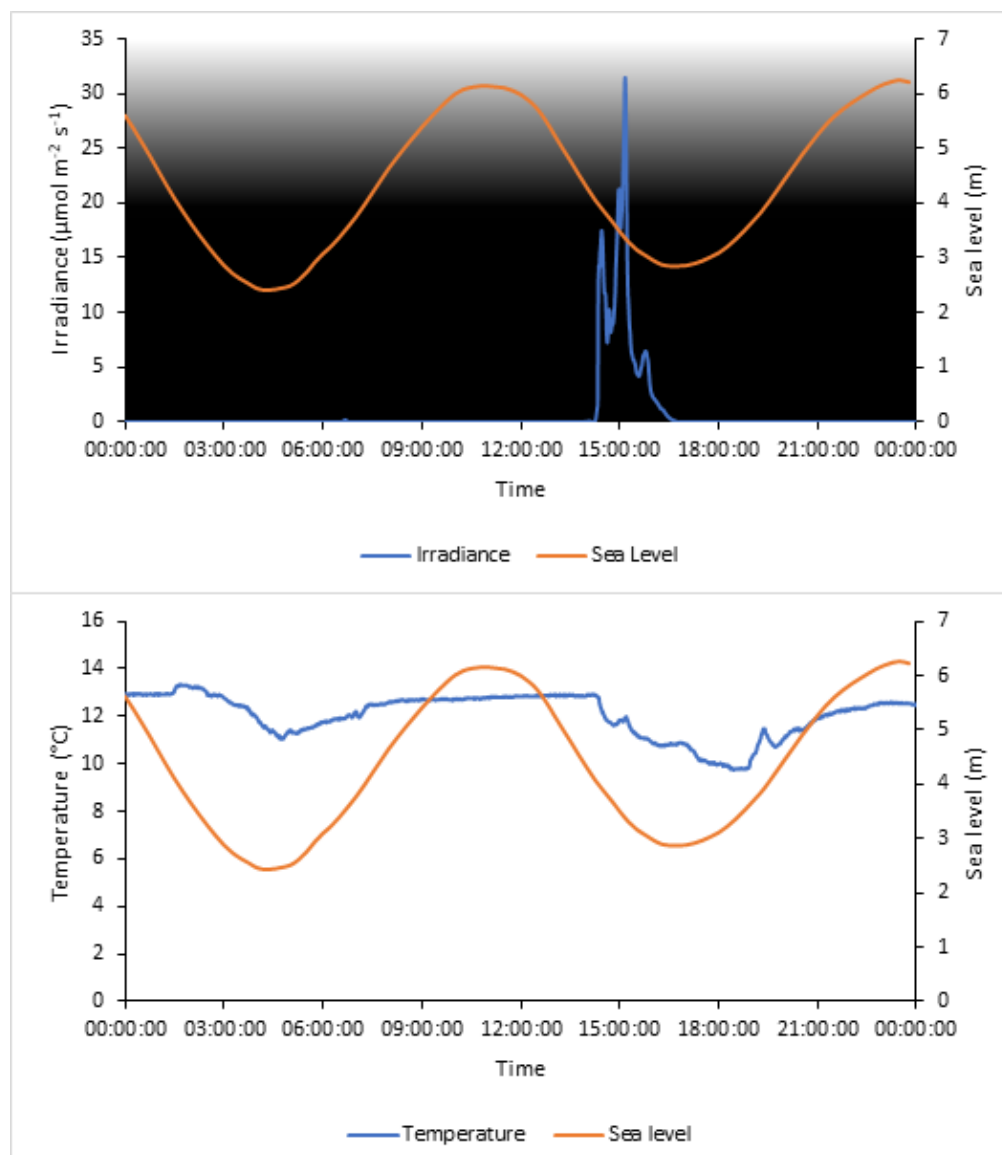
Figure 8a and 8b. An example of high frequency recording of irradiance (8a) and temperature (8b) on the 1st November 2022, in comparison to tidal height data from Immingham. The shading in the graphic reflects the light intensity relative to primary production/respiration, where the darkest shading represents the value of <20 μmol m⁻² s⁻¹ (respiration) and the lighter shading represents ≤300 μmol m⁻² s⁻¹ (half P_max).

Temperature was much more consistent during the 1st of November 2022. Tidal immersion/emersion had the opposite effect compared to the data shown in Figure 7a and 7b. Where tide dropped below a height of 5.5 m temperature decreased gradually on both instances of a retreating tide, e.g. from 12.4 °C at 03:35 to 11.41 °C at 04:20. Then immersion occurred on an incoming tide and increased and stabilised the seagrass bed temperature, maintaining the temperature within a range of 12.7 and 12.87 °C. This indicated that upon emersion the winter air is colder than the more stable temperature of the estuarine water. The data shown in figures 7a, 7b

and 8a,8b show how the conditions experienced by the seagrass bed alters depending on the time of year. Figures 7a and 7b show the conditions experienced within the growth season, in contrast, figures 8a and 8b show the conditions experienced at the end of the growth season where *Zostera noltei* begins to shed its blades.

The average temperature experienced in the months of study show are shown below, the trend shows a gradual decline in temperature as the season changes to autumn and winter.
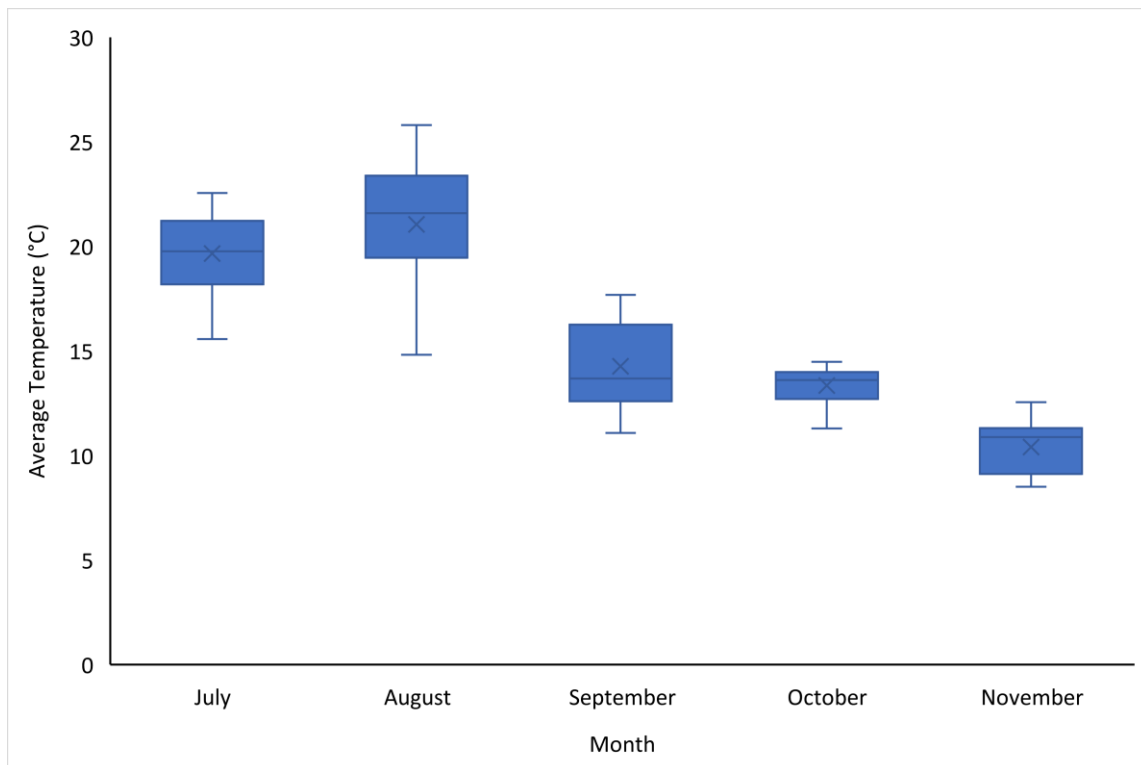
Figure 9. Daily average temperatures shown as a box-whisker plot for the 5 months of recorded data.

The boxes show the 25th/75th percentile with the solid line representing the median, the whiskers represent the above and below bounds to 1.5* the Interquartile Range. The data in Figure 9 shows August as the warmest month of the year and November as the coldest which is to be expected.

Humber Estuary Nutrient Analysis

The ammonium and nitrate levels found within the Humber estuary are of interest when investigating the overall health and recovery ability of the seagrass at Spurn Point, as ammonium and nitrates in high concentrations may have a negative impact on *Zostera noltei* (Van Katwijk et al., 1997)

Table 1. *Monthly ammonium and nitrate concentrations in the River Humber over the course of the research period in 2022, Environment Agency. (2022), Sampling point ID 'AN-CONT29' referred to as 'Sunk Island'.*

Determinand	Jan	Feb	Mar	Apr	May	Jun	Jul	Aug	Sept	Oct	Nov
Ammoniacal Nitrogen, NH3-N (mg l^{-1})	<0.007	0.013	0.03	<0.02	<0.02	<0.02	<0.02	0.02	<0.02	0.021	<0.02
Nitrate, NO3 (mg l^{-1})	1.1	0.797	1.39	1.3	1.3	0.993	0.685	0.613	0.711	0.852	1.99

The data in Table 1 shows the estuarine ammonium and nitrate concentrations that were found in the River Humber, at the closest recording station to the seagrass at Spurn. The data demonstrates relatively low levels of both nutrients, consistent with levels found in the North Sea (Thewes et al., 2022). This suggests that the water around this station is typically well mixed with the open sea, the average salinity for the Humber Estuary is 20.2 ppt (Marshall & Elliott, 1998) and values for salinity from the same buoy station being between 23.2-31.9 ppt which also supports this suggestion. The historic data that the Environment Agency publish from this station since 2008 showed the ammoniacal nitrogen concentrations varied within a narrow range of <0.007 to 0.03 mg l^{-1}. Occasional higher values were recorded at this station e.g. on the 3rd February 2010, at 0.105 mg l^{-1} and on the 6th June 2019 at 0.149 mg l^{-1}.

Short-term Gas Exchange Measurements

Other than the first enclosure experiment at a site with 0% seagrass coverage, which showed an increase in CO_2 by 15 ppm, all other experiments showed an initial drop in CO_2 after the first 5 minute interval whilst exposed to light (Figure 10). The largest decrease of 57 ppm was recorded at a site with 30% seagrass coverage. All experiments showed a drop in CO_2 for the remaining time intervals throughout their respective incubation periods whilst exposed to ambient light. The lowest final concentration of CO_2 after the illuminated period was 220 ppm and occurred in the 30% coverage dome, resulting in a total reduction in CO_2 concentration of 212 ppm after the first 15 minutes. During the following 15 minute dark period of the experiment, both the dome with 39%

coverage and the first experiment at 0% showed an increase in CO_2 of 2 ppm and 1 ppm respectively, whereas the other experiments showed a continued decline with 65 ppm being the largest decline during darkness shown by the 75% coverage experiment (Figure 10).
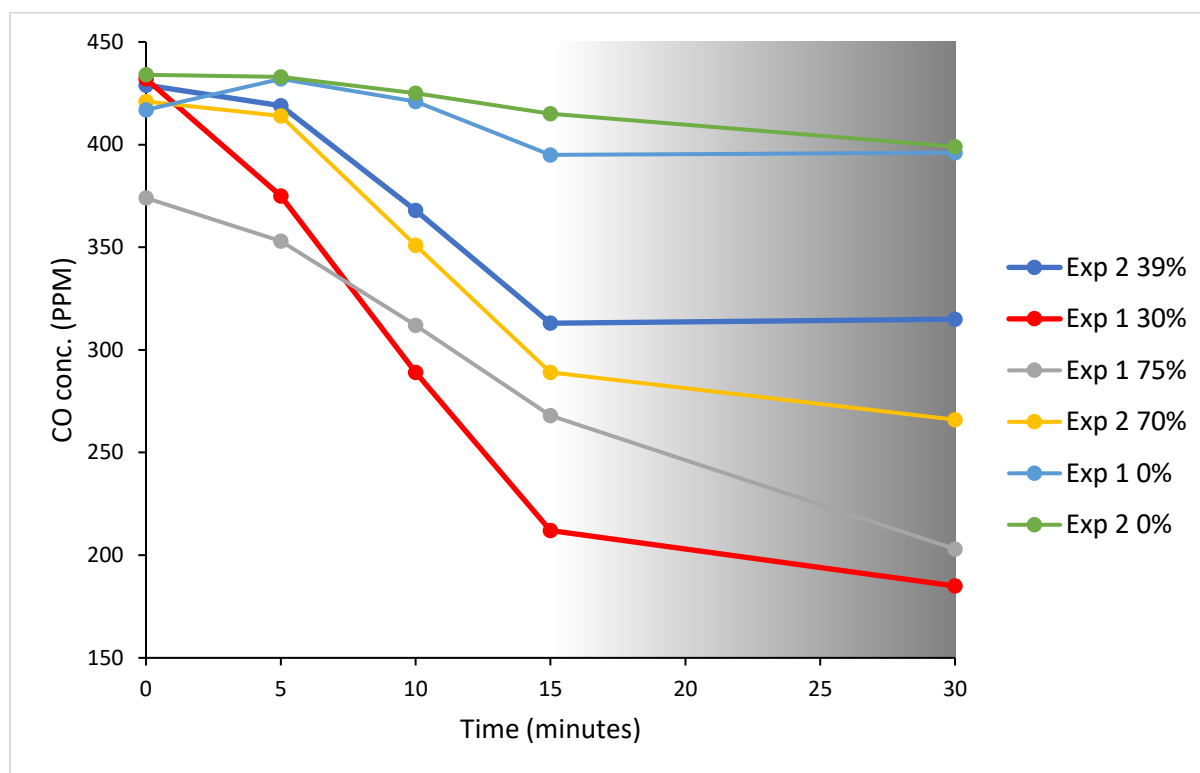
Figure 10. Change in CO_2 concentration within the isolated environment of a hemispherical transparent dome over a total period of 30 minutes. The first 0 to 15 minutes were illuminated by ambient solar light and the following 15 minutes shaded to darkness, illustrated in the graphic by shading from 15-30 minutes. Experiment 1 and 2 were carried out on 13/09/2022 and 16/09/2022. The percentage cover of Zostera noltei for each enclosure experiment is described in the legend.

The results from the enclosure experiments were then analysed in terms of photosynthetic rate (and dark respiratory rate) in units of mg C m^{-2} h^{-1} against both irradiance and temperature (Figure 11 and Figure 12). To best display the results the 5 minute intervals of daylight-exposed experiments and the 15 minute dark-covered interval have been collected and grouped within their respective seagrass densities, of which there were three groups: 0%, 50% and 100%. The three groups were derived from the original experimental design, where each of the two experiments were selected in the field by eye to fall under one of the three categories, they were later analysed using the Image J software and the true percentage cover of *Z. noltei* was calculated and can be seen in Figure 10. Consequently, they are once again categorised into their respective groups to allow ease of analysis. The recording after the first 5 minutes has been removed from each experiment to mitigate any

delay that the infra-red gas monitor experienced when responding to initial changes in CO_2 after enclosure.
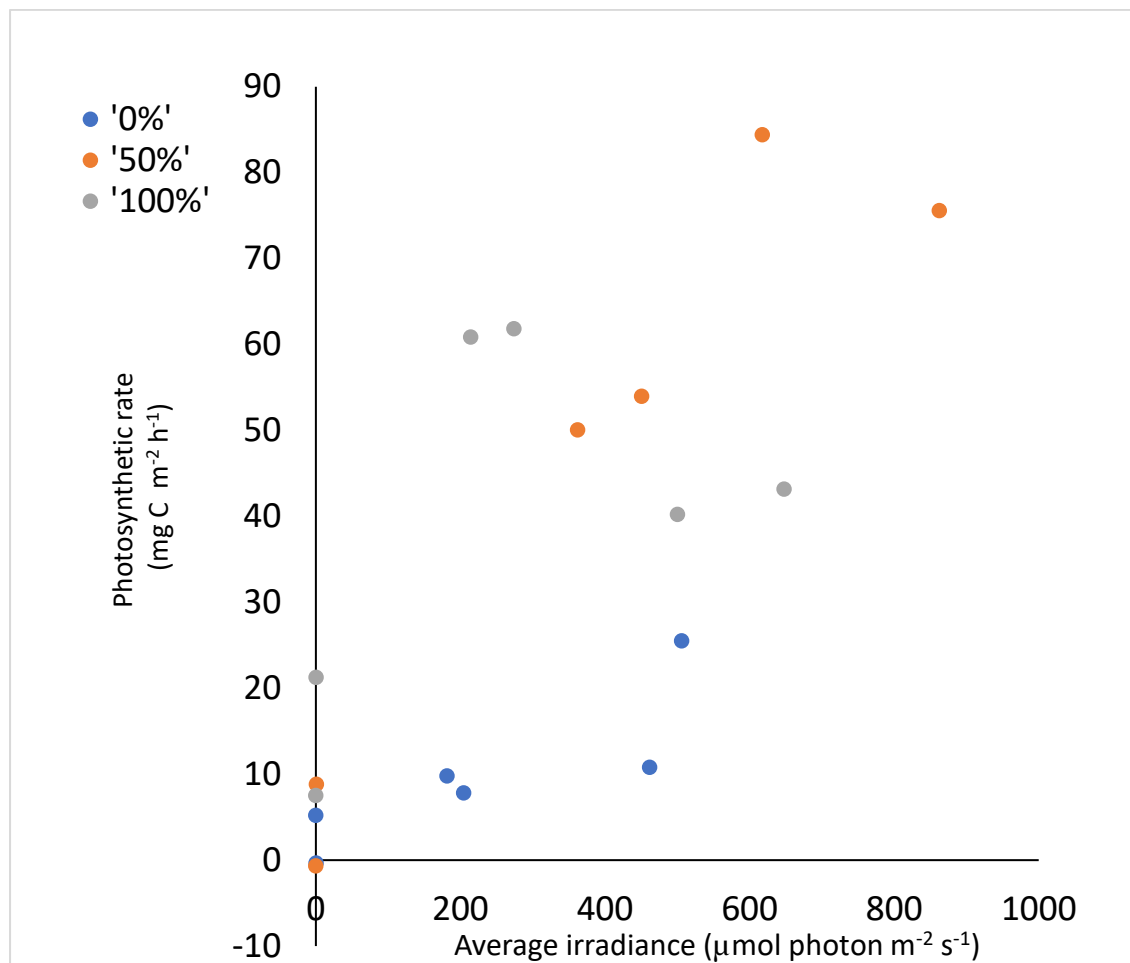
Figure 11.Photosynthesis versus irradiance response experiments at: '0', '50' and '100'% coverage of Zostera noltei showing photosynthetic CO₂ uptake in relation to mean irradiance during discrete 5 min periods.

The scatter of the data in the irradiance plot varied considerably, thus not allowing statistical analysis of the photosynthesis-irradiance relationship, but showed a general pattern from which key values could be taken forward for initial modelling. The points categorised as 0% seagrass cover (e.g. 'bare' sediment) showed low photosynthetic rates in the range of 8 to 26 mg C m^{-2} h^{-1}. A slight, and gradual, increase in photosynthetic rate could be seen as irradiance increased for this group. This suggested the presence of other autotrophs not visible to the naked eye that are also contributing to photosynthetic activity. The data categorised as '50% seagrass cover' displayed a strong photosynthetic response to increasing irradiance, with much higher rates of carbon fixation than the bare sediment. Photosynthetic rate increased linearly with irradiance, with the highest rate of photosynthesis being 84 mg C m^{-2} h^{-1} at an irradiance of 617 µmol m^{-2} s^{-1}. At the highest irradiance, of 862 µmol m^{-2} s^{-1} a slightly lower photosynthetic rate was recorded. Within the category of '100%

seagrass cover' photosynthetic rates in the light appeared lower than those at '50% cover', with the highest photosynthetic rate value being 62 mg C m^{-2} h^{-1}. Light saturation of photosynthesis occurred at a lower irradiance (274 µmol m^{-2} s^{-1}) than for the '50%' category (peak from 600 to 800 µmol m^{-2} s^{1}). An increase in the concentration of CO_2 due to respiration of the seagrass community in darkness was to be expected, but it can be seen that low, positive rates of carbon fixation were recorded in darkness for four out of six experiments after 15-minute incubation periods.

As in Figure 11, the site-specific percentage covers of seagrass were collated into the three generalised groups for analysis. The photosynthetic rate (mg C m^{-2} h^{-1}) was once again displayed as the dependent variable, with temperature as the independent variable in Figure 12. The figure contains two periods of incubation at each of the three percentage cover groups, with the first 5 minute interval removed to allow for the delay in the monitor as described previously. The other intervals at 10 and 15 minutes are included as well as the 15-minute period of darkness.
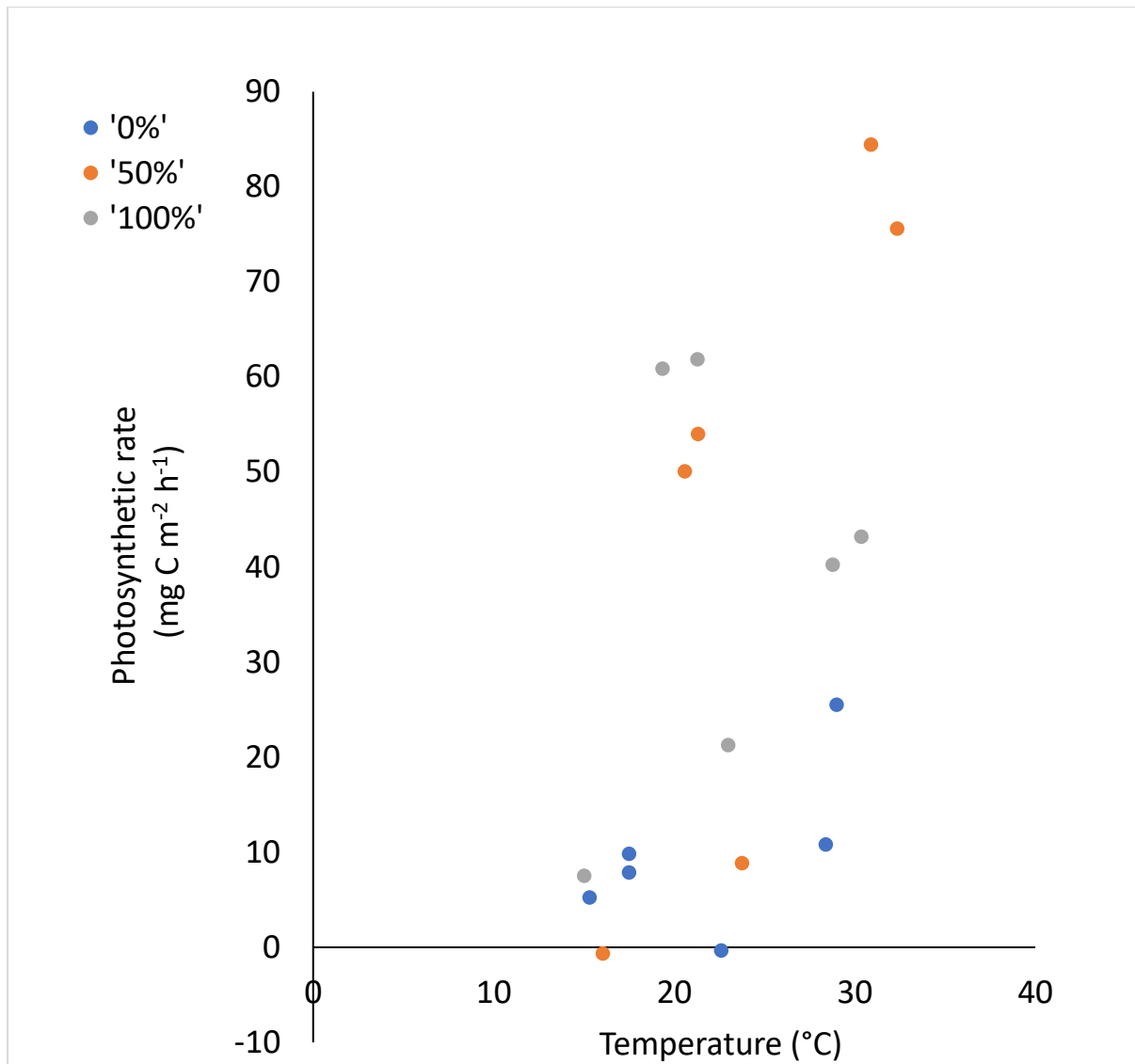
Figure 12. Results of two incubation periods of the bell jar experiments at: '0', '50' and '100'% coverage of Zostera noltei with respect to mean temperature during the incubation. As in the previous figure the data shows the 5 minute intervals of each experiment.

Again, the scatter of the results appeared quite varied, but showed a clear trend between increasing temperature and increasing photosynthetic rate, modified by the density of seagrass. The points at '0%' seagrass cover (bare sediment) with the exception of one point at around 22°C, all experienced slight positive photosynthetic rates and displayed a linear relationship with increasing temperature. This relationship was replicated within the '50%' group of percentage cover, with the only exception being one of the two data points recorded in darkness, which would be expected to show a negative photosynthetic rate. The results for the recordings at '100%' are interesting as they suggest that slightly lower temperatures are more optimal to produce a higher photosynthetic rate, with

temperatures of around 20°C producing rates of around 60 mg C m^{-2} h^{-1}, whilst at a temperature of around 30°C rates of between 40-50 mg C m^{-2} h^{-1} were recorded.

Estimation of daily net carbon fixation rates: method (1) from short-term gas exchange experiments

Over the study period, the seagrass bed experienced changing ambient conditions, including temperature and irradiance. It is appropriate to investigate the calculated integrated daily primary production (NPP) over the months of study to understand in more depth the productive capacity of the *Zostera noltei* throughout different seasons. This was done by allocation of photosynthetic and respiratory rates derived from the short-term measurements to each hour of each day for the period July to November.
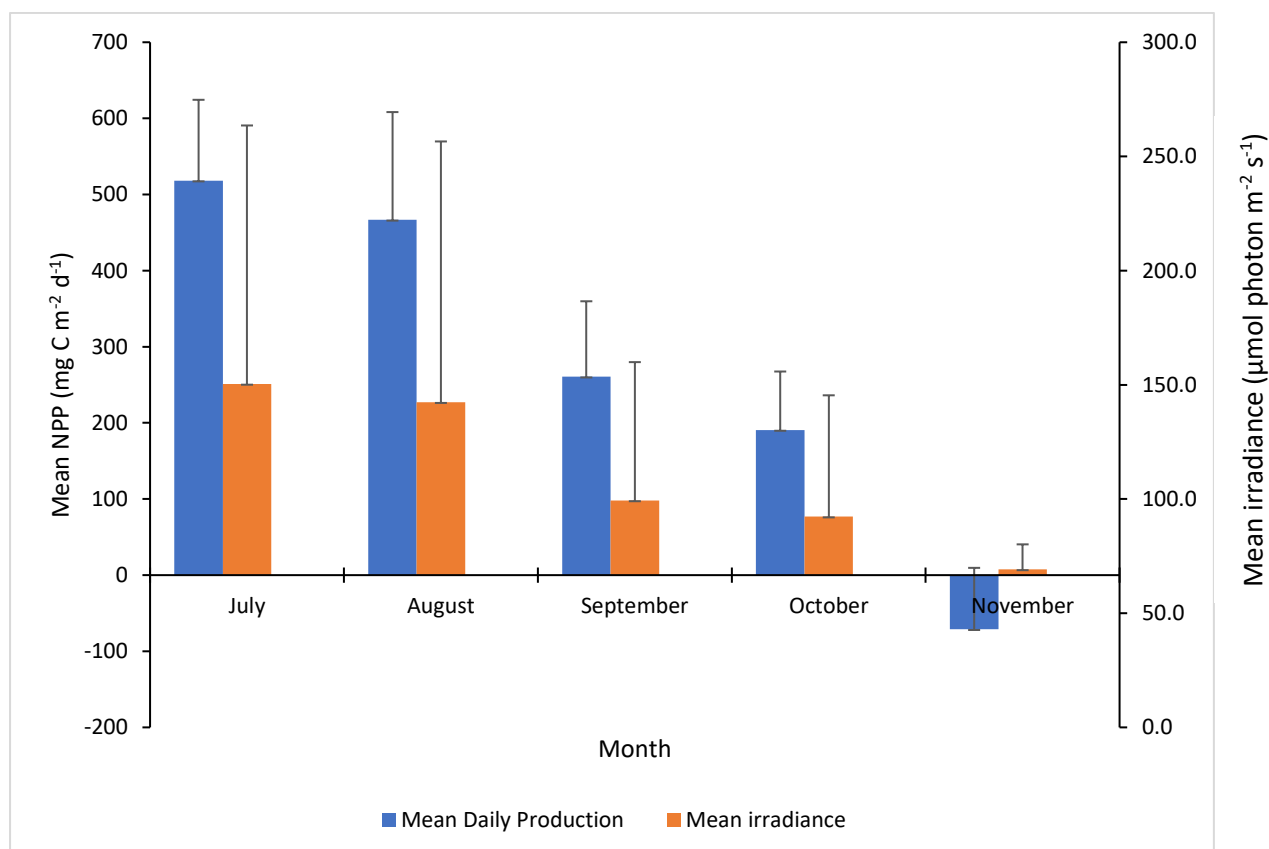
Figure 13. Changes in the mean daily NPP and mean irradiance, over the 5 month study period from July to November 2022 with standard deviations shown.

Carbon storage was variable between months (F=121.3, p<0.01). In estimating the carbon storage/release of *Zostera noltei* over the 5-month period of light data it was found that July was the month with the highest average daily NPP (Figure 13**Error! Reference source not found.**, Table 4), with a mean daily rate of 520 mg C m^{-2} d^{-1} stored. This was then followed by a slightly lower value of

466 mg C m^{-2} d^{-1} in August and a steep decrease in September to 260 mg C m^{-2} d^{-1}, and a further decrease to 190 mg C m^{-2} d^{-1} in October. Within-month variability in daily NPP was high, as shown by the standard deviations, with the irradiance received by the seagrass bed varying with changing cloud cover and tidal timing.

Positive NPP was calculated for the period of four months from July to October, with values showing a decreasing trend from the summer maximum. In November, at which point photosynthetic carbon uptake during the increasingly short irradiance periods was insufficient to offset dark respiration, it was estimated that a net daily carbon release of 71 mg C m^{-2} d^{-1} occurred due to the respiration of the seagrass becoming greater than photosynthesis as the season changed into autumn and winter.

The within-month distribution of net daily primary production thus calculated is shown in Figure 14
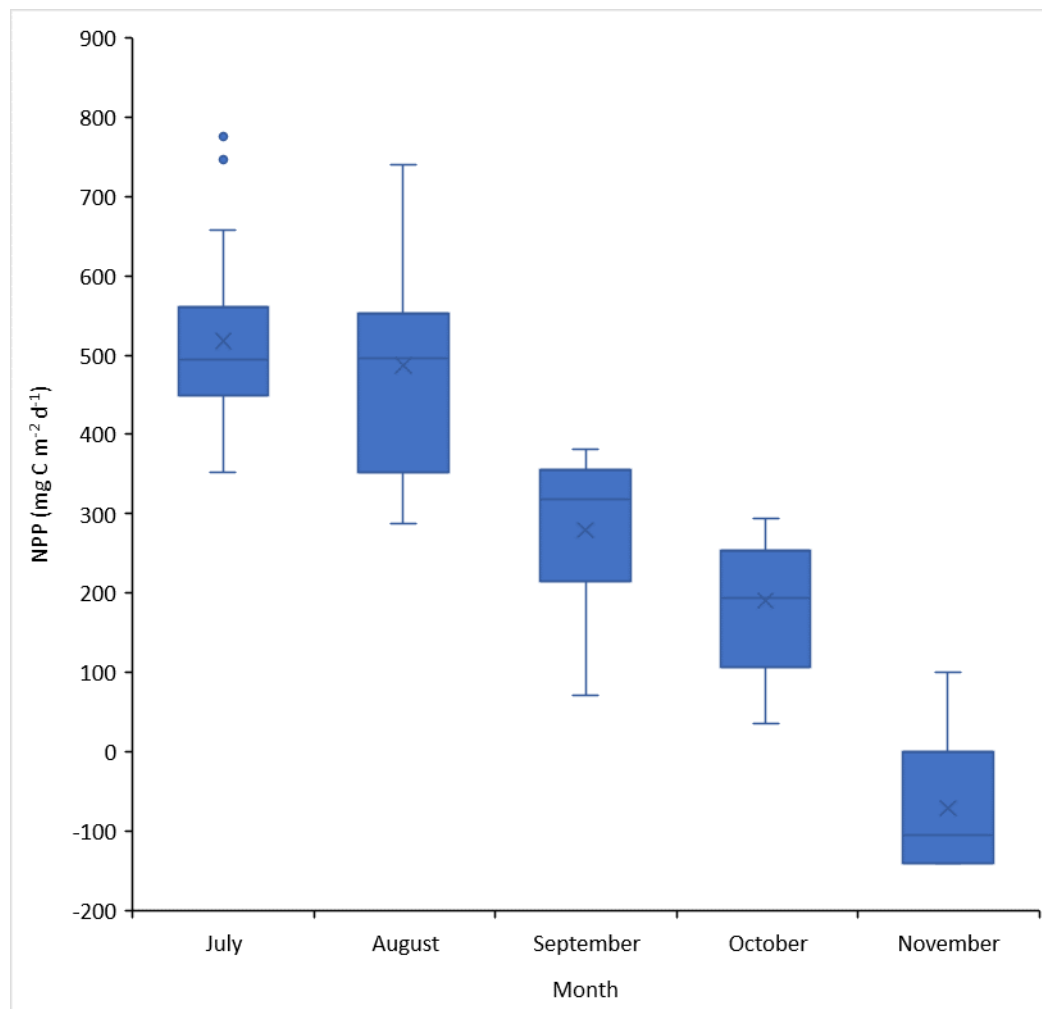
Figure 14. The distribution of the daily net primary production of Zostera noltei over a 5 month study period.

The boxes show the 25th/75th percentile with the solid line representing the median, the whiskers represent the above and below bounds to 1.5* the Interquartile Range. The solid dots seen in the month of July show the outliers in the data set.

Two months of relatively high productivity occurred in July and August, with very similar upper quartiles both showing NPPs predominantly over 500 mg C m^{-2} d^{-1}. Whilst they both are noticeably productive months, the spread of the interquartile range in August (199.9) is much larger than in July (111.7), suggesting that the weather conditions in August were beginning to become less consistent with typical Summer conditions, for example the lowest value calculated in August was 288.1 mg C m^{-2} d^{-1} in comparison to July which had a lowest value at 352.8 mg C m^{-2} d^{-1}. In July two outliers of 776.2 and 746.8 mg C m^{-2} d^{-1} were calculated, likely representing the two examples of the marine heatwaves that occurred in July, with high temperatures and irradiances.

In September and October, a steep decline in NPP was calculated. As shown in Figure 14 the spread of the interquartile range, 141.1 and 147.0 mg C m^{-2} d^{-1} respectively, was relatively low. This suggests that the days throughout September and October, whilst having much lower light intensities and shorter day lengths, were quite consistent. This is to be expected as Summer becomes Autumn and the daylight hours decreased, alongside the solar intensity. There were no cloud-free heatwave events of the type measured in July, again further reducing the available light for photosynthesis. In November a further decrease in NPP can be seen, where the entire interquartile range was negative. The spread of the interquartile range was low at 138.6 mg C m^{-2} d^{-1} showing that during this month the light intensities were consistently too low to sustain photosynthesis and allowed for respiration to be the primary state. There is no whisker below the box for November which suggests that the lower quartile encapsulated the minimum bounds from the data. Daily daylight hours were significantly reduced, with the average irradiance of November being 7.5 µmol m^{-2} s^{-1}, a decline of just over 243 µmol m^{-2} s^{-1} compared to the average irradiance of July which was 251 µmol m^{-2} s^{-1}. The highest irradiance value recorded in November was 874.95 µmol m^{-2} s^{-1} compared to 2122.28 µmol m^{-2} s^{-1} in July. As a direct result, the ability of *Zostera noltei* to photosynthesise also declined.

A Turkey (HSD) statistical test was done to analyse if there was any significant differences in NPP between the tested months. The test represents differences with a confidence interval of 95%.

Table 2. Turkey (HSD) Analysis of differences between monthly categories of NPP .

Contrast	Difference	Standardized difference	Critical value	Pr > Diff	Significant
July vs November	589.330	19.514	2.784	**<0.0001**	Yes
July vs October	327.644	10.239	2.784	**<0.0001**	Yes
July vs September	238.980	6.853	2.784	**<0.0001**	Yes
July vs August	30.975	0.924	2.784	0.887	No
August vs November	558.355	17.117	2.784	**<0.0001**	Yes
August vs October	296.669	8.651	2.784	**<0.0001**	Yes
August vs September	208.005	5.624	2.784	**<0.0001**	Yes
September vs November	350.350	10.308	2.784	**<0.0001**	Yes
September vs October	88.664	2.491	2.784	0.102	No
October vs November	261.686	8.432	2.784	**<0.0001**	Yes
Turkey's d critical value:			3.938		

Table 3.The outcome of the Turkey (HSD) analysis of difference with relative groups marking difference.

Category	LS means	Standard error	Lower bound (95%)	Upper bound (95%)	Groups		
July	518.280	22.055	474.458	562.102	A		
August	487.305	25.267	437.100	537.510	A		
September	279.300	27.012	225.629	332.971		B	
October	190.636	23.187	144.565	236.707		B	
November	-71.050	20.630	-112.042	-30.058			C

From the statistical test it is clear that with the exception of 'July vs August' and 'September vs October' every month was significantly different in regard to calculated NPP. There is less than 5% probability that these differences are due to chance shown by p values of <0.0001.

The monthly totals of carbon fixed were similar in July and August at 14.0 and 15.5 gC m^{-2}, decreasing to 7.8 and 5.7 gC m^{-2} in September and October, and becoming negative in November. Thus, a total of 41 gC for each metre of seagrass >30% can be estimated for the July-November period.

Table 4 Summary of potential daily and monthly NPP values for seagrass quadrats with percentage cover higher than 30%.

Month	Mean Daily Production (mg C m^{-2} d^{-1})	Standard deviation	Mean 24 h irradiance (µmol m^{-2} s^{-1})	Standard deviation	Sum monthly production (gC m^{-2})
July	518.3	±106.1	251.2	±339.5	15.5
August	466.7	±141.5	227.2	±342.5	14.0
September	260.7	±99.1	98.1	±181.7	7.8
October	190.6	±76.8	74.4	±159.39	5.7
November	-71.1	±80.6	7.5	±32.9	-2.1
			Total PP (gC m^{-2})		41.0

Assuming that seagrass blades emerge in April, reach half their maximum density in May, and have peak coverage extending from June to September (see following section), then annual carbon fixation extrapolated from the short-term incubations can be estimated as a total of 57.5 gC m^{-2} (Table 3).

Table 5. Monthly primary production rates according to blade density.

Month	PP
January	-2.1
February	-2.1
March	-2.1
April	2.0
May	7.5
June	15.5
July	15.5
August	14.0
September	7.8
October	5.7
November	-2.1
December	-2.1

Total PP (gC   57.5
    m^{-2})

Estimation of daily net carbon fixation rates: method (2) from Seasonal Growth Analysis

Throughout the 6-month period of the study, 9 visits took place from early April until the middle of September. The general trend of the replicated quadrats appears to be an increase in percentage cover up until the eighth recording at 127 days in mid-August, which was then followed with a decline at most quadrats upon the last recording at 159 days in mid-September (Figure 15 for individual plots; Figure 16 for mean values). The largest percentage increase occurred at quadrat 4 which showed an increase to 89% from its original percentage cover of 22%. It is noted that due to the nature of the environment other factors play a role in the seagrass cover that the image analysis software detects, this may be as a result of high sediment load, macroalgae placement within the quadrat, poor image quality or water pools within the quadrat that were incorrectly classified as seagrass.
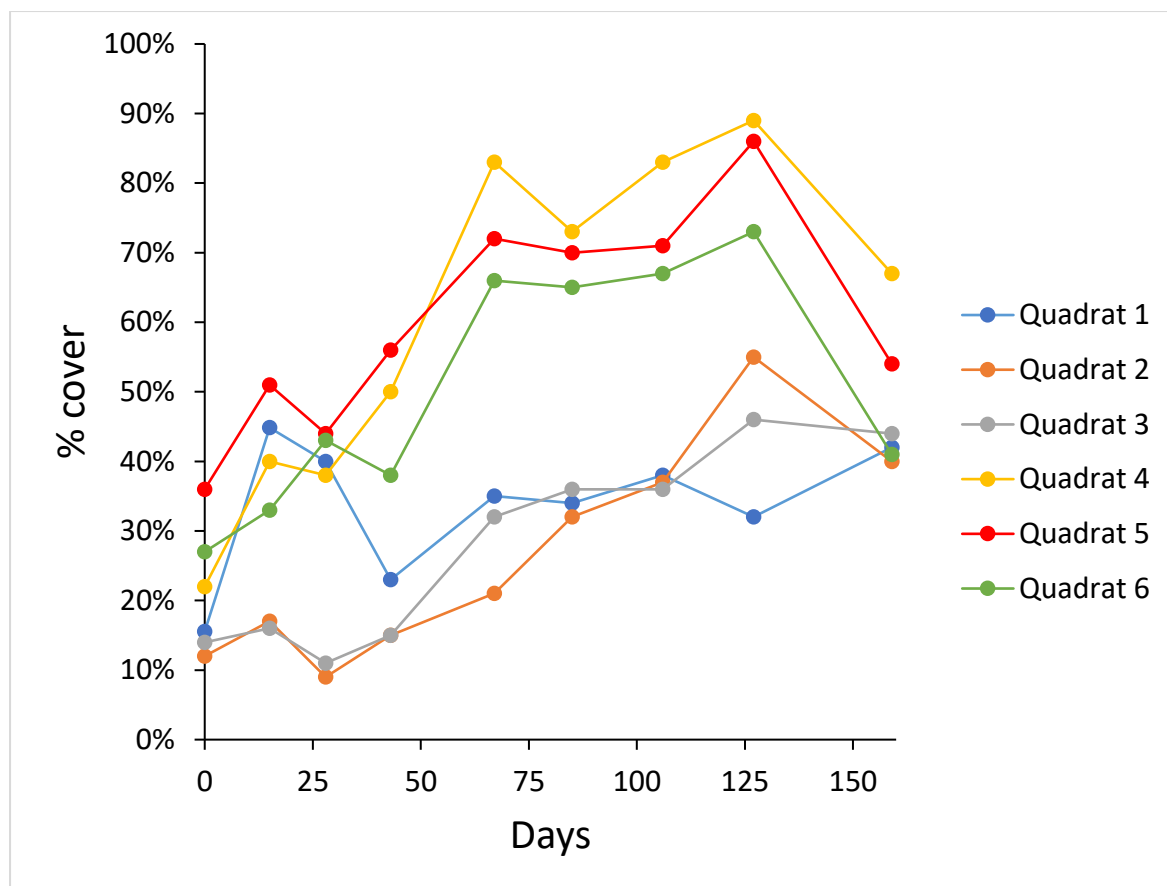
Figure 15. The progression of growth/die off of Zostera noltei at 6 selected locations at Spurn Head described as percentage cover over an 159 day period from 07/04/2022-13/09/2022. The time series at each station are exact replicates in terms of location due to the sampling design.

The results showed an initial increase from the first data point to 15 days, where 'Quadrat 1' recorded its maximum for the entire study period. Each quadrat showed a decline in the percentage cover of *Zostera noltei* after 28 days. This was noted during fieldwork as a high sediment load across the seagrass bed region, thus burying much of the seagrass, and therefore causing an apparent loss of density in the time series. The percentage cover then recovered in the following visits, continually increasing until day 127 where every quadrat with the exception of 'Quadrat 1' reached the maximum for the study period/ growth season. 'Quadrat 1' was the only quadrat to reach day 159 with an increase in percentage cover from the previous visit, the other quadrats all saw losses. This suggests that if the quadrats are representative of the bed as a whole, the end of the growth season was captured during the study period with a peak in percentage cover in July-August followed by a substantial loss (Figure 16).
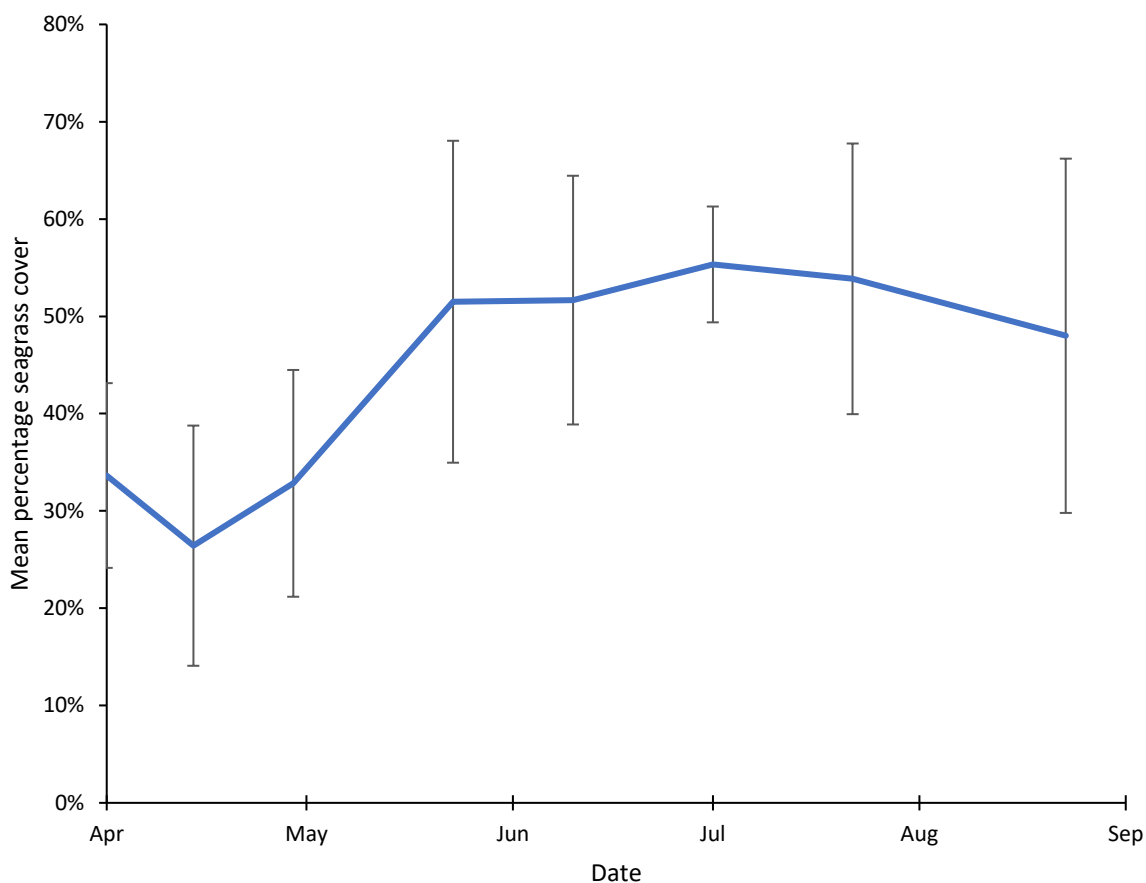
Figure 16. Mean monthly percentage seagrass cover with upper and lower limits of the 95% confidence interval.

The differences between months were found to be significant (F=7.98, p<0.01), Table 6)

Table 6 Analysis of variance for peracntage cover at 6 independent quadrats over the seven study months.

Source	DF	Sum of squares	Mean squares	F	Pr > F	p-values signification codes
1	5.000	1.077	0.215	7.977	**<0.0001**	***

Monthly variations in surface cover versus carbon storage or loss, for each quadrat location are displayed in Figure 17. For the aggregated mean values at each quadrat, the upper and lower limits of the 95% confidence interval are also displayed (Figure 18).
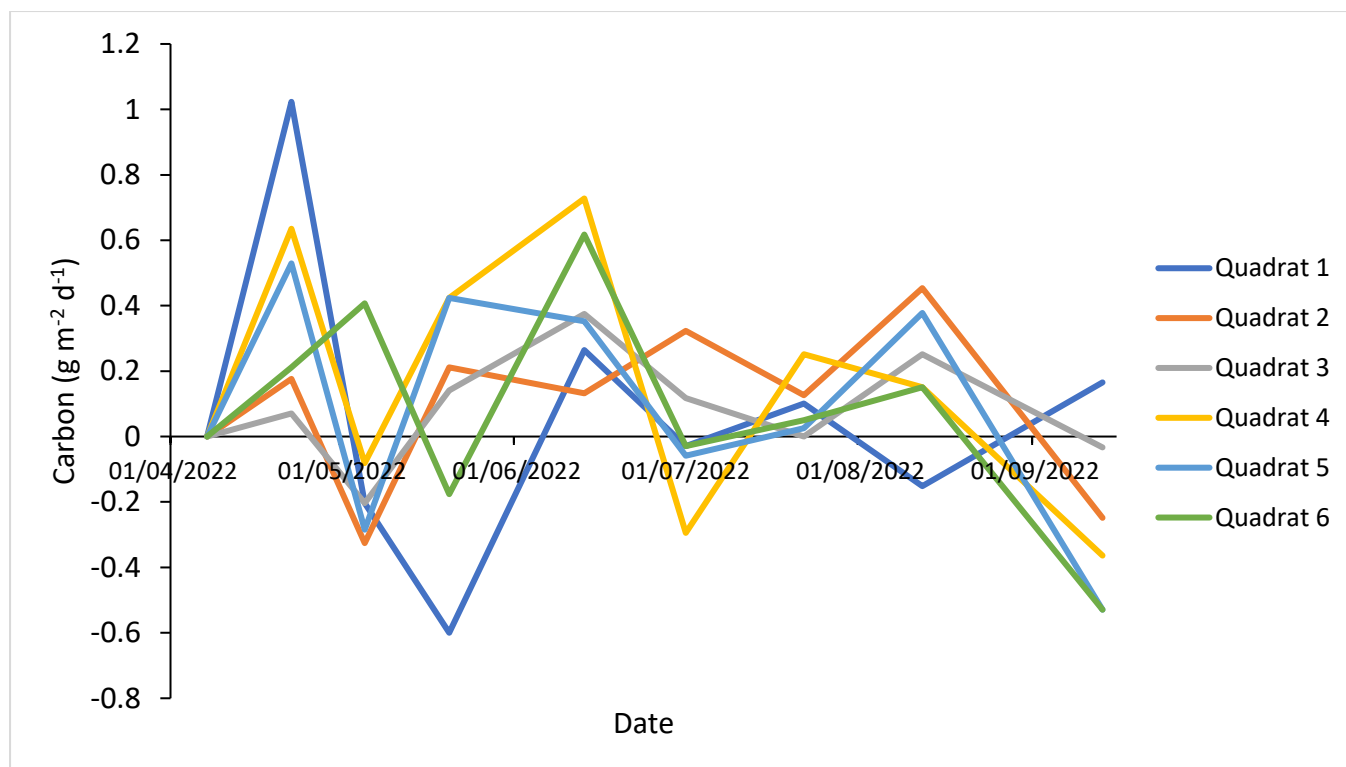
Figure 17. Between-month variations in Zostera noltei carbon gain or loss, shown at 6 quadrat stations over the study period.

Between April and May in the study period all quadrats showed a positive storage of carbon, Quadrat 1 had the largest storage of just higher than 1 g C m^{-2} d^{-1}. In May, all quadrats with the exception of 'Quadrat 6' showed a loss in carbon, as described previously in Figure 15 this was due to a high sediment load. Progressing further into May and June the net storage/release of carbon became more varied, with Quadrats 1 and 6 showing a loss later in May, however Quadrats 2, 3, 4 and 5 showed positive storage. In June, all quadrats showed a positive storage of carbon as would be expected, reaching the height of Summer and the *Zostera noltei* growth season. In early July Quadrats 4,5 and 6 showed slight losses in carbon, whilst the others maintained a positive gain. During late July all Quadrats with the exception of Quadrat 3, which showed neutral loss or gain, showed slight positive gains. In August only Quadrat 1 showed a slight loss where the other Quadrats showed positive gains. From here a noticeable decline occurs for the majority of quadrats as the end of the growth season is reached in September, other than Quadrat 1 which did not follow the trend of the others.

It is important to understand the total storage/loss of the bed as a whole. The mean data from the 6 quadrat locations enabled this to be understood. A mean of the net storage/loss across all the quadrats at each site visit was created to show this seasonal variation (Table 7).
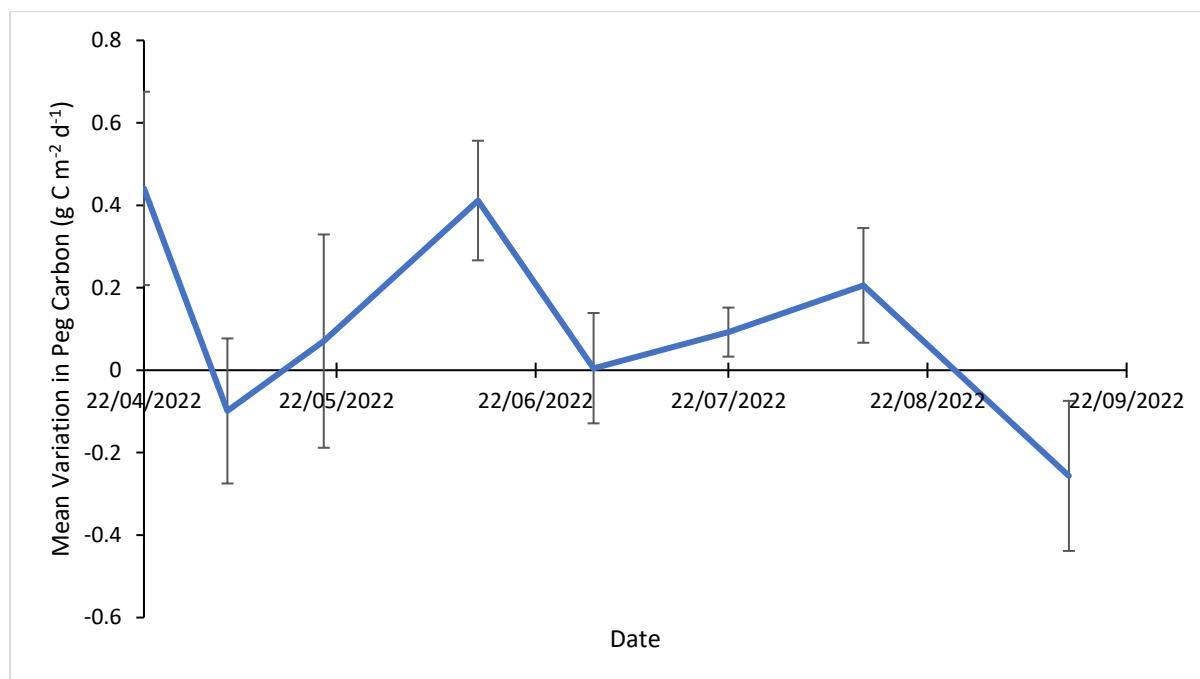
Figure 18. The mean variation of Zostera noltei Carbon storage or loss from the 6 quadrat locations at Spurn over the 6 month study period, with the upper and lower limits of the 95% confidence interval.

The above figure illustrates the variation of carbon storage and release over the time of the study. It contains the variation of the data collected through 9 site visits alongside the upper limits of the 95% confidence interval. From an initial 0.4 gC m^{-2} d^{-1}, a steep decline occurred across all quadrats showing a 0.1 gC m^{-2} d^{-1} loss in early May. As previously described, this is suggested to be due to a high sediment load which temporarily buried the seagrass. The trend shows an increase to a positive accumulation of carbon through the months of May and June, reaching the maximum for the year on the 13th June at 0.412 gC m^{-2} d^{-1}. The storage rate became 0 in the middle of June, followed by a steady positive storage through July and August to a peak of 0.206 gC m^{-2} d^{-1}. The final month displayed a strong loss of carbon of up to 0.256 gC m^{-2} d^{-1}. This is the end of the growth season where the seagrass begins to shed its blades and so heavy losses of carbon are to be expected.

This analysis of the variation of carbon throughout the study period enabled two values to be calculated for the Net Primary Production of a square meter of *Zostera noltei* throughout the study period/growth season. A sum of the total carbon differences between each quadrat throughout the 8 site visits provides us with a gain of 14.4g C m^{-2} in 159 days (Table 7). This contains the final visit in September where high loss rate of surface carbon had occurred. The inclusion of those values does not necessarily represent the carbon storage/losses during the growth season of the seagrass as we are unable to determine where exactly the 'losses' go. Therefore, the sum of the aforementioned values with the final losses of September discounted gives a value of 22.4 gC m^{-2} for the growth season. As no seagrass growth was observed outside of the study period, this value can be noted as

a maximum for the year as a whole. From here, these values may be scaled up to the size of the seagrass patch at Spurn in order to calculate the total seagrass carbon assimilation/release of the entire protected area.

Table 7. The variation of carbon stored/lost between site visits throughout the study period.

Month	date	Interval (days)	$gCm^{-2}\,d^{-1}$	$gC\,m^{-2}$
April	07/04/2022	0	N/A	N/A
April	22/04/2022	15	0.44	6.62
May	05/05/2022	13	-0.10	-1.29
May	20/05/2022	15	0.07	1.06
June	13/06/2022	24	0.41	9.88
July	01/07/2022	18	0.00	0.09
July	22/07/2022	21	0.09	1.94
August	12/08/2022	21	0.21	4.32
September	13/09/2022	32	-0.26	-8.20
	Total	159		14.41

Sediment Core Analysis

The surface sediment layers within the selected seagrass quadrats were composed of fine, well-drained sands with dry bulk densities of 1.06 to 1.66 g cm^{-3} and water contents of 19% to 41% (Figure 19). The relationship between dry bulk density of the material, and water content, followed that of previous studies (Flemming & Delafontaine, 2000; Forster & Kromkamp, 2004).
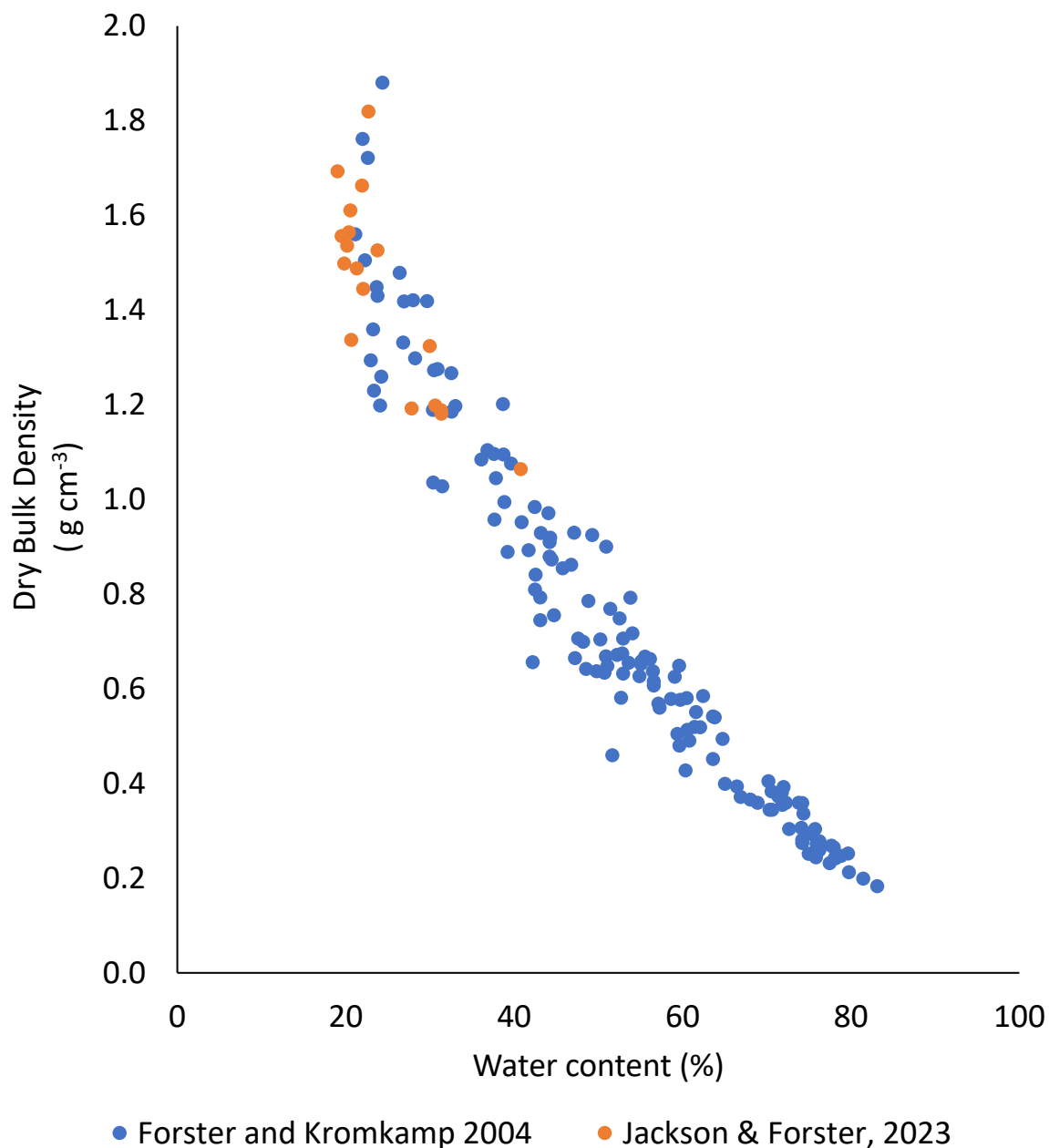
Figure 19. Relationship between sediment water content and sediment dry bulk density determined by weighing and drying material from within the seagrass bed at Spurn Point.

Seagrass blade material and seagrass rhizomes from cores of known area were sorted and weighed. Blades composed on average 47.6% of the total wet weight of plant material. Drying of the plant material at 60°C indicated a mean water content of 82.4%.

All samples excluding those taken from 'quadrat 6', for which material was lost during handling, were then analysed for elemental composition. Carbon and nitrogen contents were greater in the blade section of the seagrass rather than the rhizome/root section (See Table 8).

Nitrogen content was approximately double in the blade compared to the root/rhizome. The mean carbon content of the blades within the experiment, as a percentage of their dry weight was 37.48% in comparison to 27.96% in the root/rhizome. The results did not appear to vary according to the quadrat location that the samples were collected from. The results also agree with similar testing seen in Plus et al., (2001).

Table 8. Carbon, hydrogen and nitrogen (C, H and N) content of five samples retrieved from Spurn Head in September 2022. The values of C, H and N are shown for the blades of Zostera noltei and are presented as a percentage of total dry weight, the mean values are shown alongside the C:N atomic ratio.

Quadrat	Blades			
	C	H	N	C:N
1	36	5.52	2.87	12.54
2	38.4	5.85	3.6	10.67
3	38.4	5.84	3.35	11.46
4	40.1	6.06	3.59	11.17
5	34.5	5.37	2.77	12.45
Mean	37.48	5.73	3.24	11.67

Table 9. Carbon, hydrogen and nitrogen (C, H and N) content of five samples retrieved from Spurn Head in September 2022. The values of C, H and N are shown for the roots/rhizomes and are presented as a percentage of total dry weight, the mean values are shown alongside the C:N atomic ratio.

Quadrat	Rhizomes/Roots			
	C	H	N	C:N
1	32.6	5.73	1.33	24.51
2	30	5.31	1.08	27.78
3	23	3.97	0.79	29.11
4	26.7	4.71	1.06	25.19
5	27.5	4.88	0.87	31.61
Mean	27.96	4.92	1.03	27.64

The data given in Table 1 is a collective analysis of the 15 cores taken at 5 different quadrats that were successful under C, H, N analysis. To further analyse the data, a mean was calculated to establish the percentage of total mass of Carbon, Hydrogen and Nitrogen present in both the above ground (blades) and below ground (Rhizomes and roots) material

The values in Table 8and Table 9 allowed a C:N atomic ratio to be calculated for the above and below ground plant material, which produced a mean value of 11.67 for above ground material and 27.64 for below ground material.
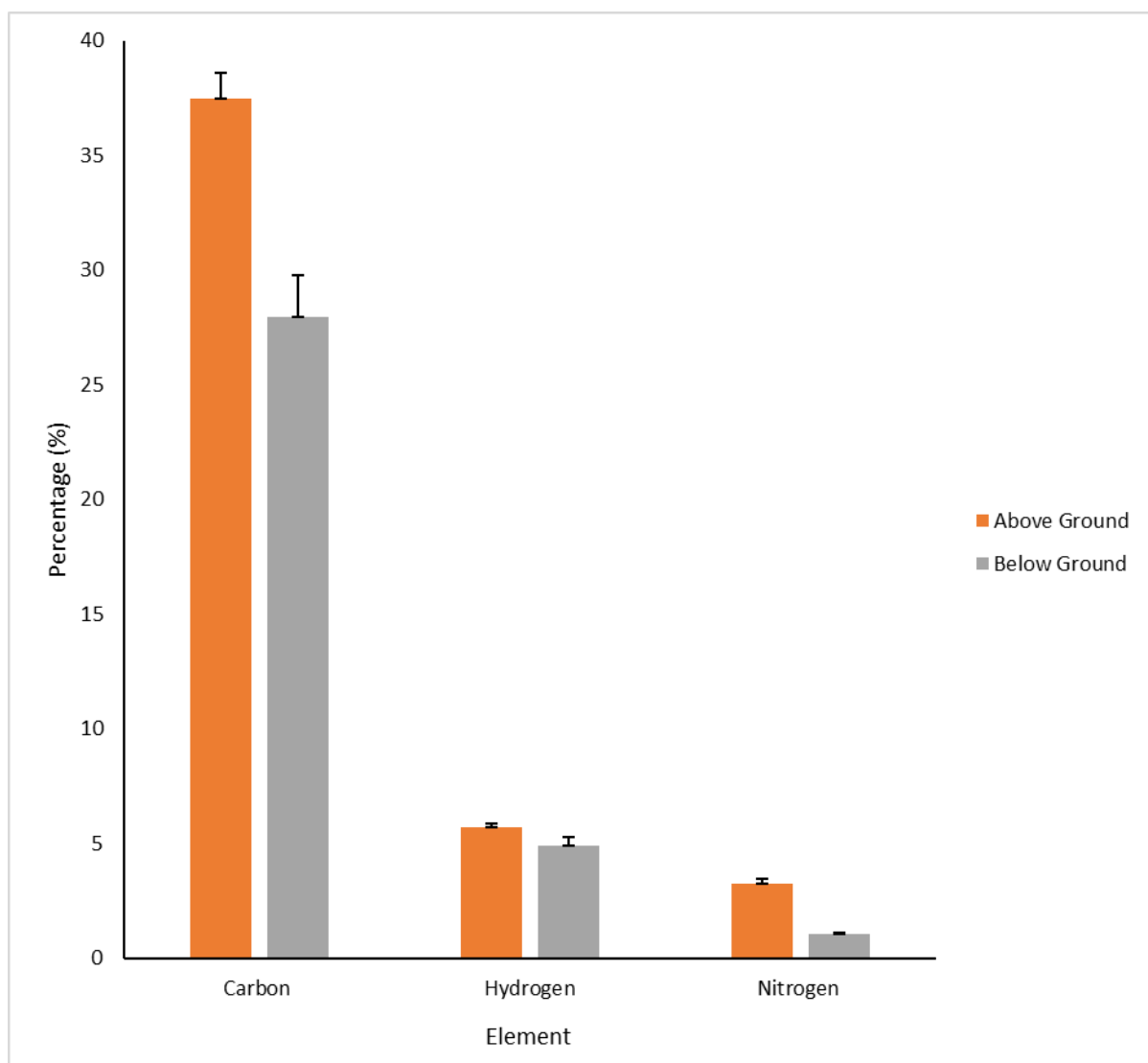
Figure 20. The carbon, hydrogen and nitrogen contents of the above and below ground material (blades and roots/rhizomes respectively) taken from the 15 syringe cores (29.45 cm3) at the 5 quadrat locations at Spurn Point (displayed as a percentage of mean total mass). Vertical bars represent the upper limits of the confidence interval to 95%.

The 95% confidence interval bars represent the upper limits of the mean elemental composition of *Zostera noltei* found in both the above and below ground cores that were successfully analysed. The confidence bars do not overlap in any of the elements investigated therefore it can be said there is a significant difference in the carbon, hydrogen and nitrogen content found in the different plant material at Spurn Point on the 13/09/2022, and that there is less than a 5% chance that this difference is due to chance.

Three single factor ANOVA tests were conducted on the above and below ground material for all three elements shown in Figure 20, all three elements displayed a significant difference between the origin of the material.

Table 10. ANOVA: Single Factor for above and below ground carbon contents.

ANOVA

Source of Variation	SS	df	MS	F	P-value	F crit
Between Groups	226.576	1	226.576	25.2734	0.001018	5.317655
Within Groups	71.72	8	8.965			
Total	298.296	9				

Table 11. ANOVA: Single Factor for above and below ground hydrogen contents.

ANOVA

Source of Variation	SS	df	MS	F	P-value	F crit
Between Groups	1.63216	1	1.63216	6.321669	0.036129	5.317655
Within Groups	2.06548	8	0.258185			
Total	3.69764	9				

Table 12. ANOVA: Single Factor for above and below ground nitrogen contents.

ANOVA

Source of Variation	SS	df	MS	F	P-value	F crit
Between Groups	11.31174	1	11.31174	132.2133	2.6E-05	5.987378
Within Groups	0.513341	6	0.085557			
Total	11.82508	7				

The significant difference between the origin of the material and the concentration of the element present is evidenced by all p-values being less than 0.05. Giving confidence that there is less than 5% chance that the difference shown is due to chance.

The mean organic carbon content of a known area was then calculated. Using the data from the C,H,N analysis it was found that an average of 32.72% of total dry plant matter (above and belowground material) was carbon. This then allowed the average blade carbon to be calculated per unit of area, using the blade/rhizome ratio data taken during dry weight analysis. The blade carbon

content of the cores taken are displayed against the percentage cover value for their respective quadrats on the 13th September 2022**Error! Reference source not found.**.
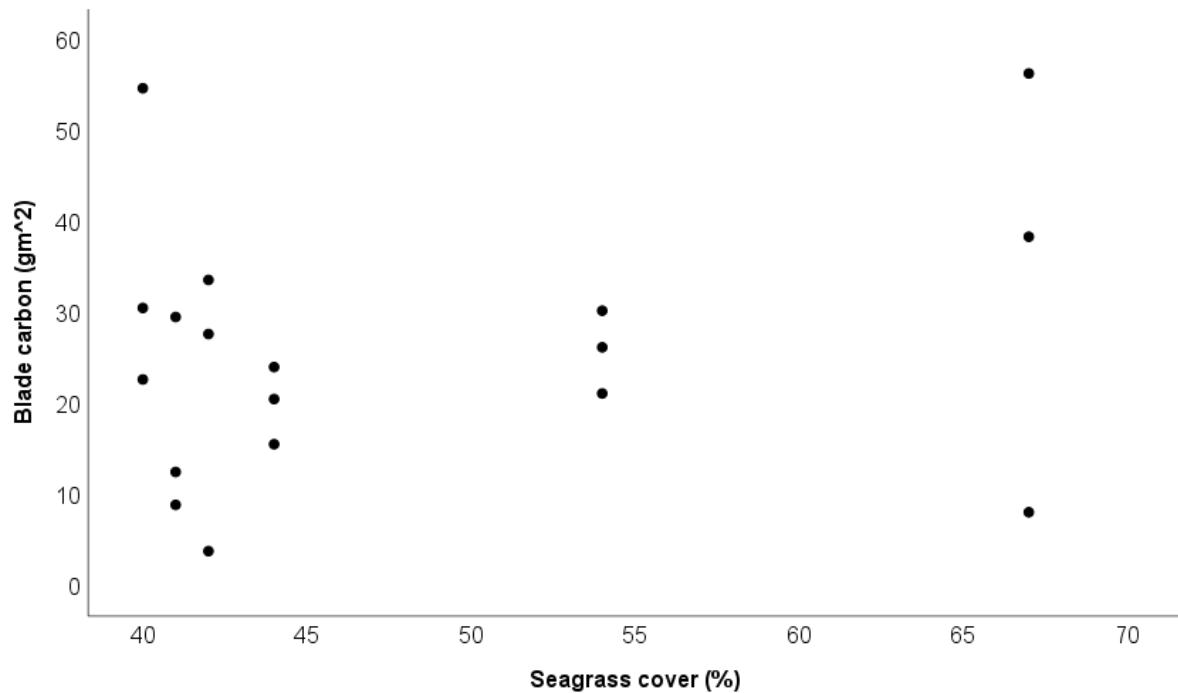
Figure 21. The mean carbon content of the blade material found at the 6 quadrat locations and the respective percentage cover of the quadrat.

The blade carbon and percentage cover mostly follow a uniform pattern with the exception of quadrat 2, which exhibited relatively high blade carbon content (35.94 g m^{-2}) in comparison to percentage cover (40%), this was expected to be due to the overlapping of blades, which would allow for the blade carbon to percentage cover ratio to be abnormally large. The initial hypothesis was that the blade carbon value would increase with an increasing percentage cover. Spearman's rank correlation analysis indicated that the two parameters were not related ($\rho = 0.034$, $p>0.05$).

Fluorescence measurements

The rapid light curves (RLC) were measured over two days of lab work with the majority being done on the day of sample collection. A total of 6 experiments were completed over the same amount of differing temperatures. During the experimentation it was difficult to hold the room's ambient

temperature to 15 and 19°C and therefore they have been discounted. The results of the RLCs displayed a clear positive correlation of the maximum rate with temperature.
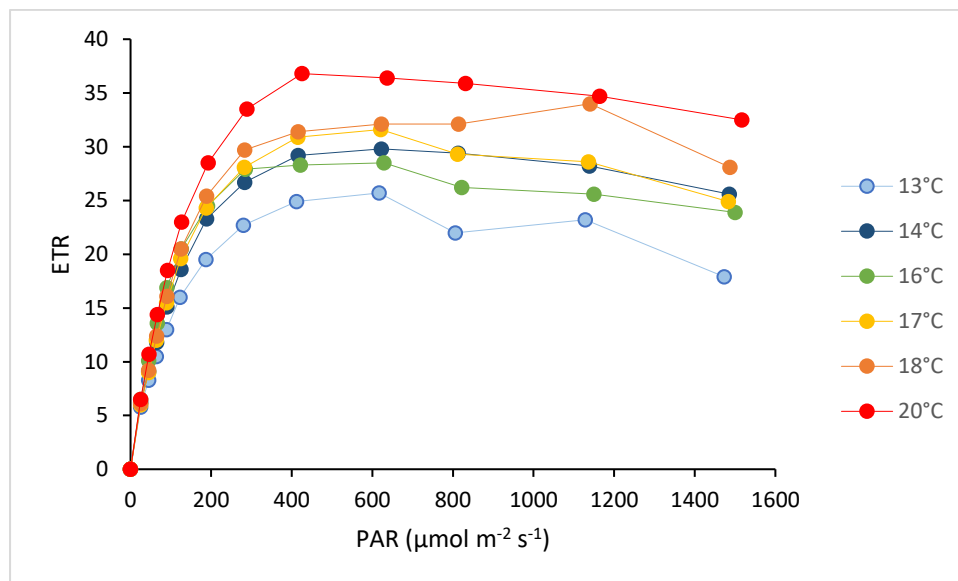
Figure 22. Rapid light curves showing the changes in the electron transport rate (ETR) of photosystem II, as a result of controlled temperature change and sequential irradiance steps produced artificially by a cold room and the MINI-PAM respectively, in a sample of Zostera noltei taken from Spurn Head.

The highest ETR being recorded during the 20°C experiment. As expected, the ETRs begin to show light saturation at around 400 µmol m^{-2} s^{-1}, and displayed a slight decline at irradiances above 800 µmol m^{-2} s^{-1} (Leuschner et al., 1998). However, other than the experiment at 13°C, no considerable decline in ETR is shown even at the highest irradiances of >1500 µmol m^{-2} s^{-1}. The experiment at 20°C simulated the most similar conditions that the seagrass would be exposed to during a typical summer's day, from which the sample of *Zostera noltei* was able to maintain an ETR of between 30 and 35 at the irradiances 600->1500 µmol m^{-2} s^{-1} therefore, complete light saturation must occur at a higher irradiance during such temperate exposure. This suggested that the population of the sample was high-light acclimated.

Discussion

Carbon Sequestration/Assimilation and Quantification

PAR and Temperature Logger Analysis

The extensive irradiance and temperature data provided by the HOBO loggers, situated within the seagrass patch at Spurn Point, gave a true reflection of the conditions that the patch was exposed to

during the 5-month testing period. A study performed in the Ria Formosa coastal lagoon, Portugal, tested the ETRs of *Z. noltei* at four different ambient PAR intervals. The intervals were 90 µmol m^{-2} s^{-1}, 300 µmol m^{-2} s^{-1}, 650 µmol m^{-2} s^{-1} and 850 µmol m^{-2} s^{-1}. The intervals at 90 and 300 µmol m^{-2} s^{-1} were measured in water and the other two were in air. The highest ETR of around 75 µmol e^{-} m^{-2} s^{-1} was recorded at 850 µmol m^{-2} s^{-1} and the lowest at 40 µmol e^{-} m^{-2} s^{-1} was recorded at 90 µmol m^{-2} s^{-1} (Silva et al., 2005). The mean irradiances for July and August in this study were 251 and 227 µmol m^{-2} s^{-1} respectively, with a decline to 98 µmol m^{-2} s^{-1} in September. This suggests that incident irradiance was sufficient for photosynthetic activity in those three months. However, optimum irradiance may have been higher than the means for the listed months. In regard to temperature, from July to August showed an increase in average temperature, with August being the warmest month on average. After August a gradual decline in average temperature occurred (Figure 9).

Throughout the study period at least one marine heatwave with full days of clear skies was recorded, where irradiances were much higher than the recorded means. An example of irradiance reaching >2000 µmol m^{-2} s^{-1} can be seen in Figure 7a. This is more than double the irradiance tested in Silva et al., (2005) and in Peralta et al., (2002) photoinhibition was stated to occur at 1000 µmol m^{-2} s^{-1} for *Z. noltei*. Therefore, it is possible that during such events *Z. noltei* will have decreased photosynthetic rates due to being saturated and may become light-stressed. In regard to the temperature tolerance of *Z. noltei*, another study from the Ria Formosa coastal lagoon, Portugal, showed a temperature tolerance of 37°C, however an increase to 39°C showed nearly 100% mortality rate for the seagrass (Massa et al., 2009). The temperatures recorded throughout our study period remained, for the most part, below these temperature levels, even during the marine heatwave event shown in Figure 7b. However, on one occasion the temperature reached 40.4°C on 17th September 2022. The temperature recorded by the logger does not necessarily reflect ambient air temperature, especially when exposed to full solar irradiance. The logger is positioned beneath the surface of the sediment and therefore reflects the temperature of the ground. Much of the seagrass does lay flat to the surface of the sediment when emersed so this may be accurate for much of the bed. However, it does not reflect the temperature of particularly dense patches of seagrass where overlapping would prevent sediment contact for much of the blades. According to Massa et al., (2009) 40.4 °C was above the temperature threshold for survival in *Z. noltei*. With increasing extreme weather events like marine heatwaves, the seagrass at Spurn may become vulnerable to heat stress and an increase in mortality may be witnessed in future years (Smith et al., 2023).

The irradiance and temperature data from the 6th July 2022, plotted against the tidal cycle from that day, demonstrated the impacts of immersion and emersion on the seagrass bed. The particular day was selected as high periods of solar irradiance (>2000 µmol m^{-2} s^{-1}) and high sediment surface temperatures (>30°C) were recorded. The Humber Estuary, as described previously is a particularly turbid body of water. This is reflected with sudden and sharp drops in irradiance in Figure 7a, where around 0.5-1 m depth of submersion was enough to decrease the irradiance to zero on an incoming tide, followed by similarly sudden and sharp increases in irradiance occur on a retreating tide. The clear change-points made it possible to notice the time when the logger/seagrass first became submerged as the temperature and irradiance would fall or rise immediately at between 4.8-5 m sea level. Together with GIS mapping of intertidal elevation for the wider area, this provides a firm base for calculation of light levels underpinning the NPP of seagrasses in regard to their time spent exposed to solar irradiance. It allows for the incident photon dose during daylight hours spent emersed to be calculated, and for periods with zero incident irradiance to be factored into the calculation.

Seagrass photosynthesis and respiration

The short-term measurements of gas exchange represent a balance of CO_2 uptake and release from different processes in the seagrass meadow that cannot clearly be separated from each other under field conditions. Measurements in the light were dominated by photosynthetic fixation of CO_2, but releases of CO_2 from respiration of seagrass, animals and bacteria in the plant-sediment matrix occur at the same time. Hence, short-term measurements are termed Net Primary Production, or more accurately Net Community Production. Subtraction of the measured respiration rate in darkness would correct the short-term measurements to give an estimate of Gross Primary Production. In the measurements made here, respiration rates were low and NPP and GPP would be similar over short timescales of less than one hour. The differences between NPP and GPP are larger when modelled over the course of a day, due to the prolonged periods of darkness due to tidal submersion of the seagrass bed. In the seagrass literature, different experimental designs and different data treatments give photosynthetic rates as GPP, NPP and NCP and care must be taken when comparing the daily NPP calculated here with rates measured by other authors.

When calculating the Net Primary Productivity (NPP) of the *Zostera noltei* population at Spurn it was possible to factor in the exact conditions experienced to increase the precision of the estimations. The values used to calculate the hourly rate were also retrieved from the seagrass at Spurn using the data provided from the set of short-term enclosure experiments, giving accurate estimates of the

maximum photosynthetic rate (P_{max}). Gas exchange measurements were made with a range of seagrass coverage and mostly higher values of irradiance and bed temperature. This again gave a more accurate representation of the meadow as a whole, as it allowed for areas of the seagrass patch that did not have 100% coverage. Whilst some areas of Spurn are heavily dense with *Zostera noltei,* much of the patch is less than 100% cover even in the height of the summer months (Figure 15). Further work with a high-resolution airborne sensor or camera would be required to quantify areas of seagrass bed according to their cover.

This analysis allowed for a representation on the impact on NPP that declining average light intensity had over a transitional period of summer to winter. Day maximum hourly NPP rates of 85 mg C m^{-2} h^{-1} were measured for *Z. noltei* at Spurn, and this rate is comparable with GPP values of 90 mg C m^{-2} h^{-1} for the same species at a study site near Roscoff, in Brittany (Ouisse et al., 2010). Using a very similar method, values of dark respiration were relatively high in that example (between 3.2 ±1.5 and 49.1 ±8.5 mg C m^{-2} h^{-1}). With these factors taken into account, our estimated maximum value, which does account for respiratory losses, appeared to be within a similar range or slightly lower.

By November the estimations indicate that the average daily irradiances are not sufficient to support a positive carbon drawdown, this is due to the shortening length of daylight hours alongside the lower solar elevation later in the year. Therefore, these lower average light conditions favour respiration and CO_2 release, as a biproduct, which is displayed in **Error! Reference source not found.** with an average loss of around 70 mg C m^{-2} d^{-1} in November. The results presented are estimations based on the two periods of enclosure experiments performed during the middle of September. More repeat data is required from the dome experiments to strengthen the values used to represent the P_{max}, half P_{max} and respiration levels, to understand if they are affected by physiological factors, such as plants entering the reproductive/carbohydrate storage period of their life cycle. This may have a negative impact on seagrass ability and readiness to effectively photosynthesise and in turn draw down carbon dioxide, which when applied to our Summer solar data where it is expected that the seagrass will be in the height of its readiness to photosynthesise (Philippart, 1995) may put our estimations more conservative than they perhaps should be. However, if dome experiments had been completed during the higher temperature and irradiance conditions in July for example, the results may have shown a limit to where the *Zostera noltei* reaches its temperature or irradiance tolerance levels and begins to shut down photosystem II (Peralta et al., 2002), reducing its photosynthetic ability. It would have proved interesting if the temperature/irradiances then declined, as to see if a subsequent recovery would then occur, where the *Z. noltei* would begin photosynthesising again.

The system used to quantify IPP in this report considered anything above 300 µmol m^{-2} s^{-1} to be at light saturation (P$_{max}$) suggesting that at any light intensity above this value, the seagrass at Spurn will be photosynthesising as effectively as it is capable of, shown from the dome experiments. This may not be true because at particularly high light intensities around 1000 µmol m^{-2} s^{-1}, *Zostera noltei* has been reported to become photoinhibited (Peralta et al., 2002). Photoinhibition occurs when the light intensity is too high for the plant to photosynthesise effectively and will begin to damage photosystem II if sustained exposure occurs (Tikkanen et al., 2014), the plant would be described as light stressed. This finding is supported by Ouisse et al., (2011), where *Zostera noltei* photosynthesised most effectively with light intensities around 639 ±174 µmol m^{-2} s^{-1}. The data provided from the laboratory PAM temperature experiment also supports this study consistently showing the highest electron transport rate (ETR) at around 600 µmol m^{-2} s^{-1}. However, the *Zostera noltei* samples taken from Spurn do not agree with Peralta et al., (2002) in that they display consistently high ETRs (>20), with the exception of the experiment at 12 °C, at irradiances in excess of 1400 µmol m^{-2} s^{-1}, displaying a positive correlation with temperature (Figure 22). However, the PAM light curves cover a very short period of time (<30 minutes). It would be interesting to see the response of the seagrass at such light intensities (>1000 µmol m^{-2} s^{-1}) for a 2hr 15 minute period as shown in Figure 7a. Sustained exposure to high light, may result in adverse light stress for the population (Duarte et al., 2017).

This provides interesting discussion as it would suggest the *Zostera noltei* community found at Spurn is adapted differently to other beds of the same species. This adaptation of the community at Spurn to support photosynthesis at a higher light intensity than previously found, is likely to be an adaptation to mitigate the lack of available PAR when immersed. The Humber Estuary is particularly turbid, with a suspended particulate matter (SPM) concentration in excess of 90 g l^{-1} (Uncles, Stephens & Law, 2006). For context, the range found in estuaries worldwide can vary between 0.1 and greater than 200 g l^{-1}. This is visualised in Figure 7a, where very shallow depths of water during times of immersion are enough to restrict the available light to zero. Such a phenomenon was also described in Vermaat & Verhagen, (1996) where *Zostera noltei* photosynthesis was restricted due to low light as a result of high turbidity in the Zandkreek estuary, Netherlands. Therefore, with very little light whilst immersed the seagrass bed will support very minimal photosynthesis, as shown in the dome experiments (Figure 10). Light becomes so limited during November that respiration becomes more dominant than photosynthesis and the overall carbon flux of the bed becomes negative. The height of the *Zostera noltei* growth season is during summer (Auby & Labourg, 1996) which coincides with the highest average light intensity for the year. Therefore, the *Zostera noltei* population at Spurn becoming adapted to sustain photosynthesis at high efficiency in high light

conditions allows the mitigation of photosynthesis lost in periods of shallow immersion due to the turbidity of the Humber. Other populations across Europe would be able to support photosynthesis underwater as shown in Ouisse et al., (2011) where the *Zostera noltei* reached P_{max} whilst immersed. Alongside continuing seagrass rewilding, The Yorkshire Wildlife Trust also have plans to reintroduce native oysters, of which populations have also declined in the area. Oysters are suspension feeders, filtering water in order to provide themselves with food, and in doing so they remove suspended particulate matter from the water column, thus reducing the turbidity (Cugier et al., 2010). If the reintroduction is successful, this may potentially reduce the turbidity of the Humber to the extent that the seagrass population at Spurn Point may be able to photosynthesise underwater. This may shift any physiological adaptations that the Spurn Point population has to current environmental conditions e.g. require low-light acclimation. It also adds speculation to the water quality during the time of Philips (1936). If the turbidity was significantly reduced, was this maybe the key factor that allowed such an extensive population of both *Zostera noltei* and *Zostera marina*? The light conditions would be particularly important for *Z. marina* due to its relatively low elevation on the shore (Figure 2). The current turbidity of the estuary drives irradiance almost instantaneously to zero after becoming submerged, which suggests that there is a tidal elevation on the mid to low shore at which *Zostera noltei* would not be exposed to sufficient irradiance to maintain a positive balance of photosynthetic gains over losses due to respiration and grazing (Flowers et al., 2023), grazing is not regarded as stored carbon as the carbon is passing to the next trophic level may eventually become remineralised by bacterial activity and released back into the atmosphere (Casal-Porras et al., 2022). This is exaggerated considering the respiration dominance in November and the steep drop off shown in October due to limited light exposure. Extending the experiment to cover months earlier in the year may prove interesting, as up until February the literature described weak levels of growth and photosynthesis (Vermaat & Verhagen, 1996; Cabaço et al., 2009; Ouisse et al., 2010; Migné et al., 2016).

The average hourly rate of NPP estimated for July equated to around 22 mg C m^{-2} h^{-1}. This was comparable to Ouisse et al., (2011) where NPP can be calculated by subtracting Community respiration (CR) from Gross Community Production (GCP).

Table 13. A comparison between the NPP of two different Zostera noltei beds. The first being Ouissé, Migne and Davoult (2011) and their findings in the Western English Channel, France displayed in the units, mg C m⁻² h⁻¹. The second being our findings at Spurn Head converted into the units mg C m⁻² h⁻¹.

Table 13. A comparison between the NPP of two different Zostera noltei beds. The first being Ouissé, Migne and Davoult (2011) and their findings in the Western English Channel, France displayed in the units, mg C m^{-2} h^{-1}. The second being our findings at Spurn Head converted into the units mg C m^{-2} h^{-1}.

Ouissé, Migne and Davoult (2011)				Jackson and Forster (2023)
Month/Year	GCP	CR	NPP	NPP
June 2008	62.91	20.98	41.93	
August 2008	115.43	51.39	64.04	
September 2008	125.89	49.53	76.36	
November 2008	47.23	8.75	38.48	
July 2022	N/A	N/A	N/A	21.6
August 2022	N/A	N/A	N/A	19.45
October 2022	N/A	N/A	N/A	7.94
November 2022	N/A	N/A	N/A	-2.96

As seen from the results in Table 13 our findings estimate a comparable NPP than that of Ouisse et al., (2011).

The estimations derived from our research are based on enclosure data collected in September. It is important to note this as a potential reason of underestimation, due to the lower light and temperature conditions recorded in that month of study in comparison to June-August. It must also be acknowledged that the literature states *Z. noltei* photosynthesises more effectively whilst submerged (Pérez-Lloréns & Niell, 1993). However, due to the high turbidity in the Spurn population, this advantage may not be present. Unlike in the highly successful populations observed in Ouisse et al., (2011), where immersed rates of both gross community production and community respiration were significantly higher than emersed. Another important difference between the two studies is the considerable amounts of epiphytes recorded within the seagrass population of Ouisse et al., (2010). This could potentially give a higher photosynthetic rate due to multiple plant and algal lifeforms occupying the space above the sediment. At Spurn, very minimal concentrations of epiphytes were observed within our population shown in Figure 11 and Figure 12 and minimal productivity was witnessed on 'bare sediment' near to the bed. The epiphytes discussed in the literature together with *Zostera noltei* have been reported to be twice as productive as *Zostera noltei* itself (Ouisse et al., 2010) which suggests that their contribution to photosynthetic activity and therefore production rates would be considerable.

The temperatures measured through the HOBO logger also introduces another area of interest, in Figure 7b the temperature during a single day of Summer is presented. The temperatures at seabed level measured on this day reached 34°C, which is a particularly high temperature for English conditions. For an intertidal species of seagrass to be exposed to such temperatures poses a threat of desiccation, photosynthetic shock and in extreme cases mortality (Mieszkowska et al., 2013). Whilst *Zostera noltei* has been described as having a high plasticity within its capacity to adapt to environmental change (Cabaço et al., 2009), it is also apparent that the species does still have a temperature capacity within it may survive. The species of seagrass as previously mentioned has capacity to survive temperatures of ≤37°C, with just two degrees higher resulting in a mortality rate of nearly 100% (Massa et al., 2009). This is quite concerning with the current trends of climate change, where global near surface temperatures have already reached 1.0-1.1°C higher than preindustrial levels, and are predicted to reach 2.7°C by the end of the century (Issa et al., 2023). This prediction would apply immense pressure on the *Zostera noltei* population at Spurn. Further experiments are required to establish the upper limit of temperature for growth and survival. At present, it is thought that *Zostera noltei* has an optimum temperature for photosynthesis of around 29°C (Penhale, 1977), which is relatively high considering the species inhabits the U.K., which has a temperate climate averaging around 20°C in Summer (Taleghani, 2022).

On the use of enclosure Experiments

The two bell jar experiments were conducted in the middle of September under ambient solar light and temperature conditions. The incident solar light was dependent on cloud cover during the experiments. The temperature within the chamber increased over the time of the experiment to end slightly higher than the ambient air temperature, as a result of the lack of air flow and the nature of an isolated heat-trapping environment. Temperature and irradiance co-varied. Using natural solar radiation and undisturbed seagrass achieved a more reliable data set when compared to any similar experiments where artificial light sources may be used, or condition variables are controlled (Zimmerman, 2021). The results here encapsulate a true representation of *in situ* varying light and temperature conditions.

The experiments were intentionally carried out over areas as close to 0, 50 and 100% cover of *Zostera noltei*. This was with the purpose of being able to notice any difference with the trends of CO_2 assimilation over different coverage and develop an understanding of the bed as a whole rather than focusing on areas of maximum density. Where *Zostera noltei* appeared denser, it was originally expected to be more photosynthetically active than patches of lesser density. However, there are

factors which limit this expectation. When *Zostera noltei* is not submerged then it lays flat, which in dense bed areas causes much bending and overlapping of blades (Fonseca & Kenworthy, 1987). Blades stack on top of each other and restrict the light availability to the rows of blades not on the surface. This overlapping or 'self-shading' contributes to positive and negative factors for the seagrass. It is suggested that this self-shading allows the *Zostera noltei* to protect itself against desiccation in periods of intense solar irradiance and soaring temperatures (Azcárate-García et al., 2022), conditions that were measured during our investigation and survived by the *Zostera noltei* population. The negative point of view from overlapping blades, is the losses of photosynthetic activity due to a reduction in light impacted blades whilst the seagrass is emersed (Clavier et al., 2011). When *Zostera noltei* becomes submerged the overlapping is mitigated and the buoyant blades stand up, separating from each other and presenting a maximum surface area to intercept light (Sandoval-Gil et al., 2015). However, as explained earlier the Humber estuary is particularly turbid and cannot support *Zostera noltei* photosynthesis in water depths >0.5m, therefore the seagrass at Spurn will have a somewhat limited photosynthetic capacity, supported by Ouisse et al., (2011) where higher density areas of *Zostera noltei* do not necessarily equate to higher production levels.

It must be acknowledged that the results of the enclosure experiments within this study are across two experimental periods within the same month and at the end of the *Zostera noltei* growth season (Migné et al., 2016) and should therefore be considered exploratory. However, they provide a strong base as a unique and perhaps preliminary investigation into the seagrass bed at Spurn. With simple alterations to the experimental design, such as including a battery powered fan internally to the dome in order to mix the air and potentially a CO_2 monitor with a faster response time, the low-cost methodology may prove very effective in understanding the photosynthetic capacity of the seagrass bed at Spurn Point (Azcárate-García et al., 2022). With these caveats, the data does show clear trends in the response to irradiance and temperature, and provided a basis from which to produce model-based estimations of NPP at the daily and monthly time scales. It showed that a higher average irradiance increased the photosynthetic rate of the autotrophic organisms within the dome. This was to be expected within reason, as an increase in available light will increase photosynthetic activity up until a point where the photosystems become saturated and another variable becomes the limiting factor (Penhale, 1977). It would also be expected that increasing the percentage cover of *Zostera noltei* to a certain extent within the dome, should increase the photosynthetic capacity within the environment. This was not a trend that was evident from the data, as the highest photosynthetic rate was 84 mg C m^{-2} h^{-1} within a 5-minute period of a '50%' seagrass cover experiment. Rates of NPP measured were similar to those previously recorded for *Zostera noltei,* and

were higher than those recorded for microphytobenthos in much of the literature (Woelfel et al., 2010; Frankenbach et al., 2020). However, when compared to common macroalgae photosynthetic rates of up to 298.6 mg C m^{-2} h^{-1} (Iannuzzi et al., 1996), the NPP values of *Zostera* are lower.

The reasoning behind higher productivity at lower percentage cover could be due to a number of factors, including the aforementioned self-shading effect. Possible factors are; experiments were done relatively late in the growing season of *Zostera noltei* (Auby & Labourg, 1996), whereby some plants may have entered a more mature stage within the plant's life cycle (Alexandre et al., 2006) with more effort being spent in other areas of their physiology, for example carbohydrate storage or reproduction. This was supported by the results of the seasonal quadrat analysis that showed the loss of blade material in September. Another factor could be that the algal epiphyte concentration may vary between areas of the seagrass bed. High densities of epiphytes could increase NPP as a result of the additional photosynthetic activity (Ouisse et al., 2010). However, at Spurn the epiphyte concentration within the bed was very low, with overgrowth of filamentous algae or diatoms not visibly noticeable on plant leaves as it is reported to be in the literature (Martínez-Crego et al., 2014).

Particularly dense sections of seagrass bed may allow the seagrass to avoid desiccation on hot summer days by retaining moisture, and thus cooling the surface through evaporation. Mechanisms to protect against photoinhibition are also likely to be important, such as restricting the photosynthetic capacity through the designation of effort to dissipating some thermal energy (Silva & Santos, 2003). It has also been suggested in Azcárate-García et al., (2022) that *Zostera noltei* have a 'high morphological plasticity', this could be an example of populational differences in morphology, where some populations become high light adapted dependent on their location within the community (Silva and Santos 2003). Similarly to irradiance, trends in NPP were shown for different temperatures, with higher temperature giving a higher photosynthetic rate. This is expected up until around 29 °C where, as previously mentioned, the optimum temperature for photosynthesis in eelgrass is met (Penhale, 1977).

The experiments done over an area of 0% coverage were expected to display a release in CO_2 as a result of respiring organisms on the sediment surface. However, the results showed a reduction in the CO_2 partial pressure in every illuminated interval, indicating continued carbon fixation. This would suggest that photoautotrophic microphytobenthos are still present even when the area

appears to have no recognisable photosynthetic material (De Brouwer & Stal, 2001) either to the naked eye or to the Image J software. This must also be acknowledged when understanding the photosynthetic capacity of *Zostera noltei* and the mudflat as a whole. Microphytobenthos, such as diatoms and other epiphytic algal material are often considered in the literature surrounding the carbon fixation of various species of seagrass (Hasegawa et al., 2007; Campbell & Fourqurean, 2014; Daudi et al., 2023). Their photosynthetic capacity, alongside the nature of the relationship that they have with the seagrass under investigation, is a highly discussed topic. Areal depth integrated production rates have shown microphytobenthos photosynthetic rates peak in Autumn at around 264.5 mg C m^{-2} d^{-1}, which equates to 11.02 mg C m^{-2} h^{-1} (Frankenbach et al., 2020). This value is much lower than the 84 mg C m^{-2} h^{-1} shown by *Zostera noltei* which was also within the end of the growth season that peaks in Spring/ Summer (Ganthy et al., 2013). However, it does suggest a strong reasoning for the carbon fixation that was shown on the bare sediment in this study. If, as stated previously, that the microphytobenthos is nearing the peak of its photosynthetic capacity for the year, then it is understandable that a decrease in CO_2 within the isolated environment occurred. However, due to the much lower rates during '0%' seagrass cover, shown during the enclosure experiments it suggests that even in periods of heightened photosynthesis from such autotrophs, *Zostera noltei* would remain the dominant primary producer on the mudflats at Spurn Head.

During the darkness section of these experiments, it was hypothesised that as a result of the incident irradiance being reduced to zero, there should be no light available for photosynthesis and therefore respiration would have been expected to become more dominant, releasing CO_2 to the air. This was expected to appear as an increase of CO_2 on the monitor after the 15 minutes of darkness. For one of the experiments this was true, but the other experiments showed slight positive carbon fixation rates. This showed that the respiration rate of *Zostera noltei* was much lower than that of its photosynthetic rate, which is supported by the common assumption that states respiration is equal to 10% of the P_{max} (Marsh et al., 1986). The photosynthetic and respiratory ability of *Zostera noltei* during periods of submersion and emersion is a much discussed topic in the literature, and studies tend to show results of *Zostera noltei* displaying much lower photosynthetic and respiration rates whilst emersed (Silva et al., 2005; Clavier et al., 2011, 2014), with some *Zostera* populations displaying a photosynthetic rate 2/3 of the submerged rate whilst emersed (Leuschner and Rees 1993).

With different physiological characteristics seen between the same species it could be suggested that the population adapts to the environmental conditions that it becomes exposed to. *Zostera*

noltei has a strong ability to adapt its morphology to changing environmental conditions (Peralta et al., 2005). The population of *Zostera noltei* studied in Silva et al., (2005) appears to have a similar habitat structure to the population at Spurn Point, where much of the seagrass bed is inundated with shallow microdepressions that retain estuarine water at low tide. The enclosure experiments were done over areas of microdepressions where some of the plant material was in fact submerged. The water within the microdepressions at Spurn is very clear as the suspended sediment usually found in the turbid Humber water has had time to settle. This is interesting because in Silva et al., (2005), it was found that the water within the microdepressions allowed for superior photosynthetic conditions for seagrass, due to the readiness of the water to dissolve CO_2 for photosynthesis (Silva, 2004; Pedersen et al., 2016) which contributes to the superior photosynthetic capacity of *Zostera noltei* whilst submerged (Ruiz-Montoya et al., 2021), as well as the transparent water to allow solar radiation to penetrate, it becomes obvious why this species is able to thrive in this area of the mudflat.

It was noted during fieldwork that the monitor used for the experiments had a slight delay from the reading it displayed of CO_2 ppm to the true reading at that given time. Hence, the initial 5 minutes during which equilibration occurred were not used. The monitor took around 60 seconds for it to return to normal ambient air concentrations when the enclosure was removed so values at the end of 15 minute experimental periods should reflect true conditions in both the ambient light section and the darkness section. For future replication of methodology, it may be logical to replace the CO_2 monitor to a model with no delay.

The lack of circulation of the gases inside the dome is another area which may be improved. Without any circulation within the enclosure, the gas that the monitor is measuring may not be a true representation of the CO_2 composition of the total gas in the enclosure. This may be resolved simply through the addition to a battery powered fan, which may be attached to the dome similarly to the monitor with Velcro strips. Such additions have been made to similar experiments in water filled bell jars (Asmus et al., 2000). This would also enable faster gaseous exchange between the meter and any photosynthetic or respiring organisms present, again providing for a more reliable data set.

Seasonal Growth Analysis

This section of experimentation was designed with the need for a non-destructive seasonal variation analysis in regard to the primary productive potential of *Zostera noltei*. The literature describes

Zostera noltei beds having pronounced seasonal variation in regard to their blade growth and die back (Vermaat & Verhagen, 1996). As an initial study into the bed, it was essential to gain understanding of the seasonal dynamics that were displayed at Spurn. Where other studies were able to take substantial cores and calculate the seasonal variation in biomass to estimate the productivity of *Zostera noltei* (Auby & Labourg, 1996), this study was restricted to non-destructive surveys by legislation protecting the site (Bateman et al., 2020). Therefore, it was seen as more suitable to study seasonal variation through change in percentage cover using a repeatable photographic quadrat technique. The methodology is arguably superior to destructive core-sampling estimations due to the ability to collect repeated samples of the exact location and therefore same plant material over a sustained period of time (6 months). Stratified sampling (Miller & Ambrose, 2000) was deemed appropriate for the location as it allowed for an interpretation to be made of the bed in its entirety, encompassing the rather intermittent nature of the *Zostera noltei* bed. It allowed for areas of particularly dense material (>80% cover) to be monitored but also areas that maintain a much lower percentage cover even throughout the height of their growth season in Spring and Summer (Hansen & Reidenbach, 2013) showing <40% cover. The majority of the quadrat pegs with the exception of quadrat 2, that can be easily replaced, have remained in place after the experiment finished and into 2023, allowing for subsequent projects to potentially reuse in future years and produce a timeline of data that could become a staple in understanding the bed's progression through the future. One limitation identified, specifically compared to core analysis, is that quadrat experiments only analyse the blade material above the sediment. Therefore, this method of analysis is unable to take into account any belowground carbon stores, showed potentially in the expansion of the root/rhizome network.

Image J was useful in identifying the percentage cover of the images taken at the stations (Lirman et al., 2007). However, there were limitations to the process. The colour threshold tool within ImageJ allowed the green of the *Zostera noltei* to become enhanced by altering the brightness of the cropped image. The ROI Manager tool would then be used to select these areas and calculate the number of pixels within the area detected. It was found that the Image J thresholding tool could not distinguish between pools of estuarine water remaining in the dimples of sediment sometimes found within the quadrat. In addition to this the quadrat used was made from tubed plastic guttering, which was quite large. The guttering, in times of direct sunlight sometimes caused shadowing within the quadrat, that was picked up within the image and again was difficult to threshold e.g. classify the areas of shadow to the dark green of the eelgrass. These limitations were mitigated by the alteration of the image with the brightness tool within the software. Often an

increase in brightness filtration reduced the shadowing effect and caused pools of water to reduce in size. Mitigation of edge effects was also done through the cropping of each image to include as much of the inside of the quadrat as deemed suitable, then the percentage cover was calculated as a percentage of the cropped image, leading to a more accurate estimation of percentage cover. It was also noted that working with a handheld camera on mudflats proved relatively difficult, especially when considering the need to be as minimally destructive as possible. Therefore, if the experiment was to be repeated, to ensure high quality replicates upon each visit. It would be suggested that a camera trap should be, if possible, connected in some capacity to the quadrat and the quadrat should be remade using different material that would not cast such shadows as previously described to lessen and strengthen the analysis workload post fieldwork. Alternatively, a camera with an infra-red band for vegetation would improve classification accuracy.

Core analysis

Using core samples to provide analysis into the structure of the seagrass bed and the composition of the above and below ground material proved very effective. It allowed the elemental composition, particularly the carbon and nitrogen content, to be studied and understood from an alternative perspective to that already explored in this study. Unfortunately, the Leco CHN analyser was unsuccessful with the sample taken from quadrat 6, due to loss of material whilst handling.

An attempt was made to calculate a conversion factor for the percentage of surface *Zostera noltei* material found at Spurn to units of carbon. High variability and a low number of data points meant that a relationship between these two parameters could not be found   (Figure 21**Error! Reference source not found.**). The analysis may have been stronger if the individual square section of the quadrat where the core sample had been taken, was made subject to the ImageJ analysis rather than using the percentage cover from the entire quadrat, as sometimes the percentage cover varied within each quadrat. The anomaly shown in quadrat 2 having a high carbon content relative to its determined percentage cover of *Zostera noltei*, could be an example of overlapping where the percentage cover may not accurately represent the biomass present, as a result of the positioning of the blades when they lay flat upon emersion.

The dry bulk density of a sediment describes the particulate matter of the sediment and the water content found within the sediment. It allows for a prediction of the texture of the sediment under investigation (Verstraeten & Poesen, 2001). As shown in Figure 19 the sediment type at Spurn fits

uniformly on the previous studies findings, describing that the sediment at Spurn varies slightly but is predominantly very fine with a relatively low water content.

The C:N ratio of *Zostera noltei* varies seasonally, and it is at its highest in Summer and lowest in Winter (Xu et al., 2021). This was supported by our findings in the blade material which displayed a C:N of 11.67 (Table 8). However, the root/rhizome material was found to have a relatively high C:N of 27.64.This appears to be relatively low and would suggest rapid mineralisation and release of nitrogen (Biswas & Micallef, 2019). *Z. noltei* is known to be a seasonal and fast-growing species (Peralta et al., 2002), this suggests that the eelgrass species requires a faster supply of nitrogen in order to maintain periods of fast growth, in comparison to more slower growing species that would maintain higher C:N ratios, such as *Posidonia oceanica* that have been seen to display shoot C:N atomic ratios up to 26 and rhizome ratios up to 19.9 (Scartazza et al., 2017). This also suggests that the plant actively stores carbohydrates during the September period, when the cores were taken. The rhizome is described as the primary organ for carbohydrate storage (Vermaat & Verhagen, 1996). A large carbohydrate store in the belowground material and reduced C:N in the blade material in the Winter months when blade breakoff is prominent suggests that the plant may have entered a carbohydrate storage period of its lifecycle. Also, the loss of carbon accounted for in the percentage cover decline during the quadrat analysis in later months, may not be as dramatic as calculated.

Collective Analysis and Comparison

Using the previously discussed analyses in conjunction with each other, we were able to provide a carbon assimilation quantification from two different angles. Firstly, the enclosure experiments gave realistic values of P_{max}, half P_{max} and respiration, and logging of irradiance provided an accurate time series. Using the tidal curve, value of Net Primary Production rate was modelled for the study period of 159 days and also for the entire year (Table 4, Table 5). An estimate was made of 57.5 gC m^{-2} over this period. The area of the *Zostera noltei* bed as of 2022, was estimated at 10,467.4 m^2. Therefore, the bed size multiplied by our productivity factor per square meter estimated an overall productivity during the growth season for the bed to be 602 kg carbon fixed each year.

The core sampling and quadrat analysis allowed a conversion factor for seagrass percentage cover to blade carbon per square meter and the carbon values per month were analysed to give an overall increase or decrease in plant biomass over the growing season. The sum of these values, divided by the number of quadrats would produce the average total blade carbon gain/loss in a square meter

of seagrass bed. It is estimated that 14.2 g C m^{-2} was stored, which when multiplied by the seagrass area gives a carbon fixation of 149 kg C in the entire bed.

This estimate is lower than that calculated for NPP over the same period, but included the loss of carbon in the final field visit in September (Figure 14), where it is believed that the loss was predominantly due to the break-off of blades. Therefore, it is relevant to investigate the productivity of the bed of *Zostera noltei* disregarding the losses in September. In this case, the productivity becomes 22.4 g C m^{-2} in 159 days or 234 kg C in the entire bed.

Hence it can be said with confidence that the annual carbon capture of the Spurn seagrass lies in the range from 22.4 to 57.5 gC m^{-2}. As both of these values do consider the losses of Carbon through various means in their life cycle, these values represent the Net Primary Productivity (NPP). These values agree with those found in (Prior, 2023) of 0.5 to 47 gC m^{-2} y^{-1} in Canada, but are on the low side when compared to the average global seagrass sediment storage of 13,970 g OC m^{-2} found in Gouldsmith & Cooper, (2022). When compared to an undisturbed rainforest, which can produce values in excess of 1000 gC m^{-2} y^{-1} (Potter et al., 2012) it would seem the suggestion that seagrass beds can produce NPP values of '35x a rainforest' is a gross overestimation for *Zostera noltei* (Macreadie et al., 2014). The seagrass *Zostera marina* is capable of 93 gC m^{-2} y^{-1} however this estimation refers to the upper limits and the average was found to be 24.8 gC m^{-2} y^{-1} in the Northwest Pacific spanning from Southeast Alaska to Southern Oregon (Prentice et al., 2020). Another species of seagrass, *Posidonia oceanica* is more highly productive. Producing NPP values of 400-817 gC m^{-2} y^{-1} (Kennedy & Björk, 2009), this is much more productive than the population found at Spurn Point. However, this still does not reach the potential of an undisturbed rainforest. Another relevant comparison is microphytobenthos production, where on average microphytobenthos yields between 50-100 gC m^{-2} y^{-1} (Cahoon, 2006), this is slightly higher than the values observed from the population at Spurn Point and again far lower than a typical undisturbed rainforest.

The loss of carbon at the end of the growth season offers conjecture to the fate of the carbon fixed from the atmosphere. The anoxic conditions shown in the sediment at Spurn have been suggested in the literature to slow the microbial activity and therefore the decomposition of organic matter (Chapman et al., 2019), such as that lost by *Zostera noltei* during the Autumn/Winter periods. Hence, carbon blade material that is lost and then buried in the sediment may be stored from the atmosphere for longer periods. However, cast-off blades which are transported high up the shore to be deposited in the salt marsh would be exposed to air for a prolonged period before eventual burial. During this time microbial degradation and consumption by invertebrates would recycle some of the carbon back to the atmosphere (Casal-Porras et al., 2022). The long-term fate of carbon fixed

by macrophytes in general (seagrass, seaweeds, mangroves, salt marshes) is a key area in blue carbon studies, and one that requires further study in the Spurn and wider Humber region.

Taking into account the broader context, it has been widely acknowledged in the scientific literature that the average individual in the United Kingdom is accountable for an annual carbon emission of 5.15 tonnes, primarily resulting from the consumption of fossil fuels per person (Ritchie et al., 2021). In light of this fact, the carbon assimilation capacity of the seagrass patch at Spurn, estimated to be in the order of 0.23 to 0.62 tonnes per year, appears relatively insignificant. The carbon fixation of the seagrass bed at Spurn would only account for a reduction of, at best, 12% of the carbon emissions of a single individual in the UK per year. Nevertheless, rather than being viewed as a discouraging outcome, this finding should serve as motivation to augment efforts for the protection and rewilding of the seagrass population at Spurn. The significance of this can be observed through the comparison depicted in Figure 2, where the seagrass areal extant shown in Phillips (1936) is much larger, indicating that carbon assimilation would be considerably greater. An additional element of carbon storage not studied here would be the capture, and long-term storage, within the seagrass root/shoot matrix of suspended organic-rich particles from the Humber estuary.

Humber Nutrient Analysis

High nitrogen levels in the form of ammonium and nitrate, (whereby concentrations of over 0.162 mg l^{-1} for ammoniacal nitrogen are toxic to eelgrass (Van Katwijk et al., 1997)), can cause direct inhibitory effects on the primary production of *Zostera noltei* (Brun et al., 2002). Therefore, it is essential when investigating the population of seagrass at Spurn to understand the nutrient levels within its environment. The results from Table 1 show the potentially toxic nutrients and their composition recorded at a water quality station near to Spurn Head. The results clearly show consistently low levels of ammoniacal nitrogen, much below the 'toxic' levels. The low levels measured are unusual for an urbanised estuary (Shi et al., 2023) near to a city.

Hull is a historically industrial city, with a busy shipping lane (Buor, 2015). Industrial activity, alongside sewage disposal and agricultural activity has the potential to increase the ammoniacal nitrogen and nitrate levels of estuarine water close to large cities (Cave et al., 2003; Jones, 2006). The original depiction of the seagrass bed at Spurn in Philip (1936), shows much greater coverage than is currently present. The Humber Estuary was deemed at risk of high nitrate levels and ammoniacal nitrogen and is therefore covered under certain legislation, restricting the industrial, sewage and farming activity that impact the nutrient content of the Humber (Cave et al., 2003). It is not unreasonable to suggest that nutrient levels of ammoniacal nitrogen could have increased to

above the toxicity level of 0.126 mg l^{-1} during the second half of the 20th century (Jones, 2006), or in the years prior to the legislation being introduced. However, nutrient data is sparse from this period of time, rendering this discussion speculative. In Head, (1970) there is a suggestion that between 45-50 tonnes N d^{-1} was discharged by the Humber estuary into the North Sea. If this level of these nutrients in the Humber estuary were present, then it is possible to understand why the seagrass bed size dramatically reduced since the bed size described in Philips (1936). Now that the ammoniacal nitrogen and nitrate levels have stabilised at low concentrations the intertidal areas may be suitable for restoration of seagrass, as is planned by The Yorkshire Wildlife Trust team at Spurn and their rewilding projects. Speculation to why a fraction of the population of seagrass was able to survive could include the dilution of estuarine water from the freshwater runoff that is apparent in channels upon visits at low tide to the site at Spurn (Uncles, Stephens & Harris, 2006). The dilution may have been sufficient enough to allow the toxicity of the aforementioned nutrients to be mitigated.

Pulse Amplitude Modulation Fluorometry

The analysis using the MINI-PAM (Walz GmbH, Germany) and the self-built mesocosm proved invaluable for this project. It allowed for the ability of the *Zostera noltei* population at Spurn to be understood in regard to their photosynthetic ability under controlled temperature and light conditions. The temperature conditions were measured between 13 and 20°C and it was noted that with increasing temperature a relatively uniform ETR increase occurred. This temperature range was within the limits of temperatures that the cold room could allow, therefore the experiment could be improved using a heater for example that could maintain temperatures >20°C as to understand the impact this would have on the *Zostera noltei*. The results of the MINI-PAM (Walz GmbH, Germany) provided the irradiance points at which the *Zostera noltei* plants performed most effectively. This enabled further analysis into the logger and CO_2 enclosure data, as the modelled data was used to provide a photosynthetic carbon assimilation maximum and release due to respiration. PAM data provided confirmation of the irradiance levels that fit within the bounds of the light-saturated photosynthetic range for *Zostera noltei* (P_{max}), the irradiance range where this was estimated to be at half (half P_{max}), and then the range of irradiance where photosynthesis is effectively zero.

The data presented for this section provides a broad estimate of the P-I and P-T curves, however further investigation is needed to determine more detailed results. This is currently ongoing in a secondary investigation.

Conclusion

- The first hypothesis of the study was that the *Zostera noltei* is expected to have environmental pressures that impact the health, distribution and physiology of the population, namely light intensity and exposure to light. In order to investigate this, we established an experiment using the MINI-PAM and a cold room laboratory. This allowed for us to perform fluorescence measurements in a temperature- controlled environment. The outcome of this experiment showed that the samples of *Z. noltei* were photosynthetically healthy, all successfully produced RLCs that displayed the light intensity where the samples were performing within their capacity of photosynthesis, which uniformly occurred at around 400 μmol m^{-2} s^{-1}. Across all temperature ranges the samples maintained ETRs near their capacity for each given temperature showing only minimal reductions at 1600 μmol m^{-2} s^{-1}. Therefore, the samples show a healthy high-light adapted population and provided data to support an in-depth estimation of carbon assimilation.

- The temperatures that could be controlled within the experiment (13-20°C) were useful in showing a predicted uniform increase in photosynthetic capacity with increasing temperature, but not sufficient enough to display a temperature where the samples became inhibited.

- The second hypothesis was that the *Zostera noltei* population at Spurn will have a comparable carbon assimilation capability to other seagrass species in similar studies. To do thisa data logger located amongst the seagrass bed provided values for incident light intensity that the bed experienced over the study period. This data was used together with the fluorescence measurements, to allow calculation of the amount of time that the seagrass bed spent photosynthesising at, full capacity, half capacity and then also respiring. Short-term enclosure experiments allowed estimation of the maximum, light-saturated rate for CO_2 drawdown, which could be then transformed and extrapolated into gC m^{-2} h^{-1}and gave an annual estimate of 57.5 gC m^{-2}. The total size of the seagrass bed was calculated using GIS and multiplied by the areal estimate of assimilation to give approximately 600 kg assimilated by the seagrass at Spurn in the study period. Whilst the results showed the population at Spurn is comparable to other studies, the trend was that they were on the lower side of the carbon drawdown capabilities.

- The third hypothesis was that the water quality of the Humber estuary may be insufficient to enable growth of *Zostera noltei* outside of the current distribution. The water quality of the Humber Estuary was also important to understanding the health of the current population and to provide any insight into what may have depleted the coverage of *Z. noltei* in comparison to a previous investigation. The nutrients primarily investigated in this study were ammonium and nitrate, as these have been stated in the literature to become toxic to *Z. noltei* over specific quantities. Using water quality values from a station provided by the Environment Agency that was situated relatively close to the bed at Spurn in 2022, we were able to confirm that the potentially toxic nutrients were much below the suggested toxicity levels. In the past, ammonium and nitrate levels may have been higher during the 1940s to 1980s period in which the seagrass areas were greatly reduced. The surviving population at the high shore may survive as a result of the freshwater run off, from predominantly unfarmed land on the peninsula at Spurn, which dilutes the nutrient concentrations in the estuarine water.

- The fourth hypothesis was that the experiments should show biomass increase through from spring into summer and then reduce again into autumn and winter. At the beginning of the study period, we set out to establish a consistent measure of *Z. noltei* percentage cover of the bed. This was key in understanding the seasonality of the growth season of the patch of *Z. noltei*, in regard to the progression of growth and die-off and in what months this occurs. Reductions in cover were noted early in the growth season, due to a high sediment load on top of the bed during low tide. Monthly cover estimates were calibrated with carbon content data to allow the estimation of carbon at any given percentage cover of *Z. noltei*. Through this, losses and gains of blade carbon could be estimated. A lower annual carbon fixation of 21 gC m^{-2} was estimated using this method, and a total carbon fixation for the entire seagrass bed of 202 kg C. We found that biomass was at its lowest in April, then increased into summer where it peaked in July, then gradually decreased into September.

- The final hypothesis was that the carbon and nitrogen balance of the above and belowground material will reflect the physiological characteristics of the *Zostera noltei* population at Spurn and that the sediment characteristics will vary slightly across the bed. A higher carbon content in the root/rhizome matrix during the end of the growth season was found. This suggested that the population of *Z. noltei* at Spurn entered a carbohydrate storage period of their lifecycle actively storing carbon. The sediment characteristics did vary slightly across the bed, with some showing finer particulate matter and others slightly larger and sandy, this was described by the dry bulk density analysis.

References

Airoldi, L. & Beck, M. (2007) Loss, Status and Trends for Coastal Marine Habitats of Europe. In *Oceanography and Marine Biology: An Annual Review*, 345–383.

Alexandre, A., Cabaço, S., Santos, R. & Serrão, E.A. (2006) Timing and success of reproductive stages in the seagrass Zostera noltii. *Aquatic Botany*, 85(3). Available online: https://doi.org/10.1016/j.aquabot.2006.05.002.

Annuar, M. & Anas, M. (2021) *The role of the seagrass Zostera noltii on sand transport across an intertidal sand flat in Ryde, Isle of Wight*. University of Southampton .

Asmus, R.M., Sprung, M. & Asmus, H. (2000) Nutrient fluxes in intertidal communities of a South European lagoon (Ria Formosa) - Similarities and differences with a northern Wadden Sea bay (Sylt-Rømø Bay). *Hydrobiologia*, 436. Available online: https://doi.org/10.1023/A:1026542621512.

Auby, I. & Labourg, P.J. (1996) Seasonal dynamics of Zostera noltii Hornem. In the Bay of Arcachon (France). *Journal of Sea Research*, 35(4). Available online: https://doi.org/10.1016/S1385-1101(96)90754-6.

Auby, I., Sauriau, P.-G., Oger-Jeanneret, H., Hily, C., Dalloyau, S., Rollet, C., Trut, G., Fortune, M., More, M. & Rigouin, L. (2014) Protocoles de suivi stationnel des herbiers à zostères pour la Directive Cadre sur l'Eau (DCE) Zostera marina-Zostera noltei. Version 2.

Azcárate-García, T., Beca-Carretero, P., Cara, C.L., Villamayor, B., Cosnett, E., Bermejo, R., Hernández, I., Brun, F.G. & Stengel, D.B. (2022) Seasonal plant development and meadow structure of Irish and southern Spanish seagrass populations. *Aquatic Botany*, 183. Available online: https://doi.org/10.1016/j.aquabot.2022.103569.

Baez, S. (2023) Blue Carbon. In *The Ocean and Us*.

Barañano, C., Fernández, E., Morán, P., Urbieta, P. & Méndez, G. (2022) Population dynamics of a fragmented subtidal Zostera marina population affected by shell fishing. *Estuarine, Coastal and Shelf Science*, 269. Available online: https://doi.org/10.1016/j.ecss.2022.107818.

Bateman, M.D., McHale, K., Bayntun, H.J. & Williams, N. (2020) Understanding historical coastal spit evolution: A case study from Spurn, East Yorkshire, UK. *Earth Surface Processes and Landforms*, 45(14). Available online: https://doi.org/10.1002/esp.4991.

Biswas, D. & Micallef, S.A. (2019) *Safety and practice for organic food Safety and Practice for Organic Food*. Available online: https://doi.org/10.1016/C2016-0-02314-8.

De Brouwer, J.F.C. & Stal, L.J. (2001) Short-term dynamics in microphytobenthos distribution and associated extracellular carbohydrates in surface sediments of an intertidal mudflat. *Marine Ecology Progress Series*, 218. Available online: https://doi.org/10.3354/meps218033.

Brun, F.G., Hernández, I., Vergara, J.J., Peralta, G. & Pérez-Lloréns, J.L. (2002) Assessing the toxicity of ammonium pulses to the survival and growth of Zostera noltii. *Marine Ecology Progress Series*, 225. Available online: https://doi.org/10.3354/meps225177.

Brun, F.G., Hernández, I., Vergara, J.J. & Pérez-Lloréns, J.L. (2003) Growth, carbon allocation and proteolytic activity in the seagrass Zostera noltii shaded by Ulva canopies. *Functional Plant Biology*, 30(5). Available online: https://doi.org/10.1071/FP03010.

Bulthuis, D.A. (1987) Effects of temperature on photosynthesis and growth of seagrasses. *Aquatic Botany*, 27(1). Available online: https://doi.org/10.1016/0304-3770(87)90084-2.

Buor, J. (2015) *Applying System Dynamics Modelling To Building Resilient Logistics: A Case of the Humber Ports Complex* . The University of Hull.

Burdick, D.M., Short, F.T. & Wolf, J. (1993) An index to assess and monitor the progression of wasting disease in eelgrass Zostera marina. *Marine Ecology Progress Series*, 94(1). Available online: https://doi.org/10.3354/meps094083.

Cabaço, S., Machás, R. & Santos, R. (2009) Individual and population plasticity of the seagrass Zostera noltii along a vertical intertidal gradient. *Estuarine, Coastal and Shelf Science*, 82(2). Available online: https://doi.org/10.1016/j.ecss.2009.01.020.

Cahoon, L. (2006) Upscaling primary production estimates: regional and global scale estimates of microphytobenthos production. *Koninklijke Nederlandse Akademie Van* [Preprint], (1995).

Campbell, J.E. & Fourqurean, J.W. (2014) Ocean acidification outweighs nutrient effects in structuring seagrass epiphyte communities. *Journal of Ecology*, 102(3). Available online: https://doi.org/10.1111/1365-2745.12233.

Canadell, M.B., Gómez-Gener, L., Clémençon, M., Lane, S.N. & Battin, T.J. (2021) Daily entropy of dissolved oxygen reveals different energetic regimes and drivers among high-mountain stream types. *Limnology and Oceanography*, 66(4). Available online: https://doi.org/10.1002/lno.11670.

Cave, R.R., Ledoux, L., Turner, K., Jickells, T., Andrews, J.E. & Davies, H. (2003) The Humber catchment and its coastal area: From UK to European perspectives. In *Science of the Total Environment*. Available online: https://doi.org/10.1016/S0048-9697(03)00093-7.

Chapman, S.K., Hayes, M.A., Kelly, B. & Adam Langley, J. (2019) Exploring the oxygen sensitivity of wetland soil carbon mineralization. *Biology Letters*, 15(1). Available online: https://doi.org/10.1098/rsbl.2018.0407.

Christianen, M.J.A., van Belzen, J., Herman, P.M.J., van Katwijk, M.M., Lamers, L.P.M., van Leent, P.J.M. & Bouma, T.J. (2013) Low-Canopy Seagrass Beds Still Provide Important Coastal Protection Services. *PLoS ONE*, 8(5). Available online: https://doi.org/10.1371/journal.pone.0062413.

Clavier, J., Chauvaud, L., Amice, E., Lazure, P., Van Der Geest, M., Labrosse, P., Diagne, A., Carlier, A. & Chauvaud, S. (2014) Benthic metabolism in shallow coastal ecosystems of the Banc d'Arguin, Mauritania. *Marine Ecology Progress Series*, 501. Available online: https://doi.org/10.3354/meps10683.

Clavier, J., Chauvaud, L., Carlier, A., Amice, E., Van der Geest, M., Labrosse, P., Diagne, A. & Hily, C. (2011) Aerial and underwater carbon metabolism of a Zostera noltii seagrass bed in the Banc d'Arguin, Mauritania. *Aquatic Botany*, 95(1). Available online: https://doi.org/10.1016/j.aquabot.2011.03.005.

Couto, T., Duarte, B., Caçador, I., Baeta, A. & Marques, J.C. (2013) Salt marsh plants carbon storage in a temperate Atlantic estuary illustrated by a stable isotopic analysis based approach. *Ecological Indicators*, 32. Available online: https://doi.org/10.1016/j.ecolind.2013.04.004.

Cugier, P., Struski, C., Blanchard, M., Mazurié, J., Pouvreau, S., Olivier, F., Trigui, J.R. & Thiébaut, E. (2010) Assessing the role of benthic filter feeders on phytoplankton production in a shellfish farming

site: Mont Saint Michel Bay, France. *Journal of Marine Systems*, 82(1–2). Available online: https://doi.org/10.1016/j.jmarsys.2010.02.013.

Cyronak, T., Andersson, A.J., D'Angelo, S., Bresnahan, P., Davidson, C., Griffin, A., Kindeberg, T., Pennise, J., Takeshita, Y. & White, M. (2018) Short-Term Spatial and Temporal Carbonate Chemistry Variability in Two Contrasting Seagrass Meadows: Implications for pH Buffering Capacities. *Estuaries and Coasts*, 41(5). Available online: https://doi.org/10.1007/s12237-017-0356-5.

Daudi, L.N., Uku, J.N. & De Troch, M. (2023) Effects of habitat complexity on the abundance and diversity of seagrass leaf meiofauna communities in tropical Kenyan seagrass meadows. *Aquatic Botany*, 187. Available online: https://doi.org/10.1016/j.aquabot.2023.103651.

Deguette, A., Barrote, I. & Silva, J. (2022) Physiological and morphological effects of a marine heatwave on the seagrass Cymodocea nodosa. *Scientific Reports*, 12(1). Available online: https://doi.org/10.1038/s41598-022-12102-x.

Deguette, A., Silva, J.M.S. da & Barotte, I. (2021) *The effects of a marine heatwave on seagrasses cymodocea nodosa and zostera marina in Ria Formosa, Portugal: photosynthetic activity & oxidative stress indicators*. Universidade do Algarve.

Duarte, B., Pedro, S., Marques, J.C., Adão, H. & Caçador, I. (2017) Zostera noltii development probing using chlorophyll a transient analysis (JIP-test) under field conditions: Integrating physiological insights into a photochemical stress index. *Ecological Indicators*, 76. Available online: https://doi.org/10.1016/j.ecolind.2017.01.023.

Duarte, B., Repolho, T., Paula, J.R., Caçador, I., Matos, A.R. & Rosa, R. (2022) Ocean Acidification Alleviates Dwarf Eelgrass (Zostera noltii) Lipid Landscape Remodeling under Warming Stress. *Biology*, 11(5). Available online: https://doi.org/10.3390/biology11050780.

Duarte de Paula Costa, M., Adame, M.F., Bryant, C. V., Hill, J., Kelleway, J.J., Lovelock, C.E., Ola, A., Rasheed, M.A., Salinas, C., Serrano, O., Waltham, N., York, P.H., Young, M. & Macreadie, P. (2023) Quantifying blue carbon stocks and the role of protected areas to conserve coastal wetlands. *Science of the Total Environment*, 874. Available online: https://doi.org/10.1016/j.scitotenv.2023.162518.

Flemming, B.W. & Delafontaine, M.T. (2000) Mass physical properties of muddy intertidal sediments: Some applications, misapplications and non-applications. *Continental Shelf Research*, 20(10–11). Available online: https://doi.org/10.1016/S0278-4343(00)00018-2.

Flowers, G.J.L., Needham, H.R., Bulmer, R.H., Lohrer, A.M. & Pilditch, C.A. (2023) Going under: The implications of sea-level rise and reduced light availability on intertidal primary production. *Limnology and Oceanography* [Preprint]. Available online: https://doi.org/10.1002/lno.12347.

Foden, J. (2007) Assessment metrics for littoral seagrass under the European Water Framework Directive; outcomes of UK intercalibration with the Netherlands. *Hydrobiologia*, 579(1). Available online: https://doi.org/10.1007/s10750-006-0402-y.

Foden, J. & Brazier, D.P. (2007) Angiosperms (seagrass) within the EU water framework directive: A UK perspective. *Marine Pollution Bulletin*, 55(1–6). Available online: https://doi.org/10.1016/j.marpolbul.2006.08.021.

Fonseca, M.S. & Kenworthy, W.J. (1987) Effects of current on photosynthesis and distribution of seagrasses. *Aquatic Botany*, 27(1). Available online: https://doi.org/10.1016/0304-3770(87)90086-6.

Forster, R.M. & Kromkamp, J.C. (2004) Modelling the effects of chlorophyll fluorescence from subsurface layers on photosynthetic efficiency measurements in microphytobenthic algae. *Marine Ecology Progress Series*, 284. Available online: https://doi.org/10.3354/meps284009.

Frankenbach, S., Ezequiel, J., Plecha, S., Goessling, J.W., Vaz, L., Kühl, M., Dias, J.M., Vaz, N. & Serôdio, J. (2020) Synoptic Spatio-Temporal Variability of the Photosynthetic Productivity of Microphytobenthos and Phytoplankton in a Tidal Estuary. *Frontiers in Marine Science*, 7. Available online: https://doi.org/10.3389/fmars.2020.00170.

Franzitta, M., Repolho, T., Paula, J.R., Caçador, I., Matos, A.R., Rosa, R. & Duarte, B. (2021) Dwarf eelgrass (Zostera noltii) fatty acid remodelling induced by climate change. *Estuarine, Coastal and Shelf Science*, 261. Available online: https://doi.org/10.1016/j.ecss.2021.107546.

Ganthy, F., Sottolichio, A. & Verney, R. (2013) Seasonal modification of tidal flat sediment dynamics by seagrass meadows of Zostera noltii (Bassin d'Arcachon, France). *Journal of Marine Systems*, 109–110(SUPPL.). Available online: https://doi.org/10.1016/j.jmarsys.2011.11.027.

Gitelson, A., Arkebauer, T., Viña, A., Skakun, S. & Inoue, Y. (2021) Evaluating plant photosynthetic traits via absorption coefficient in the photosynthetically active radiation region. *Remote Sensing of Environment*, 258. Available online: https://doi.org/10.1016/j.rse.2021.112401.

Gouldsmith, V. & Cooper, A. (2022) Consideration of the carbon sequestration potential of seagrass to inform recovery and restoration projects within the Essex Estuaries Special Area of Conservation (SAC), United Kingdom. *Journal of Coastal Conservation*, 26(4). Available online: https://doi.org/10.1007/s11852-022-00882-3.

Green, A.E., Unsworth, R.K.F., Chadwick, M.A. & Jones, P.J.S. (2021) Historical Analysis Exposes Catastrophic Seagrass Loss for the United Kingdom. *Frontiers in Plant Science*, 12. Available online: https://doi.org/10.3389/fpls.2021.629962.

Gruber, R., Gurbisz, C., Borum, J. & Kemp, M. (2022) Estuarine Ecology. In *Estuarine Ecology*, 106–108.

Hansen, J.C.R. & Reidenbach, M.A. (2013) Seasonal Growth and Senescence of a Zostera marina Seagrass Meadow Alters Wave-Dominated Flow and Sediment Suspension Within a Coastal Bay. *Estuaries and Coasts*, 36(6). Available online: https://doi.org/10.1007/s12237-013-9620-5.

Hasegawa, N., Hori, M. & Mukai, H. (2007) Seasonal shifts in seagrass bed primary producers in a cold-temperate estuary: Dynamics of eelgrass Zostera marina and associated epiphytic algae. *Aquatic Botany*, 86(4). Available online: https://doi.org/10.1016/j.aquabot.2006.12.002.

Head, P.C. (1970) Discharge of nutrients from estuaries. *Marine Pollution Bulletin*. Available online: https://doi.org/10.1016/0025-326X(70)90256-0.

Hendriks, I.E., Olsen, Y.S., Ramajo, L., Basso, L., Steckbauer, A., Moore, T.S., Howard, J. & Duarte, C.M. (2014) Photosynthetic activity buffers ocean acidification in seagrass meadows. *Biogeosciences*, 11(2). Available online: https://doi.org/10.5194/bg-11-333-2014.

Houseago, R.C., Hong, L., Cheng, S., Best, J.L., Parsons, D.R. & Chamorro, L.P. (2022) On the turbulence dynamics induced by a surrogate seagrass canopy. *Journal of Fluid Mechanics*, 934. Available online: https://doi.org/10.1017/jfm.2021.1142.

Iannuzzi, T.J., Weinstein, M.P., Sellner, K.G. & Barrett, J.C. (1996) Habitat disturbance and marina development: An assessment of ecological effects. I. Changes in primary production due to dredging and marina construction. In *Estuaries*. Available online: https://doi.org/10.2307/1352231.

Issa, R., Robin van Daalen, K., Faddoul, A., Collias, L., James, R., Chaudhry, U.A.R., Graef, V., Sullivan, A., Erasmus, P., Chesters, H. & Kelman, I. (2023) Human migration on a heating planet: A scoping review. *PLOS Climate*, 2(5). Available online: https://doi.org/10.1371/journal.pclm.0000214.

Istomina, E.A., Luzhkova, N.M. & Khidekel', V. V. (2016) Birdwatching tourism infrastructure planning in the Ria Formosa Natural Park (Portugal). *Geography and Natural Resources*, 37(4). Available online: https://doi.org/10.1134/S1875372816040120.

IUCN. 2022. The IUCN Red List of Threatened Species. Version 2022-2. https://www.iucnredlist.org. Accessed on [16/07/2023].

Jones, P.D. (2006) Water quality and fisheries in the Mersey estuary, England: A historical perspective. *Marine Pollution Bulletin*, 53(1). Available online: https://doi.org/10.1016/j.marpolbul.2005.11.025.

Van Katwijk, M.M., Vergeer, L.H.T., Schmitz, G.H.W. & Roelofs, J.G.M. (1997) Ammonium toxicity in eelgrass Zostera marina. *Marine Ecology Progress Series*, 157. Available online: https://doi.org/10.3354/meps157159.

Kennedy, H. & Björk, M. (2009) Seagrass meadows. In Laffoley, D. & Grimsditch, G. (eds), 23–26.

Kowalski, J.L., Cammarata, K., DeYoe, H. & Vatcheva, K. (2023) Metabolic responses of Halodule wrightii to hyposalinity. *Aquatic Botany*, 186. Available online: https://doi.org/10.1016/j.aquabot.2023.103628.

Lebreton, B., Richard, P., Galois, R., Radenac, G., Brahmia, A., Colli, G., Grouazel, M., André, C., Guillou, G. & Blanchard, G.F. (2012) Food sources used by sediment meiofauna in an intertidal Zostera noltii seagrass bed: A seasonal stable isotope study. *Marine Biology*, 159(7). Available online: https://doi.org/10.1007/s00227-012-1940-7.

Lefebvre, A., Thompson, C.E.L., Collins, K.J. & Amos, C.L. (2009) Use of a high-resolution profiling sonar and a towed video camera to map a Zostera marina bed, Solent, UK. *Estuarine, Coastal and Shelf Science*, 82(2). Available online: https://doi.org/10.1016/j.ecss.2009.01.027.

Leuschner, C., Landwehr, S. & Mehlig, U. (1998) Limitation of carbon assimilation of intertidal Zostera noltii and Z. marina by desiccation at low tide. *Aquatic Botany*, 62(3). Available online: https://doi.org/10.1016/S0304-3770(98)00091-6.

Lirman, D., Gracias, N.R., Gintert, B.E., Gleason, A.C.R., Reid, R.P., Negahdaripour, S. & Kramer, P. (2007) Development and application of a video-mosaic survey technology to document the status of coral reef communities. *Environmental Monitoring and Assessment*, 125(1–3). Available online: https://doi.org/10.1007/s10661-006-9239-0.

Lonsdale, J.A., Leach, C., Parsons, D., Barkwith, A., Manson, S. & Elliott, M. (2022) Managing estuaries under a changing climate: A case study of the Humber Estuary, UK. *Environmental Science and Policy*. Available online: https://doi.org/10.1016/j.envsci.2022.04.001.

Machás, R., Santos, R. & Peterson, B. (2006) Elemental and stable isotope composition of Zostera noltii (Horneman) leaves during the early phases of decay in a temperate mesotidal lagoon.

Estuarine, Coastal and Shelf Science, 66(1–2). Available online: https://doi.org/10.1016/j.ecss.2005.07.018.

Macreadie, P.I., Baird, M.E., Trevathan-Tackett, S.M., Larkum, A.W.D. & Ralph, P.J. (2014) Quantifying and modelling the carbon sequestration capacity of seagrass meadows - A critical assessment. *Marine Pollution Bulletin*, 83(2). Available online: https://doi.org/10.1016/j.marpolbul.2013.07.038.

Makri, D., Melillos, G., Kalogirou, E. & Hadjimitsis, D. (2023) Seagrass mapping in Cyprus area of interest with pixel-based classification. In. Available online: https://doi.org/10.1117/12.2663484.

Marino, R., Hayn, M., Howarth, R., Giblin, A. & McGlathery, K. (2021) High rates of nitrogen fixation associated with epibiota on Zostera marina in a nitrogen-enriched temperate lagoon, Cape Cod, MA.

Marsh, J.A., Dennison, W.C. & Alberte, R.S. (1986) Effects of temperature on photosynthesis and respiration in eelgrass (Zostera marina L.). *Journal of Experimental Marine Biology and Ecology*, 101(3). Available online: https://doi.org/10.1016/0022-0981(86)90267-4.

Marshall, S. & Elliott, M. (1998) Environmental influences on the fish assemblage of the Humber estuary, U.K. *Estuarine, Coastal and Shelf Science*, 46(2). Available online: https://doi.org/10.1006/ecss.1997.0268.

Marshall, S & Elliott, M. (1998) Estuarine Coastal and Shelf Science\rEnvironmental influences on the fish assemblage of the Humber estuary, UK. *Estuarine Coastal and Shelf Science*, 46.

Martínez-Crego, B., Olivé, I. & Santos, R. (2014) CO2and nutrient-driven changes across multiple levels of organization in Zostera noltii ecosystems. *Biogeosciences*, 11(24). Available online: https://doi.org/10.5194/bg-11-7237-2014.

Massa, S.I., Arnaud-Haond, S., Pearson, G.A. & Serrão, E.A. (2009) Temperature tolerance and survival of intertidal populations of the seagrass Zostera noltii (Hornemann) in Southern Europe (Ria Formosa, Portugal). *Hydrobiologia*, 619(1). Available online: https://doi.org/10.1007/s10750-008-9609-4.

Mazarrasa, I., Lavery, P., Duarte, C.M., Lafratta, A., Lovelock, C.E., Macreadie, P.I., Samper-Villarreal, J., Salinas, C., Sanders, C.J., Trevathan-Tackett, S., Young, M., Steven, A. & Serrano, O. (2021) Factors Determining Seagrass Blue Carbon Across Bioregions and Geomorphologies. *Global Biogeochemical Cycles*, 35(6). Available online: https://doi.org/10.1029/2021GB006935.

McHenry, J., Rassweiler, A., Hernan, G., Dubel, A.K., Curtin, C., Barzak, J., Varias, N. & Lester, S.E. (2023) Geographic variation in organic carbon storage by seagrass beds. *Limnology and Oceanography* [Preprint]. Available online: https://doi.org/10.1002/lno.12343.

McHenry, J., Rassweiler, A., Hernan, G., Uejio, C.K., Pau, S., Dubel, A.K. & Lester, S.E. (2021) Modelling the biodiversity enhancement value of seagrass beds. *Diversity and Distributions*, 27(11). Available online: https://doi.org/10.1111/ddi.13379.

McLeod, E., Chmura, G.L., Bouillon, S., Salm, R., Björk, M., Duarte, C.M., Lovelock, C.E., Schlesinger, W.H. & Silliman, B.R. (2011) A blueprint for blue carbon: Toward an improved understanding of the role of vegetated coastal habitats in sequestering CO2. *Frontiers in Ecology and the Environment*. Available online: https://doi.org/10.1890/110004.

Mieszkowska, N., Firth, L. & Bentley, M. (2013) Impacts of climate change on intertidal habitats. *MCCIP Science Review*, xxx(November 2013).

Migné, A., Davoult, D., Spilmont, N., Ouisse, V. & Boucher, G. (2016) Spatial and temporal variability of CO2 fluxes at the sediment-air interface in a tidal flat of a temperate lagoon (Arcachon Bay, France). *Journal of Sea Research*, 109. Available online: https://doi.org/10.1016/j.seares.2016.01.003.

Miller, A.W. & Ambrose, R.F. (2000) Sampling patchy distributions: Comparison of sampling designs in rocky intertidal habitats. *Marine Ecology Progress Series*, 196. Available online: https://doi.org/10.3354/meps196001.

La Nafie, Y.A., de los Santos, C.B., Brun, F.G., van Katwijk, M.M. & Bouma, T.J. (2012) Waves and high nutrient loads jointly decrease survival and separately affect morphological and biomechanical properties in the seagrass Zostera noltii. *Limnology and Oceanography*, 57(6). Available online: https://doi.org/10.4319/lo.2012.57.6.1664.

Oracion, E.G., Miller, M.L. & Christie, P. (2005) Marine protected areas for whom? Fisheries, tourism, and solidarity in a Philippine community. *Ocean and Coastal Management*, 48(3-6 SPEC. ISS.). Available online: https://doi.org/10.1016/j.ocecoaman.2005.04.013.

Ouisse, V., Migné, A. & Davoult, D. (2010) Seasonal variations of community production, respiration and biomass of different primary producers in an intertidal Zostera noltii bed (Western English Channel, France). *Hydrobiologia*, 649(1). Available online: https://doi.org/10.1007/s10750-010-0254-3.

Ouisse, V., Migné, A. & Davoult, D. (2011) Community-level carbon flux variability over a tidal cycle in Zostera marina and Z. Noltii beds. *Marine Ecology Progress Series*. Available online: https://doi.org/10.3354/meps09274.

Ouisse, V., Riera, P., Migné, A., Leroux, C. & Davoult, D. (2012) Food web analysis in intertidal Zostera marina and Zostera noltii communities in winter and summer. *Marine Biology*, 159(1). Available online: https://doi.org/10.1007/s00227-011-1796-2.

Pedersen, O., Colmer, T.D., Borum, J., Zavala-Perez, A. & Kendrick, G.A. (2016) Heat stress of two tropical seagrass species during low tides - impact on underwater net photosynthesis, dark respiration and diel in situ internal aeration. *New Phytologist*, 210(4). Available online: https://doi.org/10.1111/nph.13900.

Penhale, P.A. (1977) Macrophyte-epiphyte biomass and productivity in an eelgrass (Zostera marina L.) community. *Journal of Experimental Marine Biology and Ecology*, 26(2). Available online: https://doi.org/10.1016/0022-0981(77)90109-5.

Peralta, G., Brun, F.G., Hernández, I., Vergara, J.J. & Pérez-Lloréns, J.L. (2005) Morphometric variations as acclimation mechanisms in Zostera noltii beds. *Estuarine, Coastal and Shelf Science*, 64(2–3). Available online: https://doi.org/10.1016/j.ecss.2005.02.027.

Peralta, G., Pérez-Lloréns, J.L., Hernández, I. & Vergara, J.J. (2002) Effects of light availability on growth, architecture and nutrient content of the seagrass Zostera noltii Hornem. *Journal of Experimental Marine Biology and Ecology*, 269(1). Available online: https://doi.org/10.1016/S0022-0981(01)00393-8.

Pérez-Lloréns, J.L. & Niell, F.X. (1993) Temperature and emergence effects on the net photosynthesis of two Zostera noltii Hornem. morphotypes. *Hydrobiologia*, 254(1). Available online: https://doi.org/10.1007/BF00007765.

Philip, G. (1936) An Enalid Plant Association in the Humber Estuary. *The Journal of Ecology*, 24(1). Available online: https://doi.org/10.2307/2256275.

Philippart, C.J.M. (1995) Seasonal variation in growth and biomass of an intertidal Zostera noltii stand in the Dutch wadden sea. *Netherlands Journal of Sea Research*, 33(2). Available online: https://doi.org/10.1016/0077-7579(95)90007-1.

Plus, M., Deslous-Paoli, J.M., Auby, I. & Dagault, F. (2001) Factors influencing primary production of seagrass beds (Zostera noltii Hornem.) in the Thau lagoon (French Mediterranean coast). *Journal of Experimental Marine Biology and Ecology*, 259(1). Available online: https://doi.org/10.1016/S0022-0981(01)00223-4.

Polte, P., Schanz, A. & Asmus, H. (2005) The contribution of seagrass beds (Zostera noltii) to the function of tidal flats as a juvenile habitat for dominant, mobile epibenthos in the Wadden Sea. *Marine Biology*, 147(3). Available online: https://doi.org/10.1007/s00227-005-1583-z.

Potter, C., Klooster, S. & Genovese, V. (2012) Net primary production of terrestrial ecosystems from 2000 to 2009. *Climatic Change*, 115(2). Available online: https://doi.org/10.1007/s10584-012-0460-2.

Prentice, C., Poppe, K.L., Lutz, M., Murray, E., Stephens, T.A., Spooner, A., Hessing-Lewis, M., Sanders-Smith, R., Rybczyk, J.M., Apple, J., Short, F.T., Gaeckle, J., Helms, A., Mattson, C., Raymond, W.W. & Klinger, T. (2020) A Synthesis of Blue Carbon Stocks, Sources, and Accumulation Rates in Eelgrass (Zostera marina) Meadows in the Northeast Pacific. *Global Biogeochemical Cycles*, 34(2). Available online: https://doi.org/10.1029/2019GB006345.

Prior, J. (2023) *Carbon Sequestration of Eelgrass Meadows in Clayoquot Sound, BC: An Identification of the Environmental Drivers of Sediment Carbon Variability*. University of Victoria .

Ralph, P.J. & Gademann, R. (2005) Rapid light curves: A powerful tool to assess photosynthetic activity. *Aquatic Botany*, 82(3). Available online: https://doi.org/10.1016/j.aquabot.2005.02.006.

Repolho, T., Duarte, B., Dionísio, G., Paula, J.R., Lopes, A.R., Rosa, I.C., Grilo, T.F., Caçador, I., Calado, R. & Rosa, R. (2017) Seagrass ecophysiological performance under ocean warming and acidification. *Scientific Reports*, 7. Available online: https://doi.org/10.1038/srep41443.

Ritchie, H., Roser, M. & Rosado, P. (2021) *CO2 and Greenhouse Gas Emissions: Germany: CO2 Country Profile OurWorldInData*.

Ruiz-Montoya, L., Sandoval-Gil, J.M., Belando-Torrentes, M.D., Vivanco-Bercovich, M., Cabello-Pasini, A., Rangel-Mendoza, L.K., Maldonado-Gutiérrez, A., Ferrerira-Arrieta, A. & Guzmán-Calderón, J.M. (2021) Ecophysiological responses and self-protective canopy effects of surfgrass (Phyllospadix torreyi) in the intertidal. *Marine Environmental Research*, 172. Available online: https://doi.org/10.1016/j.marenvres.2021.105501.

Saiful, S.A., Hj. Talib, K., Mat, M.A., Yusof, O.M. & Zalil, S.A. (2012) Height discrepancies based on various vertical datum. In *Proceedings - 2012 IEEE Control and System Graduate Research Colloquium, ICSGRC 2012*. Available online: https://doi.org/10.1109/ICSGRC.2012.6287171.

Sandoval-Gil, J.M., Barrote, I., Silva, J., Olivé, I., Costa, M.M., Ruiz, J.M., Marín-Guirao, L., Sánchez-Lizaso, J.L. & Santos, R. (2015) Plant-water relations of intertidal and subtidal seagrasses. *Marine Ecology*, 36(4). Available online: https://doi.org/10.1111/maec.12230.

Scartazza, A., Moscatello, S., Gavrichkova, O., Buia, M.C., Lauteri, M., Battistelli, A., Lorenti, M., Garrard, S.L., Calfapietra, C. & Brugnoli, E. (2017) Carbon and nitrogen allocation strategy in Posidonia oceanica is altered by seawater acidification. *Science of the Total Environment*, 607–608. Available online: https://doi.org/10.1016/j.scitotenv.2017.06.084.

Scott, A.L., York, P.H., Duncan, C., Macreadie, P.I., Connolly, R.M., Ellis, M.T., Jarvis, J.C., Jinks, K.I., Marsh, H. & Rasheed, M.A. (2018) The role of herbivory in structuring tropical seagrass ecosystem service delivery. *Frontiers in Plant Science*, 9. Available online: https://doi.org/10.3389/fpls.2018.00127.

Shi, J., Zhu, Y., Feng, Y., Yang, J. & Xia, C. (2023) A Prompt Decarbonization Pathway for Shipping: Green Hydrogen, Ammonia, and Methanol Production and Utilization in Marine Engines. *Atmosphere*. Available online: https://doi.org/10.3390/atmos14030584.

Short, F.T. & Neckles, H.A. (1999) The effects of global climate change on seagrasses. *Aquatic Botany*. Available online: https://doi.org/10.1016/S0304-3770(98)00117-X.

Silva, J. & Santos, R. (2003) Daily variation patterns in seagrass photosynthesis along a vertical gradient. *Marine Ecology Progress Series*, 257. Available online: https://doi.org/10.3354/meps257037.

Silva, J., Santos, R., Calleja, M.L. & Duarte, C.M. (2005) Submerged versus air-exposed intertidal macrophyte productivity: From physiological to community-level assessments. *Journal of Experimental Marine Biology and Ecology*, 317(1). Available online: https://doi.org/10.1016/j.jembe.2004.11.010.

Silva, J.M.S. da (2004) *The Photosynthetic Ecology of Zostera noltii*. Universidade do Algarve.

Smith, K.E., Burrows, M.T., Hobday, A.J., King, N.G., Moore, P.J., Sen Gupta, A., Thomsen, M.S., Wernberg, T. & Smale, D.A. (2023) Biological Impacts of Marine Heatwaves. *Annual Review of Marine Science*. Available online: https://doi.org/10.1146/annurev-marine-032122-121437.

Sudo, K., Quiros, T.E.A.L., Prathep, A., Luong, C. Van, Lin, H.J., Bujang, J.S., Ooi, J.L.S., Fortes, M.D., Zakaria, M.H., Yaakub, S.M., Tan, Y.M., Huang, X. & Nakaoka, M. (2021) Distribution, Temporal Change, and Conservation Status of Tropical Seagrass Beds in Southeast Asia: 2000–2020. *Frontiers in Marine Science*, 8. Available online: https://doi.org/10.3389/fmars.2021.637722.

Taleghani, M. (2022) Air Pollution within Different Urban Forms in Manchester, UK. *Climate*, 10(2). Available online: https://doi.org/10.3390/cli10020026.

Tang, K.H.D. & Hadibarata, T. (2022) Seagrass Meadows under the Changing Climate: A Review of the Impacts of Climate Stressors. *Research in Ecology*, 4(1). Available online: https://doi.org/10.30564/re.v4i1.4363.

Thewes, D., Stanev, E. V. & Zielinski, O. (2022) Steps Toward Modelling the Past and Future North Sea Ecosystem With a Focus on Light Climate. *Frontiers in Marine Science*, 9. Available online: https://doi.org/10.3389/fmars.2022.818383.

Tikkanen, M., Mekala, N.R. & Aro, E.M. (2014) Photosystem II photoinhibition-repair cycle protects Photosystem i from irreversible damage. *Biochimica et Biophysica Acta - Bioenergetics*, 1837(1). Available online: https://doi.org/10.1016/j.bbabio.2013.10.001.

Tyler-Walters, H. (2008) *Common eelgrass (Zostera (Zostera) marina)*.

Tyler-Walters, H. & d'Avack, E. (2015) Ruppia maritima in reduced salinity infralittoral muddy sand.

Uncles, R.J., Stephens, J.A. & Harris, C. (2006) Runoff and tidal influences on the estuarine turbidity maximum of a highly turbid system: The upper Humber and Ouse Estuary, UK. *Marine Geology*, 235(1-4 SPEC. ISS.). Available online: https://doi.org/10.1016/j.margeo.2006.10.015.

Uncles, R.J., Stephens, J.A. & Law, D.J. (2006) Turbidity maximum in the macrotidal, highly turbid Humber Estuary, UK: Flocs, fluid mud, stationary suspensions and tidal bores. *Estuarine, Coastal and Shelf Science*, 67(1–2). Available online: https://doi.org/10.1016/j.ecss.2005.10.013.

Vermaat, J.E. & Verhagen, F.C.A. (1996) Seasonal variation in the intertidal seagrass Zostera noltii Hornem.: Copuling demographic and physiological patterns. *Aquatic Botany*, 52(4). Available online: https://doi.org/10.1016/0304-3770(95)00510-2.

Verstraeten, G. & Poesen, J. (2001) Variability of dry sediment bulk density between and within retention ponds and its impact on the calculation of sediment yields. *Earth Surface Processes and Landforms*, 26(4). Available online: https://doi.org/10.1002/esp.186.

White, A.J. & Critchley, C. (1999) Rapid light curves: A new fluorescence method to assess the state of the photosynthetic apparatus. *Photosynthesis Research*, 59(1). Available online: https://doi.org/10.1023/A:1006188004189.

Woelfel, J., Schumann, R., Peine, F., Flohr, A., Kruss, A., Tegowski, J., Blondel, P., Wiencke, C. & Karsten, U. (2010) Microphytobenthos of Arctic Kongsfjorden (Svalbard, Norway): Biomass and potential primary production along the shore line. *Polar Biology*, 33(9). Available online: https://doi.org/10.1007/s00300-010-0813-0.

Wu, X. and Parsons, D.R. (2019) 'Field investigation of bedform morphodynamics under combined flow', Geomorphology, 339, pp. 19–30. doi:10.1016/j.geomorph.2019.04.028.

Wyer, D.W., Boorman, L.A. & Waters, R. (1977) Studies on the distribution of Zostera in the outer Thames Estuary. *Aquaculture*, 12(3). Available online: https://doi.org/10.1016/0044-8486(77)90062-X.

Xu, S., Zhou, Y., Wang, P., Wang, F., Zhang, X., Yue, S., Zhang, Y., Qiao, Y. & Liu, M. (2021) Temporal-spatial variations in the elemental and stable isotope contents of eelgrass (Zostera marina L.) in the Bohai Sea and Yellow Sea, northern China: Sheath as a novel ecological indicator for geochemical research. *Ecological Indicators*, 121. Available online: https://doi.org/10.1016/j.ecolind.2020.107181.

Zimmerman, R.C. (2021) Scaling up: Predicting the Impacts of Climate Change on Seagrass Ecosystems. *Estuaries and Coasts*, 44(2). Available online: https://doi.org/10.1007/s12237-020-00837-7.

Zoffoli, M.L., Gernez, P., Rosa, P., Le Bris, A., Brando, V.E., Barillé, A.L., Harin, N., Peters, S., Poser, K., Spaias, L., Peralta, G. & Barillé, L. (2020) Sentinel-2 remote sensing of Zostera noltei-dominated intertidal seagrass meadows. *Remote Sensing of Environment*, 251. Available online: https://doi.org/10.1016/j.rse.2020.112020.

Acknowledgements

Appendices

Appendix 1. A time series of images taken above quadrat station 1.
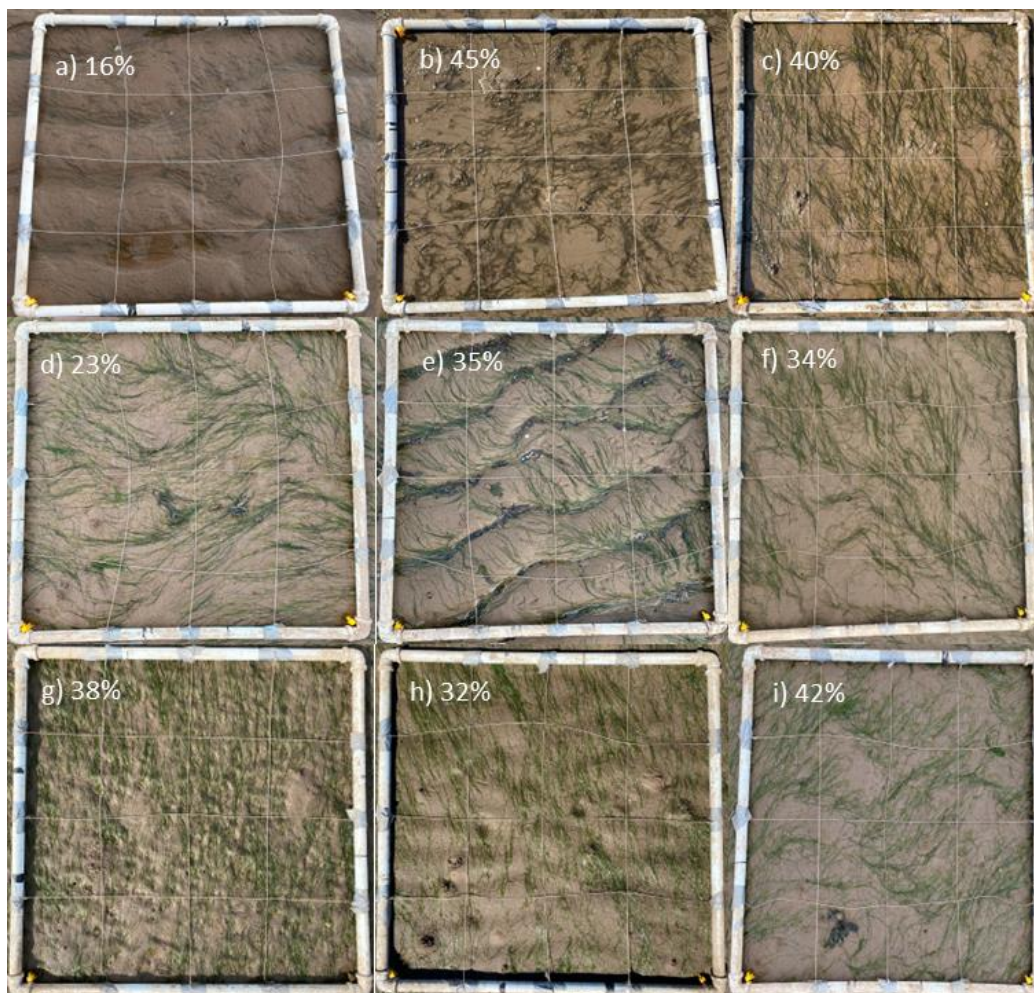
Appendix 2. A time series of images taken above quadrat station 2.
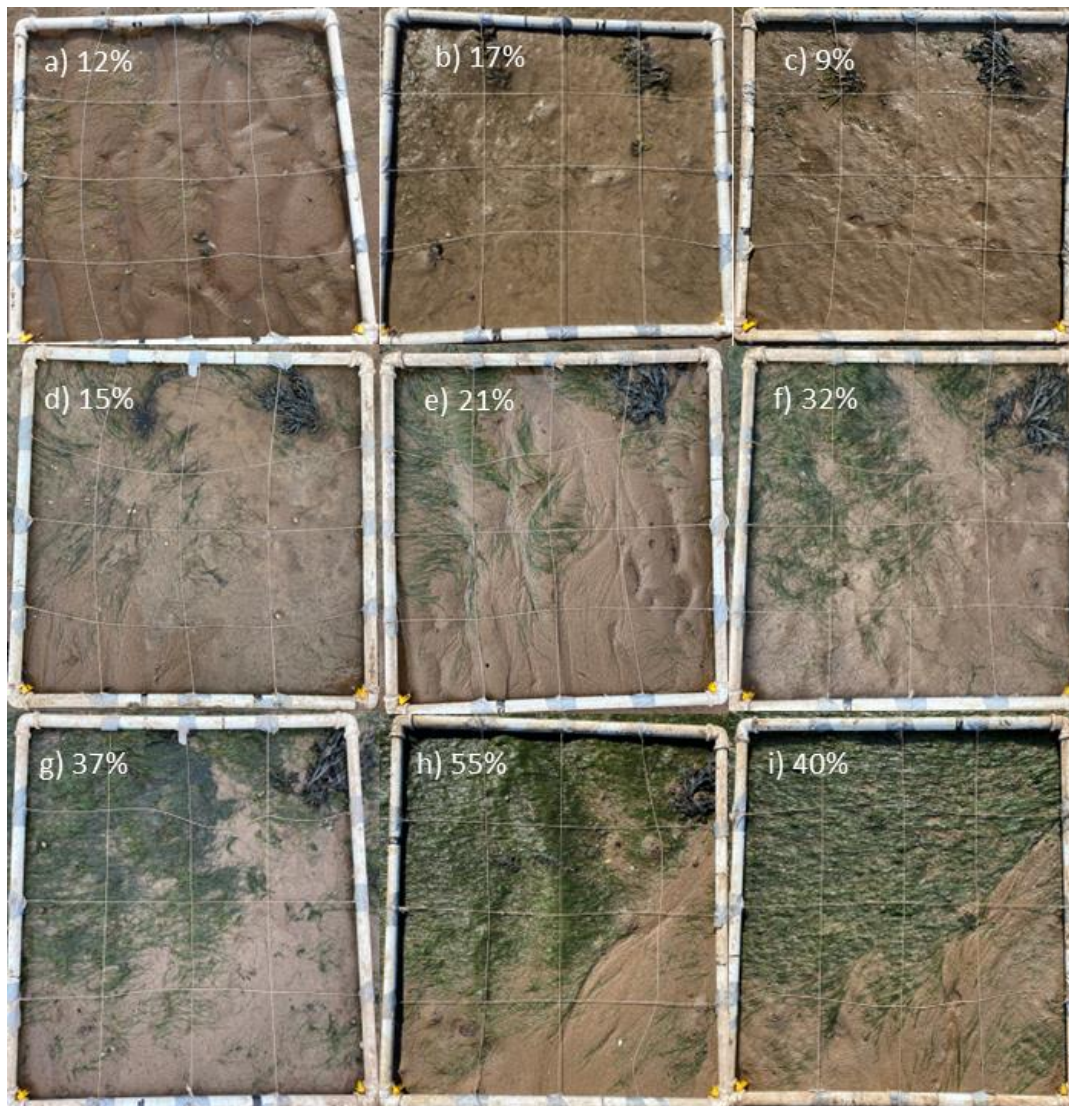
Appendix 2. A time series of images taken above quadrat station 2.

Appendix 3. A time series of images taken above quadrat station 3.
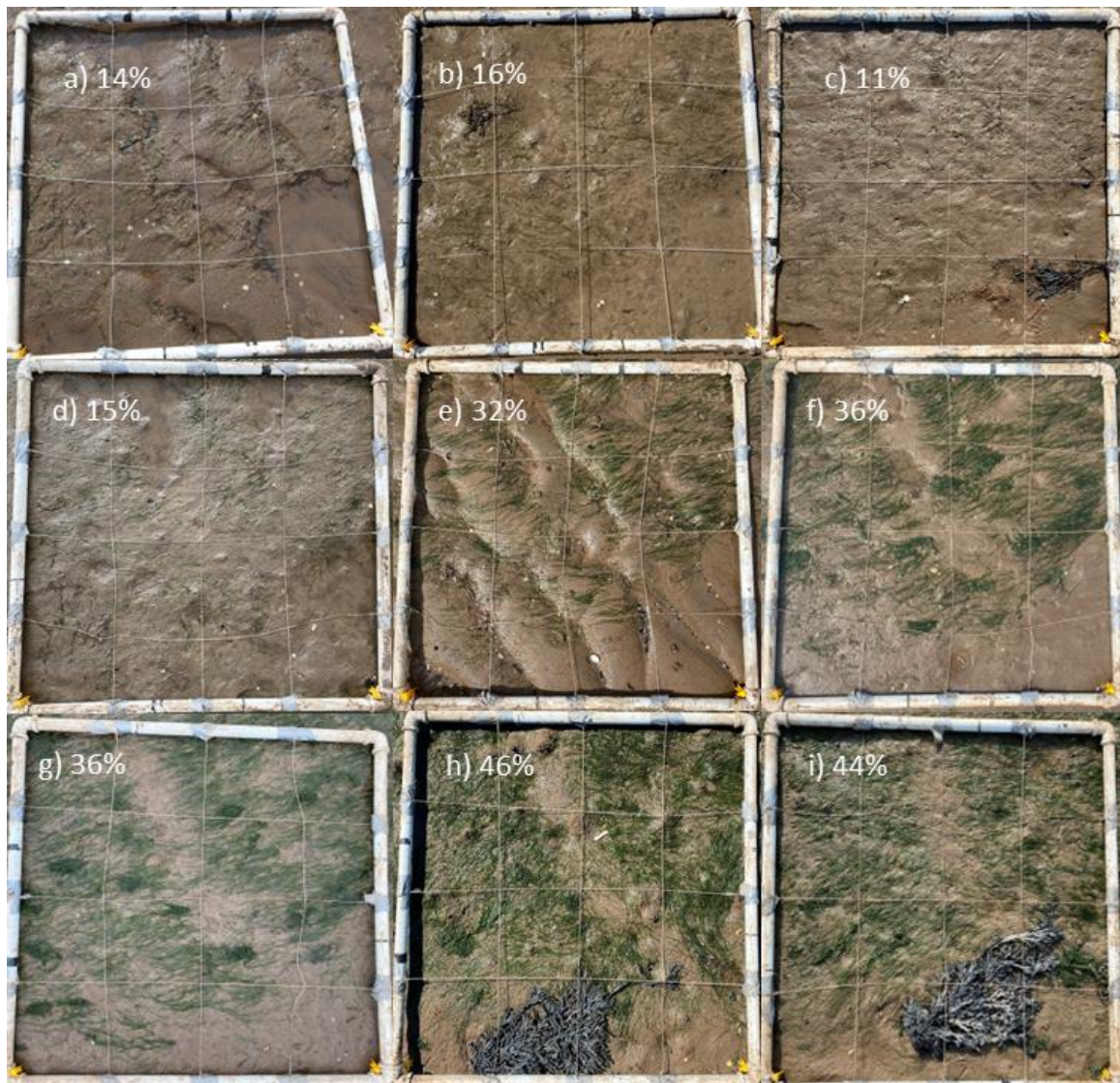
Appendix 4. A time series of images taken above quadrat station 4.
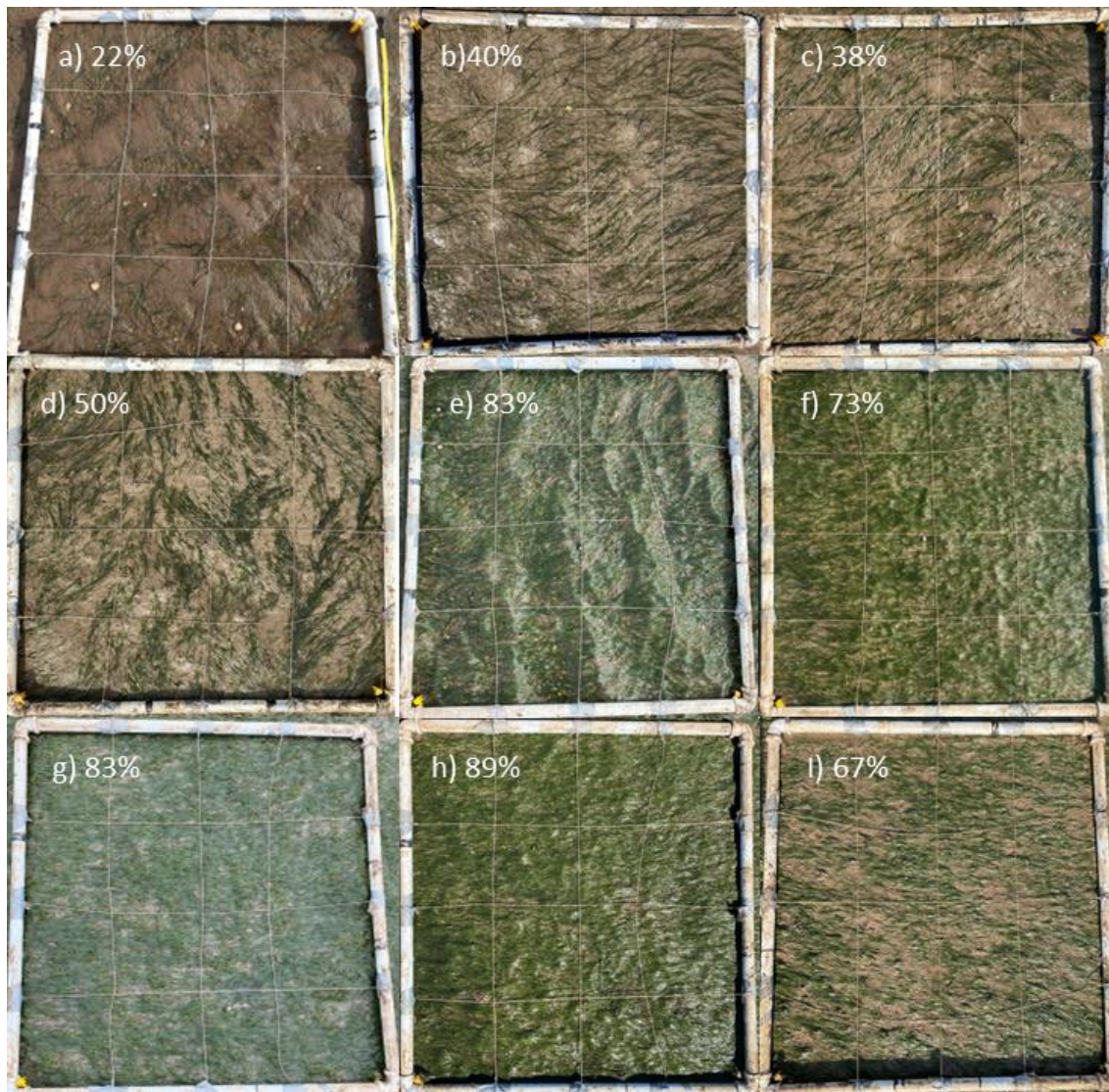
Appendix 5. A time series of images taken above quadrat station 5.
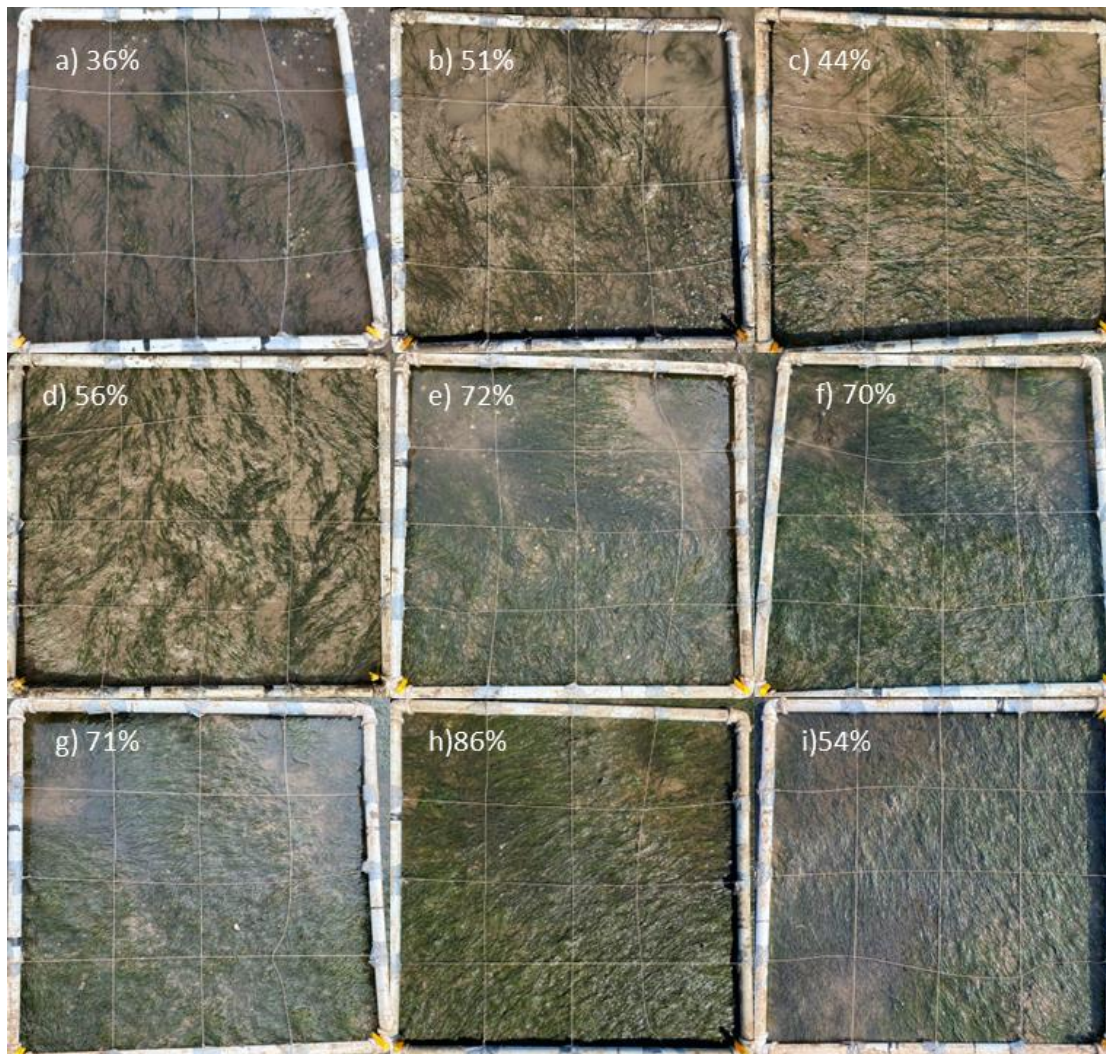
Appendix 6. A time series of images taken above quadrat station 6.
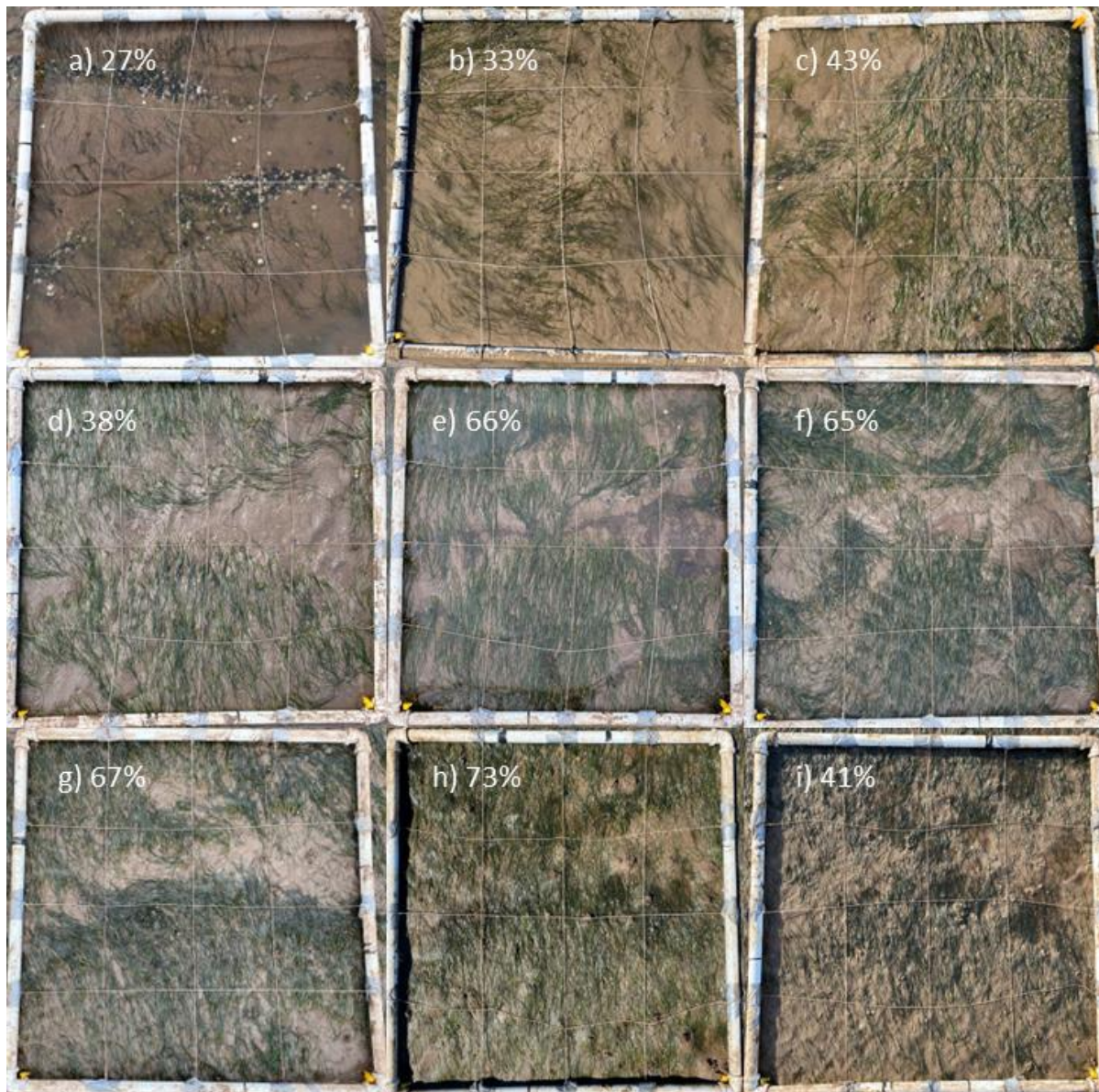
Appendix 7. Core sample wet and dry weights.

Sediment							
Crucible_weight	subsample/crucible_wet_weight	wet_weight_g	Subsample/crucible_dry_weight	dry_weight_g	water_weight_g	water_content_percent	DW/WW ratio
16.67	22.07	5.4	20.92	4.25	1.15	21.30	79%
10.19	15.52	5.33	14.48	4.29	1.04	19.51	80%
15.56	23.17	7.61	21.62	6.06	1.55	20.37	80%
18.69	27.08	8.39	25.24	6.55	1.84	21.93	78%
9.7	18.07	8.37	16.35	6.65	1.72	20.55	79%
17.14	24.92	7.78	23.44	6.3	1.48	19.02	81%
14.26	21.93	7.67	20.19	5.93	1.74	22.69	77%
14.95	23.01	8.06	21.23	6.28	1.78	22.08	78%
9.94	17.87	7.93	16.27	6.33	1.6	20.18	80%
15.85	23.61	7.76	21.45	5.6	2.16	27.84	72%
15.47	21.71	6.24	19.84	4.37	1.87	29.97	70%
14.98	22.72	7.74	20.35	5.37	2.37	30.62	69%
17.01	22.43	5.42	20.22	3.21	2.21	40.77	59%
9.25	15.63	6.38	13.63	4.38	2	31.35	69%
9.88	18.63	8.75	15.89	6.01	2.74	31.31	69%
16.22	24.59	8.37	22.6	6.38	1.99	23.78	76%
17.23	27.73	10.5	25.65	8.42	2.08	19.81	80%
10.32	18.79	8.47	17.04	6.72	1.75	20.66	79%
						24.65	75%

Appendix 8. Core sample weights and carbon conversion using C,H,N analysis

plant_wet_g	total_plant_dry_g	plant_water_g	plant_carbon_g	total_seagrass_carbon_g_m2	blade_seagrass_carbon_g_m2	mean_blade_seagrass_carbon_g_m2	%_cover_september
0.27	0.07	0.2	0.023	46.66	27.65		
0.5	0.09	0.41	0.029	59.99	33.59		
0.07	0.01	0.06	0.003	6.67	3.81	21.68	42
0.86	0.15	0.71	0.049	99.98	54.64		
0.71	0.13	0.58	0.043	86.65	30.51		
0.35	0.07	0.28	0.023	46.66	22.66	35.94	40
0.39	0.08	0.31	0.026	53.33	20.51		
1.01	0.13	0.88	0.043	86.65	24.02		
0.18	0.03	0.15	0.010	20.00	15.55	20.03	44
0.52	0.07	0.45	0.023	46.66	8.08		
0.44	0.11	0.33	0.036	73.32	38.33		
0.91	0.16	0.75	0.052	106.65	56.26	34.22	67
0.28	0.05	0.23	0.016	33.33	26.19		
0.71	0.09	0.62	0.029	59.99	21.12		
1.43	0.18	1.25	0.059	119.98	30.21	25.84	54
0.7	0.1	0.6	0.033	66.66	29.52		
0.15	0.04	0.11	0.013	26.66	8.89		
0.24	0.03	0.21	0.010	20.00	12.50	16.97	41